Maintenance and function of antigen-specific CD4 T cells within the lung during tuberculosis

Albanus Moguche

A Dissertation

Submitted in partial fulfillment of the

requirements for the degree of

Doctor of Philosophy

University of Washington

2014

Reading Committee:

Kevin B. Urdahl, MD, PhD, Chair

Pamela J. Fink, PhD

Marion Pepper, PhD

Program Authorized to Offer Degree:

Department of Immunology

University of Washington

Abstract

Maintenance and function of antigen-specific CD4 T cells within the lung during tuberculosis

ALBANUS OBONSI MOGUCHE

Chair of Supervisory Committee:
Kevin B. Urdahl, M.D., Ph.D.
Department of Immunology

Tuberculosis (TB) is a chronic pulmonary disease caused by the intracellular bacterium *Mycobacterium tuberculosis* (Mtb). Even though CD4 T cells are critical for containing Mtb, the immune system rarely eradicates the bacteria, necessitating the maintaining of an antigen-specific CD4 T cell response throughout the course of infection. How this response is maintained is not currently well understood. Here we show that in a murine model of TB, Mtb-specific CD4 T cells are subjected to chronic antigenic stimulation. Despite this chronic antigenic stimulation, a subset of these Mtb-specific CD4 T cells expressing the inhibitory receptor PD-1 exhibits hallmarks of memory T cells and their maintenance requires intrinsic expression of ICOS, the transcription factor Bcl6, and the chemokine receptor CXCR5.

Furthermore we find that a majority of KLRG1$^+$ IFN-γ producing CD4 T cells are located in the lung-associated vasculature and not in the lung parenchyma as previously thought. However, the PD-1$^+$ population that shares features with follicular helper (Tfh) and memory T cells is principally located within the lung parenchyma. This distribution can be largely explained by considering the TB granuloma as a tertiary lymphoid structure that forms within the

Mtb infected lung parenchyma. Contrary to previous reports, we found naïve $CD44^{low}$ CD4 T cells are excluded from lung parenchyma of uninfected mice but migrate into the lungs of Mtb-infected mice in a CCR7 dependent manner. PD-1^{+} Mtb-specific CD4 T cells express high levels of CD69 but have low levels of sphingosine-1-phosphate receptor 1 (S1PR1) and the transcription factor KLF2. In contrast, terminally differentiated $KLRG1^{+}$ type 1 helper T cells (Th1) cells exhibit elevated expression of S1PR1 and KLF2, but are $CD69^{low}$. These expression profiles likely explain the differential localization of these Mtb-specific cell populations and suggest that when effector Th1 cells are generated within the granuloma or draining lymph nodes, they egress into the blood in an S1P1R mediated manner. Our results help explain why the frequency of Th1 cells circulating in the blood does not correlate with immune protection, and provides a framework for understanding how immunity against TB is shaped by CD4 T cell trafficking into and out of granulomas.

Finally, we found that CD4 T cells recognizing Mtb antigens expressed throughout infection have a reduced capacity to produce protective cytokines and are restricted in their ability to control Mtb due to persistent stimulation by antigen. Conversely, CD4 T cells that recognize different Mtb antigens whose expression wanes with chronic infection have a limited capacity to mediate protection because of suboptimal stimulation by cognate antigen.

Collectively, these studies expand our understanding of the mechanisms that promote the maintenance and function of antigen-specific CD4 T cells in the lung during TB. The insights gained should aid in the rational design of new vaccines, not only against TB, but also against other chronic disease conditions in which maintenance of antigen specific CD4 T cells is paramount.

Table of Contents

List of figures

Figure **Page**

Chapter III

Chapter IV

List of tables

List of abbreviations

Ag85B	Antigen 85B
Akt	Protein Kinase B (PKB)
APCs	Antigen Presenting Cells
BCG	Bacillus Calmette–Guérin
Bcl6	B-cell lymphoma 6 protein
CCR7	C-C chemokine receptor type 7
CFSE	Carboxyfluorescein succinimidyl ester
CFU	Colony Forming Units
CTLs	Cytotoxic T lymphocytes
CXCL9	C-X-C Motif chemokine 9
CXCL10	C-X-C Motif chemokine 10
CXCL11	C-X-C Motif chemokine 11
CXCL13	C-X-C Motif chemokine 13
CXCR3	CXC Chemokine Receptor 3
CXCR5	CXC Chemokine Receptor 5
DCs	Dendritic Cells
DST	Directly Supervised Therapy
ESAT-6	Early Secreted Antigenic Target protein 6kDa
HIV-AIDS	Human immunodeficiency virus infection /acquired immunodeficiency syndrome
HRP	Horseradish peroxidase
i.n.	Intranasal
i.p.	Intraperitoneal
i.v.	Intravenous
ICOS	Inducible Co-stimulator
ICOSL	Inducible Co-stimulator Ligand
IFN-γ	Interferon gamma
IL-2	Interleukin 2
IL-12	Interleukin 12
IL-17	Interleukin 17
IL-18	Interleukin 18

IL-21	Interleukin 21
iNOS	Inducible Nitrogen Oxide Synthase
KLRG1	Killer cell Lectin-like Receptor subfamily G member 1
LDLN	Lung draining lymph node
MDR-TB	Multi-drug-resistant tuberculosis
MFI	Mean Fluorescence Intensity
MHCI	Major histocompatibility complex Class I Molecules
MHCII	Major histocompatibility complex Class II Molecules
Mtb	*Mycobacterium tuberculosis*
MyD88	Myeloid differentiation primary response gene 88
OD	Optical Density
PD1	Programmed Death Protein 1
PDIM	phthiocerol dimycocerosate
pLNs	Pulmonary lymph nodes
PE	Phyco-erythrin
RNI	Reactive Nitrogen Intermediates
ROI	Reactive Oxygen Intermediates
s.c.	Subcutaneous
S1P	Sphingosine-1-phosphate
S1PR	Sphingosine-1-phosphate Receptor
TB	Tuberculosis
Th1	Type 1 Helper T cells
Th2	Type 2 Helper T cells
Th17	Type 17 Helper T cells
TLR2	Toll Like Receptor 2
TNF	Tumor Necrosis Factor
Tregs	Regulatory T cells
WHO	World Health Organization
WT	Wild Type
XDR-TB	Extensively drug-resistant tuberculosis

Acknowledgements

First I would like to acknowledge Dr. Kevin Urdahl for being a great supportive and understanding mentor, for encouraging me to think critically and to consider all possibilities. Thanks very much for allowing me to pursue my passion and desire to make one tiny contribution in the fight against one of the most frustrating global diseases. I also would want to thank current and previous lab members for their enthusiasm and hard work and critical thinking that facilitated my research in the lab. Many thanks goes to Dr. Shahin Shafiani, Dr. Ryan Larson, Corey Clemons, Crystal Dinh and Dr. Kristin Adams who all contributed in one-way or the other to make my project a success. Special thanks to Dr. Ryan Larson for the many and long hours spend to help me do my experiments. Also thanks to Dr. Chris Plaisier (ISB) for helping to analyze the RNAseq data. Great thanks to my Ph.D. committee members, Dr. Pamela Fink, Dr. David Rawlings, Dr. Brian Iritani and Dr. Marion Pepper for their advice. Special thanks go to Dr. Pamela Fink and Dr. Marion Pepper for not only serving in my reading committee but also for helping and facilitating many aspects of my research. I appreciate the support from everyone in the immunology department and especially Peggy McCune for making my graduate school not only a success but also an enjoyable one. Thanks to my classmates who have been a source of support and help for the last five years.

My friends and family deserve a special acknowledgement for their help and understanding. I am especially grateful to my wife (Meicha Geohagen-Moguche) for all the help and encouragement and for being my friend. Special thanks to my mom (Mary Gesare Moguche) an extraordinary woman who gave me all when she had none, who sacrificed what she did not have, to ensure that my future was better and brighter than hers was. Thanks to all my brothers and sisters for a journey that we all shared and struggles that we all endured. And thanks to my

son (Ethan Obonsi Moguche). You were born when I was already in graduate school but you grew so fast to understand that dad had to go to school. I will forever appreciate and cherish that memory.

I will not forget all those folks in the village back in Kenya who sacrificed the very little they had to ensure I had an education. Special thanks to Mr. Joseph Onchieku Ondieki, without whose efforts I could never have gone to high school in the first place and to Mr. Joseph Orang`i Getanke for ensuring that I had a place to stay when I was on break from school and for providing a home for me the first time I moved from the village to the city.

Many thanks to the funding agencies that made my research possible: NIH/NIAID (U19AI106761) and Paul J Allen Family Foundation that provided funding to Dr. Urdahl, Bank of America Fellowship (through GO-MAP) and NCI (Training grant T21-CA009537) that supported my training.

Dedication

To my dad Thomas Moguche Kiboma

Chapter I: Introduction

Tuberculosis and Mycobacterium tuberculosis

Tuberculosis (TB) is a chronic pulmonary infection caused by bacteria of the genus Mycobacterium[1]. In humans the primary etiological agent for TB is *Mycobacterium tuberculosis* (Mtb), although the closely related *Mycobacterium bovis* (M. bovis) and other non-tuberculous mycobacteria can also cause disease[2,3]. Furthermore other non-pathogenic *Mycobacterium* species exist and whereas they do not commonly cause disease in healthy individuals, they can cause morbidity and mortality in immune compromised patients[4]. Mycobacteria are intracellular pathogens that take up residence within the host in the endosomal compartment of phagocytic cells, including macrophages, dendritic cells, and neutrophils. However, mycobacteria can also exist and replicate extracellularly[5]. The lung is the primary portal of infection as well as the most common site of disease. However, Mtb can spread via the blood or lymphatics to infect the pulmonary lymph nodes (pLNs), spleen, liver and the brain where it can cause fatal TB meningitis[6-8].

Mtb is usually spread by person-to-person transmission through inhalation of aerosolized cough droplets from infected individuals with active disease[9]. *M. bovis,* on the other hand, is transmitted from infected cattle through consumption of unpasteurized milk or contaminated meat products. Although it is a known occupational hazard for abattoir workers and meat inspectors[2], improved hygiene, milk pasteurization (or boiling for home produced milk), and stringent meat inspection standards have drastically reduced the number of TB cases due to *M. bovis* over the last century. As a result, Mtb causes the vast majority of human TB cases currently.

It is estimated that over 2 billion people worldwide are infected with Mtb and TB kills over 1 million individuals every year. In fact, despite the efforts of numerous international health agencies (including the World Health Organization (WHO), which declared TB a global health emergency 20 years ago), TB remains the second leading infectious killer worldwide[10]. The vast majority of those infected with Mtb (90-95%) display no overt signs of disease, rarely transmit infection, and remain asymptomatic for their entire lives[9,11]. These individuals are said to be latently infected and nevertheless exhibit immunologic evidence of infection (by skin test or in vitro IFN-γ release assays), and pathologic assessment of some latently infected individuals who died of other causes has revealed live Mtb in their lungs and lymph nodes[12]. There is growing evidence that latently infected individuals are not a homogeneous population, but comprise individuals harboring a broad spectrum of Mtb burdens[13,14]. On one end of the spectrum are those with the highest bacterial burdens and may be at the greatest risk of progressing to symptomatic, or active disease. On the other end, it is not known whether a proportion of those classified as latently infected by immunologic tests have actually eradicated Mtb.

About 5-10% of individuals infected with Mtb do eventually develop clinical signs of disease. The clinical signs of active TB are non-specific and varied, but in adults they include fever and chills, coughing, chest pain, blood in sputum, fatigue and weakness, lack of appetite and weight loss[9]. TB in children is usually subtler and often difficult to diagnose, as it is not uncommon for children to present with fever as their only sign. Adolescents and adults with active disease are the populations that transmit the infection to others. They develop inflammatory lesions that erode into their airways, resulting in Mtb bacilli in their sputum that can be expelled and aerosolized with forceful coughing. Because TB is usually less inflammatory in children, they rarely are the source of transmission[11]. Most active disease develops within 2

years of being infected, however, latently infected individuals can "re-activate" and develop active disease many years, or even decades, after being infected[14]. The factors that lead to progression to active disease, or disease reactivation many years later in a small percentage of those infected, are largely unknown. However, a functional repertoire of CD4 T cells is required to prevent progression to active TB. Young children and immune-compromised individuals are more likely to progress to active disease and have greater disease severity and mortality rates[15]. Those in these risk groups have an increased likelihood of dissemination to the brain and subsequent TB meningitis, contributing to their higher mortality rates[16]. However, most individuals who develop active TB were previously healthy with no known immunodeficiency.

Efforts to control and combat the TB epidemic have been met with little success due to multiple compounding factors that make its eradication and control quite difficult. Some of these factors include: 1) The sheer large number of infected people, making disease control logistically and economically unfeasible[10], 2) concentration of infected individuals in resource poor and developing countries in sub-Saharan Africa and South East Asia[10], 3) inter-connectivity of the current global population with enhanced cross border migration leading to disease spread[17], 4) emergence of multi-drug resistant (MDR-TB) and extensively drug resistant (XDR-TB) strains of Mtb making treatment with currently available antibiotics extremely difficult or impossible[18], 5) epidemic of human immune-deficiency virus and acquired immune deficiency syndrome (HIV-AIDS) in Mtb endemic areas[7,15] and 6) lack of effective vaccines against Mtb[19].

Intervention strategies to control tuberculosis

Despite the difficulties outlined above, a lot of effort and resources are being spent to develop effective ways to reduce the TB burden. One of the most effective strategies is to prevent infection and spread. Developed countries routinely screen potential immigrants for TB

as a means to maintain low TB rates in their own countries and when TB does occur, control strategies usually focus on screening and promptly treating infected people and their household contacts who might have been exposed[20,21]. The majority of TB is still caused by drug-sensitive Mtb, but even these cases require daily doses of 3-4 antibiotics for 6-9 months. This long course of treatment makes completion of an adequate course of treatment very difficult, especially since patients often feel better after a couple weeks of therapy and the drugs themselves have side effects that make people feel ill. Often individuals stop their antibiotics early, or take them inconsistently, and this practice is what has driven the global rise in drug-resistant TB. Individuals infected with MDR-TB or XDR-TB often require 7 or more very toxic antibiotics for up to two years of treatment (at a cost of ~$250,000 per patient), and even with this intensive therapy there is still a high rate of mortality. Resource rich countries try to assure that each patient is effectively treated and that the development of drug resistance is avoided by practicing directly supervised therapy (DST), which requires that health care workers physically supervise patients to ensure they take the medications[22]. However, this practice is not practical for developing countries with a high burden of TB and limited resources[23]. Therefore research efforts to develop novel drugs or interventions to shorten the duration of therapy are ongoing.

Therapeutic approaches, even when effective, are ultimately expensive. This is especially problematic given the socio-economic status of the countries with the highest TB burden. In contrast, vaccines have proven to be highly cost effective in controlling and reducing the burden of many infectious diseases and in a few cases, in globally eliminating certain infectious diseases[24,25]. Currently the only TB vaccine approved for use is Bacillus Calmette-Guerin (BCG)[9,10]. While it`s known to decrease the severity of disease, especially in young children, in whom it prevents dissemination and TB meningitis, BCG is only modestly effective in adults[16].

Because adults are responsible for transmission of TB, widespread BCG immunization has done little to stem the spread of the disease. Furthermore, unlike other vaccines (for example those against measles or chickenpox), whether BCG vaccination can prevent infection is unclear. Therefore efforts are currently underway to develop new and effective vaccines against tuberculosis.

Host immune response to Mycobacterium infection: Overview

TB is a complex infection, unlike any for which an effective vaccine has been developed. The vaccines currently used in human populations (with the exception of the shingles vaccine) mediate protection through humoral immunity[26,27]. Unfortunately, as an intracellular pathogen, antibodies have no role in natural immunity against TB[28]. Instead, Th1 cells (CD4 T cells producing IFN-γ) are critical for immunity but the frequency of these cells in the circulation of immunized individuals shows no correlation with protection[19,29,30]. Mtb is a slow growing pathogen with a lung portal of entry that modulates host immunity to delay the initiation of adaptive immunity, evade eradication, and establish chronic infection. It is abundantly clear that effective immunization against TB will require an entirely different approach than utilized for current vaccines. However, rationally devising an effective strategy will require understanding and overcoming Mtb-induced manipulation of the immune response.

Delayed transport of Mtb to the pulmonary lymph nodes

After initial infection via inhalation of cough droplets containing Mtb, the bacterium is taken up by alveolar macrophages[31]. However the inflammatory response of these sentinel cells is dampened by a virulence lipid on the surface of Mtb (phthiocerol dimycocerosate, PDIM) that mask toll-like receptors (TLR) ligands in the Mtb cell wall[32]. In addition, during this innate

phase of immunity Mtb mediates early endosomal arrest and prevents phagolysosomal fusion, further enhancing the replication-friendly niche within the host phagosome[33-35]. As a result, instead of activating and recruiting highly mycobacteriocidal macrophages, Mtb replicates under cover in cells that are relatively quiescent. Furthermore Mtb prolongs its dwell time within these replication-friendly macrophages by preventing apoptosis, but does eventually induce cell death[36,37]. Mtb is subsequently taken up by neutrophils within apoptotic bodies, which in turn undergo apoptosis and uptake by dendritic cells and inflammatory monocyte-derived phagocytes[5,38-40]. It is these latter two populations that shuttle live intracellular Mtb to the pulmonary lymph nodes (pLN), a process that does not occur until 8-10 days after infection. The adaptive immune response is initiated in the pLN only after this transport occurs[41-43].

Delayed effector T cell priming and migration to the lung

Even after the late transport of Mtb to the pLN, the onset of adaptive immunity is postponed even further by delayed effector T cell expansion and migration to the lung site of infection. Although migratory dendritic cells (DCs) harboring Mtb may participate in antigen-presentation, infected inflammatory monocyte derived cells do not[44] and these cells have to transfer their major histocompatibility I and II (MHCI and MHCII) restricted Mtb antigens to uninfected antigen presenting cells (APCs), such as lymph node (LN) resident DCs[45,46]. These uninfected DC populations are more effective at stimulating T cells than their infected counterparts, and seem to be the primary drivers of T cell priming. In addition to priming effector CD4 and CD8 T cells, Mtb-specific $Foxp3^+$ T regulatory cells (Tregs) also undergo expansion in the pLN. This Treg expansion seems to be driven by Mtb itself, as infection of the lung by other bacteria induce effector T cell expansion in the pLN without a concomitant Treg response. Mtb-specific Tregs in the pLN are highly activated and immunosuppressive and serve

to slow the expansion of effector CD4 and CD8 T cells, and delay their subsequent migration to the lungs[47-49]. These pathogen-orchestrated delays of adaptive immunity allow Mtb to replicate robustly in the lung and establish a niche for chronic infection.

CD4 T cells and tuberculosis

As an intracellular infection of the endosomal compartment, it is perhaps not surprising that CD4 T cells are central for protective immunity against TB[50]. HIV-infected individuals with low numbers or poorly functioning CD4 T cells are severely compromised in their ability to contain primary or latent Mtb infection. In fact, TB is the leading cause of death in HIV^+ persons worldwide[6,7,19,28,51,52].

Of the different CD4 T cell subsets, Th1 cells (those producing IFN-γ) are the most important for controlling Mtb infection [50,53]. Mice and humans deficient in IFN-γ or IL-12 (a cytokine required for Th1 development) are extremely susceptible to TB [50,54]. Th1 cells are thought to act primarily by producing immune-modulatory cytokines, such as IFN-γ and TNF that function to activate infected macrophages to kill Mtb, or at least curtail its growth[54,55]. However, Th1 cells can also release cytolytic molecules, like Granzyme B and perforin[56]. IFN-γ released by Mtb-specific T cells overrides early endosomal arrest of Mtb-containing phagosomes and induces phagolysosomal fusion[57]. Acidification and the release of nitric oxide and other reactive oxygen species occur within the phagolysosomal compartment, promoting Mtb killing[36,58]. Importantly, CD4 control of Mtb requires direct recognition of Mtb antigens on infected $MHCII^+$ cells[45,50]. In WT (wild type) by $MHCII^{-/-}$ mixed chimeric mice, $MHCII^{-/-}$ macrophages exhibited a much high bacterial burden that WT macrophages within the same mice[45]. Thus, cytokine production by "bystander" CD4 T cells probably has a very limited role in controlling Mtb.

Despite the importance of Th1 cells in protective immunity, the frequency of Mtb-specific Th1 cells in the blood of immunized individuals does not correlate with immune protection[19,29,30]. This seeming discrepancy has been a major point of contention and created confusion regarding the best path forward for an effective TB. In mice, the best correlate of protection is not the magnitude of the Th1 response, but the rate at which Th1 cells reach the site of infection in the lung[49,59,60]. However, why early arriving T cells are better able to control Mtb than late arriving T cells is not completely clear. Due to the central role of Th1 cells in protective immunity against TB, my thesis research focuses on elucidating how functional Th1 responses are maintained within the Mtb-infected lung. My data sheds light on why Th1 responses in the blood and lymphoid periphery do not correlate with protection, and also why early recognition of Mtb-infected cells within the lung may confer superior protection.

In addition to Th1 responses, Mtb can also induce type 2 helper (Th2), follicular helper (Tfh) and type 17 helper (Th17) effector responses. Most studies indicate that Th2 responses are actually detrimental to disease outcome[61]. Tfh cells provide help to B cells to secrete high affinity antibodies, including antibodies against Mtb. But antibodies play no role in natural immunity against Mtb[62], and thus the utility of Tfh cells during TB is unclear. In Chapter III of this thesis, however, we show that CD4 T cells with Tfh properties serve as progenitors that maintain the Mtb-specific Th1 response. Th17 cells, by secreting the cytokine IL-17, serve to recruit neutrophils to the infected lung[63]. Neutrophils can mediate protection by participating in the killing of Mtb; however a neutrophilic response can exacerbate disease by enhancing lung pathology[63]. Th17 cells and IL-17 can also enhance Mtb immunity during a memory response by accelerating the recruitment of Th1 cells into the lung and promoting a rapid recall to Mtb challenge after vaccination[64].

As previously discussed, pathogen-specific Tregs are induced in the pLN early after infection and help Mtb establish a niche in the lung by delaying the effector T cell response[47,49]. These Mtb-specific Tregs do not originate from effector CD4 T cells, but are thymically-derived cells that undergo parallel expansion with effector T cells in the pLN[48]. They peak in numbers ~3 weeks after infection, then contract and even 2 weeks later (~5 weeks post-infection) are difficult to find. Although pulmonary granulomas during chronic TB contain Tregs, they are not Mtb-specific (defined by MHCII restricted tetramers). In contrast to the host-detrimental role of Mtb-specific Tregs during the first 3 weeks of Mtb infection, our preliminary data suggests that Tregs during the chronic phase of infection are largely host-protective and serve to dampen potentially damaging inflammatory responses in the lung.

CD8 T cells during tuberculosis

CD8 T cells can also contribute to protective immunity. Mtb-specific CD8 T cells are activated through cross presentation of Mtb antigens by DCs that have taken up apoptotic infected cells, or directly recognize Mtb-infected cells[37,65]. CD8 T cells help control Mtb replication, by both perforin-mediated cytolysis of infected macrophages and direct killing of Mtb. Although the role of CD8 T cells in protective immunity during human TB is unclear, they play a relatively minor role in the mouse model and are effective primarily late during the chronic phase of infection (>200 days post-infection)[66].

Immune evasion by *Mycobacterium tuberculosis*

Although individual granuloma lesions can induce sterile immunity and clear bacteria[67], other lesions in the same host can exhibit increasing numbers of mycobacteria, despite an apparently robust T cell response. Part of the reason for this inability to clear infection is that

Mtb has evolved mechanisms to evade the host immune response[33]. As previously discussed, one of the primary mechanisms of Mtb control is that activated macrophages generate reactive oxygen intermediates (ROI) and reactive nitrogen intermediates (RNI) that have the potential to kill or restrict the replication of Mtb within the acidic phagolysosome[34]. However, Mtb has evolved mechanisms to inactivate both ROI and RNI principally by the expression of an NADH-dependent peroxidase and peroxynitrite reductase[35] and also to survive in low pH. While the precise mechanisms for this survival are not well understood, Mtb lipid-rich cell envelope (including peptidoglycan and lipoarabinomannan[58]) seem to act as an effective barrier against entry of protons induced by low pH as postulated more than 100 years ago.

During chronic infection, Mtb resides within granulomas that are bathed in a variety of immunosuppressive cytokines, including IL-10 and TGFβ (which are directly induced by an Mtb cell surface lipid, ManLAM)[68-71], as well as anti-inflammatory lipids called lipoxins[37]. These mediators are thought to restrict immune clearance of Mtb, but the mechanistic details of this immunosuppression are poorly understood.

Finally Mtb can indirectly induce the death of highly polarized Th1 cells. Infected macrophages and DCs are ultimately responsible for the killing or controlling Mtb replication[57,72]. Optimal control of Mtb to required a cognate interaction between Mtb-specific Th1 cells and infected macrophages/DCs[45]. As a result of this interaction, activated macrophages/DCs express high levels of reactive nitric oxide species and these can be toxic to effector T cells that express high levels of the transcription factor T-bet[34,73] Ultimately, this results in a reduced frequency of Th1 cells in close proximity to infected cells in the lung parenchyma. This phenomenon is explored further in chapter IV of this dissertation.

The anatomy of the immune system and lymphocyte re-circulation during TB

Naïve T cells in the steady state continuously circulate between lymphatic vessels, lymph nodes, blood, and secondary lymphoid tissues[74,75]. During an infectious challenge, naïve T cells must dwell in lymph nodes for a longer period to permit optimal T cell priming. This is achieved by a temporary increase in CD69 expression induced by cognate antigenic stimulation and/or inflammatory cytokines (especially type I interferon)[76]. Primed T cells must then egress from the lymph node and enter the blood circulation before trafficking to the site of infection. To accomplish this, CD69 expression needs to be lost or counteracted. This occurs through expression of sphingosine-1-phosphate receptors (S1PR) that are antagonistic to CD69 expression[77]. The ligand for this receptor, sphingosine-1-phosphate (S1P), is in higher concentration in blood than in the lymph nodes[78]. Upon binding S1PR, S1P provides a cue directing egress from the lymph node into blood circulation. Eventually S1PR becomes desensitized in the blood due to high concentration of S1P, and this desensitization (along with up-regulation of a variety of cell chemokine and trafficking receptors), is necessary for effector T cells to leave the blood and enter infected tissues. During Th1 mediated inflammation CXCR3 is a key chemokine receptor on Th1 CD4 T cells and it binds IFN-γ-induced chemokines, such as CXCL9, CXCL10 and CXCL11[79] to direct the migration of Th1 cells to the site of infection.

This complex sequence of events needs to be perfectly synchronized and any interference in the balance of the expression of CD69, S1P and its receptors, or the chemokines and their receptors, could alter T cell trafficking and potentially subvert immunity. Furthermore, the nature and organization of the TB granuloma (as outlined below) may profoundly impact T cell trafficking and recirculation.

***Mycobacterium* induced pathology in the host: The granuloma**

A cardinal feature of the host response to mycobacterial infections is the development of the 'tubercle' for which the disease is named and which was later described as a granuloma. The granuloma is a compact aggregate of organized macrophages, neutrophils, DCs, B and T cells, natural killer cells, fibroblasts and the epithelial cells that surround it[80]. The role of the granuloma during TB has been subject to debate for a long time. Indeed before the identification of *Mycobacterium tuberculosis* as the etiological agent for TB, it was postulated that the 'tubercle' caused the disease[1]. The idea that the granuloma sequesters and walls off Mtb has been advanced and is based on the common finding that granulomas frequently form during chronic stimulation from infectious agents or sterile non-infectious stimuli[81]. Furthermore in disease models in which granulomas are poorly formed or not formed at all, the prognosis of disease is nearly always poor[82]. Additionally single nucleotide polymorphisms (SNPs) in the genes essential for effective granuloma formation (CXCL13, CXCR5, CCR7 and IFN-γ) constitute risk factors for development of active disease following infection with Mtb[82,83]. However recent studies have also revealed that Mtb exploits granuloma formation for its own benefit[80].

Interestingly, both TB granulomas and lymph nodes are dependent on CXCL13, CXCR5, and CCR7 for their development[84,85]. Indeed, the maturation of the Mtb-induced granulomas results in ectopic lymphangiogenesis and contains all the hallmarks of lymphoid tissue, including aggregates of different cell types that are differentially located, the ability to undergo a germinal center reaction, and the ability to activate and prime T cells in-situ[69,82,85,86]. These tissue architectural changes are likely to shape how T cells circulate through the lung and have profound effects on TB outcome. In Chapter IV, we will explore how T cells enter and egress from the parenchyma of the Mtb-infected lung.

Tuberculosis vaccine development efforts

Bacillus Calmette-Guerin (BCG) is currently the only approved vaccine against TB and has been used widely in humans since 1921[9]. Despite this widespread use, TB continues to be one of the world's biggest infectious killers. A new vaccine is urgently needed, but first it is important to consider the nature of BCG and the reasons for its limited efficacy. BCG is derived from *Mycobacterium bovis* and is attenuated by the loss of critical genes necessary for virulence including the early secretory 6kDa ESAT-6 protein[87]. The efficacy of BCG vaccination is highly variable, with little to no protection in adults, and some efficacy in infants, where it prevents bacterial dissemination, especially into the brain[16]. Even though it reduces the severity of disease, whether BCG vaccination can prevent infection with Mtb is currently unclear. This is in contrast to most vaccines in which prevention of infection is the expected result. Even in infants, where it's modestly efficacious, how BCG vaccination functions is not currently understood. However it is known that the protective ability of BCG wanes over time and this is likely due to the induction of terminally differentiated Th1 cells[88]. It has been further suggested that the route of vaccination with BCG influences both the initial protective capacity and duration of that protection with concomitant airway and parenteral vaccination offering the best protection[60].

A tremendous amount of money and resources have been spent in the last few decades in efforts to improve BCG or make a new vaccine that is better than BCG. However those efforts have been met with little success, perhaps due to limitations in our understanding of how protective immunity against TB is mediated. This limited understanding is vividly demonstrated by our failure to understand why Th1 cells are absolutely critical for protection against tuberculosis[50,52,53,89], but their frequency in the blood of infected humans or in the lungs of immunized individuals does not correlate with protection against Mtb[30,90-92]. Furthermore a

recent vaccine candidate that successfully induced large numbers of Mtb-specific Th1 cells in the blood was shown to confer no greater protection than that provided by BCG alone[93,94]. Therefore there is great need to understand the basic biology of the CD4 T cell response to Mtb to inform the rational design of an effective vaccine against the global scourge of TB.

Dissertation objectives and significance

The goals of this dissertation were three-fold: 1) identify the cellular and molecular pathways that promote the maintenance of Mtb-specific CD4 T cells during chronic tuberculosis, 2) elucidate the trafficking patterns of CD4 T cells into and out of the Mtb-infected lung, and 3) determine whether chronic antigenic stimulation restricts the function and protective capacity of Mtb-specific CD4 T cells during chronic tuberculosis. Answers to these questions could not only provide basic insight into how immunity to tuberculosis is shaped, but could potentially identify new pathways that can be targeted for the rational design and development of new vaccines and immunotherapeutics.

We found that despite the continuous stimulation by cognate antigen, a subset of Mtb-specific CD4 T cells acquires characteristics of memory T cells, allowing for the maintenance of the CD4 T cell response during chronic tuberculosis. This maintenance is dependent upon ICOS-ICOSL signaling and the transcription factor Bcl6. This will be discussed in detail in Chapter III.

We also found that contrary to the previous belief of the field, most Th1 polarized Mtb-specific CD4 T cells do not localize within the lung parenchyma at the site of infection, but rather accumulate in the lung associated vasculature. This finding helps to explain the dichotomy between the absolute requirement of Th1 cells for immunity against tuberculosis and the lack of correlation between the quantity of these cells and protection. Furthermore, we found that the trafficking patterns of CD4 T cells can be largely understood if one considers pulmonary

granulomas as ectopic lymphoid tissue with similar rules governing T cell entry and egress from such sites. These findings will be discussed further in Chapter IV.

Finally we found that the ability of Mtb-specific CD4 T cells to mediate protective immunity is restricted for two opposite reasons. Some Mtb-specific T cells, such as those specific for ESAT-6, have a limited ability to produce protective cytokines due to chronic antigenic stimulation. In contrast, other Mtb-specific CD4 T cells, such as those specific for Ag85B, retain their functional capacity, but are restricted in their protective capacity due to limited cognate antigen expression. These findings are discussed in greater detail in Chapter V, and have important implications for vaccine and immunotherapeutic design.

Chapter II: Materials and Methods

Mice

C57BL/6 (B6), C57BL/6.PL (B6.PL, CD90.1), B6.SJL-Ptprc^{a}Pep3^{b}BoyJ (B6.SJL, CD45.1), B6.129S2 (Cg)-Blr1^{tm1lipp}/J (CXCR5$^{-/-}$), B6.129P2-ICOS^{tm1Mak}/J (ICOS$^{-/-}$), B10.129S2 (B6)-Igh-6^{tm1Cgn}/J (μMT$^{-/-}$), B6.129P2-Icosl^{tm1mak}/J (ICOSL$^{-/-}$), B6.Cg-Tg (TcraTcrb) 425Cbn/J (OT-II), B6.129P2-Tcrb^{tm1Mom}Tcrd^{tm1Mom}/J (TCRβ$^{-/-}$δ$^{-/-}$), Ccr7^{tm1Rfor}/J (CCR7$^{-/-}$) and C57BL/6-Tg (Nr4a1-EGFP/Cre) 820Khog/J (Nur77^{GFP}) mice were bought from Jackson laboratories and the later were used in experiments as hemi-zygotes. Heterozygous mice deficient in one allele of the Bcl6 gene (Bcl6$^{+/-}$) were maintained on a B6 background and have been described previously[95]. ESAT-6 TCR transgenic (C7) mice were provided by Dr. Eric Pamer and have been described previously[96]. Ag85B TCR transgenic (P25) mice have been previously described[97]. All mice were housed and bred under specific pathogen-free conditions at Seattle Biomedical Research Institute (SBRI) and the University of Washington. The Institutional Animal Care and Use Committee of SBRI and or the University of Washington approved all experimental protocols involving animals. All TB related work and flow cytometry on unfixed cells was performed under biosafety level-3 (BSL3) laboratory containment.

Generation of bone marrow or fetal liver chimeric mice

To generate mixed bone marrow chimeras, bone marrow cells from congenically marked WT, ICOS$^{-/-}$ or CXCR5$^{-/-}$ mice were isolated. Mature B and T cells were depleted from the bone marrow cell preparation by adding biotinylated anti-mouse CD19 to a mouse anti-CD3ε micro-bead Kit (Miltenyi Biotec). Congenically marked WT and knockout (ICOS$^{-/-}$ or CXCR5$^{-/-}$) cells were mixed in a ratio of 1:1 and 1-5 x 10^{6} cells of each strain were injected intravenously into

sub-lethally irradiated (600 Rads from a Rad Source gamma irradiator) mice deficient of T cells ($TCR\beta^{-/-}\delta^{-/-}$). As Bcl6 deficiency on a B6 background is embryonic lethal[98,99], we employed a mixed fetal liver chimera approach. For this, timed pregnancies of congenically marked WT (CD45.1 and CD45.2) and Bcl6 heterozygous mice (CD45.2) were set up. At embryonic day 15.5 or 16.5, pregnant mice were sacrificed and WT (CD45.1xCD45.2) as well as $Bcl6^{-/-}$ (CD45.2) fetuses collected. Fetal livers were isolated and teased into single cell suspension. Tail snips of the fetuses were screened for Bcl6 deficiency by PCR[99]. $Bcl6^{-/-}$ and WT fetal liver cells were then mixed at a ratio of 1:1 and injected $2x10^6$ cells of each strain were intravenously injected into lethally irradiated (1000 Rad) congenically marked B6.SJL mice. All recipient mice were put on prophylactic antibiotics for 4 weeks and their blood was screened for immune reconstitution 8-10 weeks post bone marrow or fetal liver cell transfer, followed by infection with Mtb.

Aerosol infections and bacterial load determination

Infection with a stock of Mtb H37Rv was done as previously described[66]. Briefly a stock of Mtb was sonicated before use and mice were infected in an aerosol infection chamber (Glas-Col) with ~100 colony forming units (CFU) deposited in the lungs of each mouse. Two mice were sacrificed immediately after infection to determine the infectious dose for each experiment. To determine viable numbers of CFUs, the left lung lobes of each mouse were homogenized in 0.05% Tween 80 in PBS. Ten-fold serial dilutions were made in 0.05% Tween 80 and plated on 7H10 plates. Colonies were counted after 21 days of incubation at 37°C to determine CFUs per organ.

Bacillus Calmette–Guérin (BCG), an attenuated strain of *Mycobacterium bovis* and *Listeria Monocytogenes* bacteria were grown to exponential phase and used as fresh cultures.

The approximate number of bacteria per fresh culture was determined by reading the optical density using a spectrophotometer. The calculation was based on an OD reading of 1 reflecting ~1 x 10^9 bacterial per milliliter of culture. 1 x 10^6 BCG bacteria were injected into mice intraperitoneally (i.p.) or 5 x 10^5 intranasally (i.n.). BCG was primarily used for vaccination in these studies. *Listeria Monocytogenes* was used at a dose of 1 x 10^5 intranasally primarily as an inducer of inflammation and control for Mtb infected mice. To determine the infection dose for Listeria, an aliquot of the infectious formulation was plated on culture plates overnight and colonies counted. A strain of Mtb that constitutively expresses antigen 85B (Mtb_Ag85B) has been described previously[100]. This Mtb strain was grown, maintained and prepared as Mtb H37Rv.

In vivo intravascular labeling of T cells

Intravascular T cells were labeled in vivo by intravenous (i.v.) injection of 1 μg PE conjugated antibodies against a T cell marker (CD90.2) 5-10 minutes before sacrificing the mice as previously described[101-104]. In some experiments, in vivo labeling was done by antibodies against the CD4 molecule (clone RM4-4, eBioscience) followed by ex-vivo staining for the CD4 marker using a different non cross blocking clone (RM4-5, Invitrogen).

Preparation of single cell suspensions

Lungs were perfused with 5ml of PBS via injection through the right ventricle. The perfused lungs were harvested into HEPES buffer containing liberase blendzyme 3 (Roche) and DNAse (Sigma-Aldrich). The lungs were then minced into small pieces using the gentleMacs^{TM} dissociator (Miltenyi Biotec) and incubated at 37°C for 30 min, followed by homogenization with the gentleMacs^{TM} dissociator. The single cell suspensions were then filtered using a cell

strainer. Single cell suspensions of spleens and pLNs were prepared by crushing the tissues between two glass slides. The cells were filtered using cell strainers and suspended in FACs buffer (PBS containing 2.5% fetal bovine serum and 0.1% NaN_3). For intracellular cytokine detection, incubation steps were performed in media/buffers containing Brefeldin A (Sigma-Aldrich, 10 μg/ml). For CXCR5 staining, lung cells were isolated using the enzyme free cell dissociation buffer (Invitrogen).

Cell enrichment, sorting and adoptive transfer

For adoptive transfer experiments, CD4 T cells were negatively enriched to >95% purity from spleens, pLNs and/or lungs using Miltenyi Biotec magnetic micro-beads and subsequent column purification was performed according to the manufacturer's protocol. In some cases, the negatively enriched cells were stained with anti-mouse PD-1 and anti-mouse KLRG1 antibodies (Biolegend) and sorted on a cell sorter (FACSAria, BD Bioscience). The enriched or sorted cells were transferred with or without carboxyfluorescein succinimidyl ester (CFSE) labeling into naïve or infected mice. For recall experiments, polyclonal CD4 T cells expressing PD-1 or KLRG1 were sorted from donor B6.PL (CD45.2 x CD90.1) mice 154 days post-infection with Mtb. An aliquot of sorted cells stained with ESAT-6-tetramers and injected cells were normalized to the number of ESAT-6-specific cells of which an equivalent of 5×10^4 cells were injected into naïve B6.SJL mice. Recipient mice were rested for 10 days and then challenged with low dose aerosol Mtb for 28 days.

Detection of Mtb-specific CD4 T cells

MHC class II tetramers containing amino acids 4 to 17 of the early-secreted antigenic target 6kD (ESAT-6) of Mtb were used to detect Mtb-specific CD4 T cells. Drosophila S2 cell

line transfected with pRMHa-3 vector containing the sequence for the stimulatory residues of ESAT-6 protein (QQWNFAGIEAAASA) of Mtb was a kind gift from Dr. Marc Jenkins, University of Minnesota. Production of the peptide:I-A^b monomeric molecules, and tetramerization of biotinylated peptide:I-A^b with PE or Allophycocyanin fluorophores (Prozyme), was performed as previously described[105]. In addition, Allophycocyanin conjugated tetramers (ESAT-6_{4-17}:I-A^b) were obtained from the National Institutes of Health Tetramer Core Facility. Single cell lymphocyte preparations were stained at saturating concentrations with the tetramers and incubated at room temperature for 1hr.

Cell-surface, intracellular cytokine and transcription factor staining

Fc receptors were blocked with purified anti-mouse CD16/32 (2.4G2, BD). Cells were suspended in FACS buffer and stained at saturating conditions with the anti-mouse monoclonal antibodies against CD3 (145-2C11, eBioscience), CD4 (RM4-5 Invitrogen), CD44 (1M7, eBioscience), CD8 (53-6.7, eBioscience), PD-1 (RMP1-30, Biolegend), KLRG1 (2F1, Biolegend), Ly6C (HK1.4, eBioscience), CD62L (MEL-14, eBioscience), CD127 (A7R34, eBioscience) and CD43 (S7, BD Biosciences). To exclude cells that may non-specifically bind to the tetramers, antibodies against non T cell markers: F4/80 (BM8, eBioscience), CD19 (eBio1D3, eBioscience), CD11c (N418, eBioscience), and CD11b (M1/70, eBioscience) were included in a dump channel. All staining for surface markers was done at 4°C for 30 minutes, except for CXCR3 (CXCR3-173, eBioscience), CXCR5 (2G8, BD Biosciences) and CCR7 (4B12, eBioscience) staining that was done at room temperature for 1 hour. Samples were fixed in PBS containing 2% paraformaldehyde.

Following surface staining, cells were fixed, permeabilized and stained with antibodies against intracellular markers using eBioscience fixation/permeabilization and permeabilization

buffers. For detection of inducible IFN-γ, TNF and IL-2, single cell suspensions were stimulated in vitro with $ESAT_{4-17}$ peptide (5μg/ml final concentration) or anti-CD3ε (145-2C11, BD Bioscience) and CD28 (37.51, BD Bioscience), (referred to here as anti-CD3/28) at a final concentration of 0.03μg/ml anti-CD3ε and 0.5μg/ml anti-CD28. The cells were cultured for 4 h in complete growth medium (RPMI 1640 supplemented with 10% FCS, 2 mM L-glutamine, 10 mM HEPES, 0.5 μM 2-ME, 100 U/ml penicillin, and 100 μg/ml streptomycin). Cells were washed, stained with antibodies against surface markers, permeabilized and fixed as described above. The cells were then stained using anti-mouse IFN-γ (XMG1.2, BD), anti-mouse IL-2 (JES6-5H4, Biolegend), anti-mouse TNF (MP6-XT22, eBioscience), Ki67 (SolA15, eBioscience), anti-mouse T-bet (4B10, Biolegend) and or anti-mouse Bcl6 (K112-91, BD). The cells were incubated at 4°C for 30 minutes, washed, re-suspended in PBS and analyzed by flow cytometry. In some experiments, 4 hours prior to harvest of mice for detection of direct ex vivo IFN-γ, mice were injected with Cyclosporine A (R&D Systems) intraperitoneally. Cyclosporine A (R&D Systems) was diluted in olive oil and mice were injected in 200ul volume, at a dose of 25mg/kg body weight.

RNA isolation, RNA sequencing and RNA data analysis

Lung single cells suspensions were made and stained with MHCII restricted tetramers in the presence of 1μg/ml Cyclosporine A (R&D Systems) to prevent tetramer-mediated activation of T cells. The cells were sorted using the BD-Aria directly into a buffer containing trizol. Samples were shipped to Expression Analysis (Durham, NC), RNA was isolated and amplified linearly followed by RNA sequencing. RNASeq data were analyzed at the Institute for Systems Biology (ISB) (Seattle, WA). In brief the Spliced Transcripts Alignment to a Reference (STAR) tool was used to map the RNASeq reads to University of California Santa Cruz (UCSC) mouse

genome. Aligned reads were sorted and mapped to transcripts and counts were output into a matrix using htseq-count. Quality control of samples was conducted by ensuring biological replicates clustered together more closely than samples from other test conditions using Principal Component Analysis (PCA). Differentially expressed genes were discovered by inputting the counts matrix into the DESeq2 package in R with Benjamini-Hochberg corrected p-values less than or equal to 0.05 and fold-change greater than or equal to 2.

Western blot analysis

CD4 T cells were purified by negative enrichment from WT and $ICOS^{-/-}$ mixed bone marrow chimeric mice. Cells were stained with anti-mouse PD-1, KLRG1 and the congenic markers for WT and $ICOS^{-/-}$ cells. $PD\text{-}1^{+}$and $KLRG1^{+}$ cells of WT or $ICOS^{-/-}$ origin were sorted and lysed for protein analysis by western blotting following standard techniques. Briefly nitrocellulose membranes were probed rabbit anti-phospho-Akt and rabbit anti-pan-Akt (Cell Signaling Technology) or rabbit anti-mouse beta-actin1-HRP antibody (Jackson ImmunoResearch). A secondary rat anti-rabbit-HRP antibody (Jackson ImmunoResearch) was used to detect the primary antibodies.

Data acquisition and analysis

Flow data was acquired using the BD LSRII flow cytometer and analyzed using FlowJo software (Tree Star). Data in here is represented as mean ± standard error of mean (SEM) and statistical analysis and graphical representation of data was done using GraphPad Prism software. Statistical significance was determined by unpaired two tailed Student`s t test, except for survival curves where the Mantel-Cox log rank test. The p values herein are denoted as $^{*}p \leq 0.05$, $^{**}p \leq 0.005$, $^{***}p \leq 0.0005$ and $^{****}p \leq 0.0001$.

Chapter III: Maintenance of antigen-specific CD4 T cells during chronic tuberculosis

Introduction

Despite over 80 years of global immunization with the attenuated *Mycobacterium bovis* Bacille Calmette-Guerin (BCG), TB remains a massive international health emergency, with ~ 9 million new cases of active disease and over a million deaths annually[10]. While BCG vaccination confers limited protection to infants and prevents dissemination especially into the brain and the ensuing TB meningitis, its efficacy in adults is quite limited. Furthermore BCG induced immunity wanes over time[16]. An effective vaccine is thus urgently needed, but achieving this goal has proven to be exceptionally difficult. This difficulty is highlighted by the results of a recent clinical efficacy trial since BCG itself was introduced, which showed that the vaccine candidate (MVA-85A) provided no protection beyond the very limited immunity conferred by BCG alone[94].

CD4 T cells, especially Th1 cells expressing the T-Box transcription factor TBX21 (T-bet) and having the capacity to produce the immune modulatory cytokine IFN-γ, are critical for immunity against Mtb the bacterium that causes TB. In support of the critical role Th1 cells serve to control tuberculosis, mice lacking CD4 T cells, IFN-γ, or IL-12 signaling (a pathway required for Th1 development), are profoundly susceptible to Mtb infection[50,53,54,89]. Likewise, humans with genetic deficiencies in IFN-γ or IL-12 signaling, as well as HIV-infected individuals depleted of CD4 T cells, are severely restricted in their ability to contain mycobacterial infections, including TB[15,52].

Due to the central role of T cells and IFN-γ in immunity, a common goal for all of the current TB vaccine candidates is to increase the number of Mtb-specific and IFN-γ producing T cells or atleast induce cells with the potential to rapidly differentiate into Th1 cells once an

individual is exposed to Mtb. As it has not yet been conclusively demonstrated that the immune system can clear Mtb and induce sterilizing immunity, it is imperative that a successful vaccine candidate induce a long-lived immune response[19,29,30]. To achieve this we need to better understand how CD4 T cells are induced and maintained during TB and identify the pathways that promote this maintenance.

Recently it was shown that Mtb-specific Th1 cells are heterogeneous and can be clustered into subsets with distinct functional properties[106]. Mtb-specific CD4 T cells expressing the inhibitory receptor KLRG1 exhibited the greatest capacity to produce the immune modulatory Th1 cytokines IFN-γ and TNF after in vitro stimulation. These cells represent terminally differentiated Th1 cells, as upon transfer into a second Mtb-infected host they proliferate poorly, maintain their KLRG1$^+$ phenotype, and are short-lived. In contrast, a second population of Mtb-specific CD4 T cells expresses the inhibitory receptor PD-1, but not KLRG1. These PD-1$^+$ cells are less able to produce IFN-γ than their KLRG1$^+$ counterparts. When transferred into infected hosts, they proliferate robustly, are maintained at high numbers, and have the capacity to differentiate into KLRG1$^+$ cells. These studies suggested that PD-1$^+$ CD4 T cells are critical for maintaining the Mtb-specific Th1 response during chronic infection. Importantly, two other recent studies suggested that vaccines with a high propensity to induce antigen-specific CD4 T cells expressing PD-1 confer greater and longer lasting protection than vaccines (such as BCG) that induce higher numbers of fully differentiated KLRG1$^+$ Th1 cells[88,107].

Further highlighting the role of PD-1$^+$ cells and PD-1 expression, genetic deficiency of PD-1 leads to hypersusceptibility to TB[108,109]. Given the emerging importance of the PD-1$^+$ CD4 T cells and PD-1 expression in mediating and maintaining immunity against Mtb, we sought to more fully define the phenotype and functions of CD4 T cells that express PD-1 during TB. We

further sought to elucidate the molecular pathways that promote its induction and maintenance. Identification of these pathways can provide potential novel intervention strategies in the ongoing efforts to rationally design new vaccines against tuberculosis.

Mtb-specific CD4 T cells are subjected to chronic stimulation by antigen

We used MHCII restricted tetramers to track and characterize endogenous CD4 T cells recognizing ESAT-$6_{4\text{-}17}$:I-A^b, an immunodominant CD4 T cell antigen in mice and humans[42,110]. Following infection with a low dose of aerosolized Mtb, mycobacteria replicate robustly and accumulate in the lungs until day 21 post-infection[54] (Fig. 3.1A). Concomitant with the Mtb-specific T cell response, the lung bacterial burden plateaus at ~10^6 CFU and is maintained at this level for at least 300 days. ESAT-6-specific CD4 T cells can first be reliably detected in the lungs at ~day 16 post-infection, and thereafter rapidly expand in numbers.

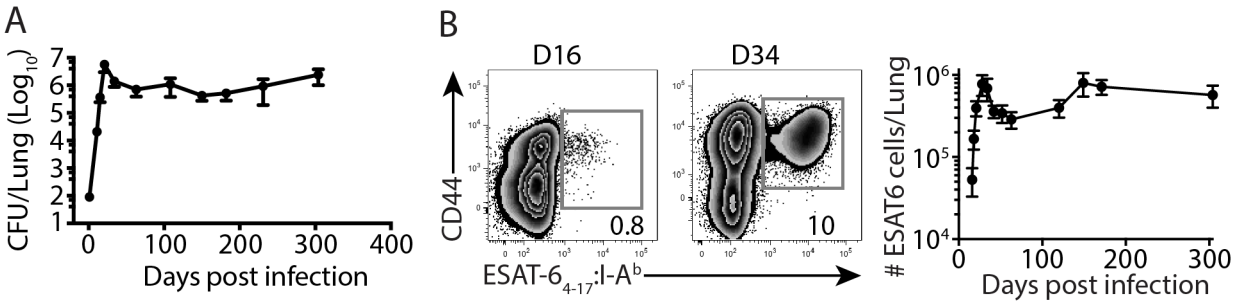

Figure 3.1: Live Mtb and Mtb-specific CD4 T cells co-exist in the lung tissue. B6 mice were infected with low dose aerosolized Mtb (~100cfu). A) Kinetics of lung bacterial burdens. B) Left panel representative flow cytometry plots depicts the frequency of ESAT-6 tetramer binding cells among lung CD4 T cells at the time points shown. The right panel shows the total number of ESAT-6 specific CD4 T cells recovered from the lungs of mice. Data represent 2 independent experiments with 4-5 mice per group and per time point. Data are presented as mean ± SEM.

At day 34 post-infection, ESAT-6-specific CD4 T cells comprise up to 10% of the total CD4 T cells in the lungs, peaking at ~10^6 total cells (Fig. 3.1B). After a modest contraction phase, this population plateaus at 3-10 x 10^5 cells until at least day 300. To test whether the high numbers of ESAT-6-specific CD4 T cells in the lungs correlated with enhanced proliferation, we

evaluated Ki67 expression. Most ESAT-6-specific but not naïve CD44^{low} CD4 T cells recovered from the lungs were Ki67^{+}, suggesting their active division (Fig. 3.2A).

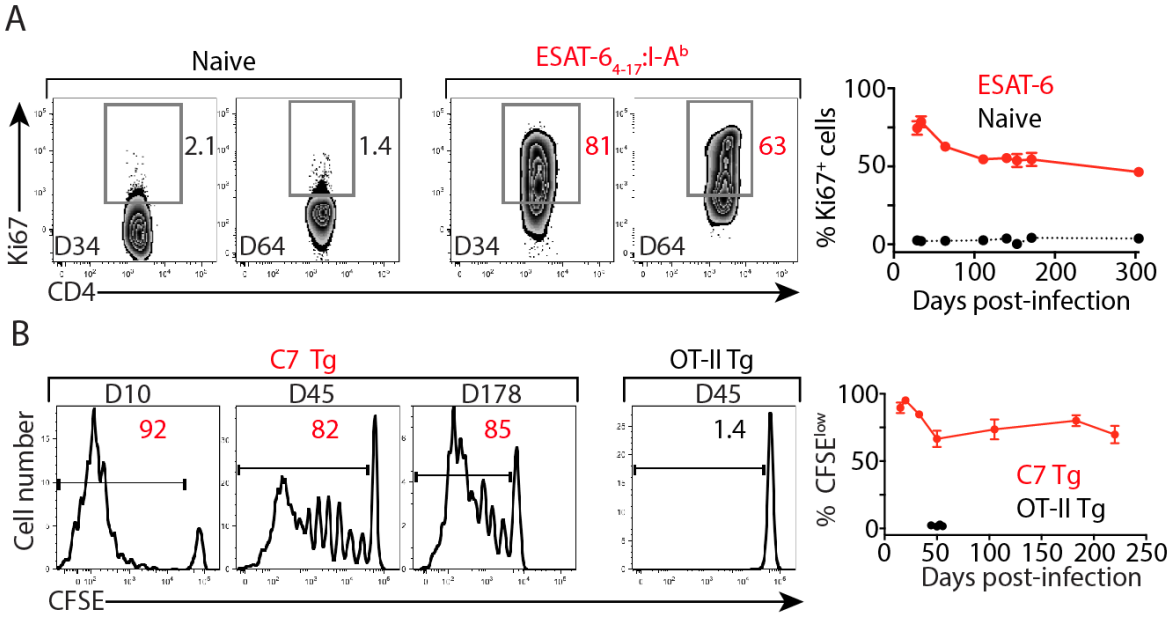

Figure 3.2: Mtb-specific CD4 T cells are characterized by extensive proliferation. A) Representative flow cytometry plots and kinetics graph depicts Ki67 expression by lung naïve CD44^{low} and ESAT-6 tetramer binding CD4 T cells. B) Naïve TCR transgenic CD4 T cells from ESAT-6 (C7 Tg) or Ovalbumin (OT-II Tg) mice were CFSE labeled and adoptively transferred into mice infected with Mtb at various time points prior. 5 days later, donor cells were isolated from the lungs and analyzed for CFSE dilution. The time points shown are the days post-Mtb infection when donor cells were transferred into mice. Data are representative of two independent experiments with 3-5 mice per group and per time point. Data are presented as mean ± SEM.

Consistent with a previous finding that ESAT-6-specific T cells proliferate throughout chronic infection[106], we observed that the percentage of tetramer-binding T cells expressing Ki67 was highest during early infection (~80% at day 34) and continued to comprise a substantial population even at 300 days. To test the antigen dependence of this proliferation, we transferred CFSE -labeled ESAT-6-specific (C7 Tg), or chicken ovalbumin-specific (OT-II Tg) CD4 T cells from TCR Tg mice into Mtb-infected hosts. The proliferation donor Tg T cells as measured by CFSE dilution mirrored our previous results with Ki67 expression in endogenous tetramer-binding cells; proliferation peaked in the first 4 weeks but remained at high levels throughout

chronic infection. Importantly, the inflammatory milieu induced by Mtb infection did not drive bystander CD4 T cell proliferation (Fig. 3.2B).

Using intracellular cytokine staining on T cells directly ex vivo without in vitro re-stimulation[48], we detected IFN-γ in CD44^{hi} tetramer binding and CD44^{hi} non-tetramer binding cells but not in CD44^{low} CD4 T cells (Fig. 3.3A). Furthermore, IFN-γ was not detected using an isotype marched control (Fig. 3.3B).

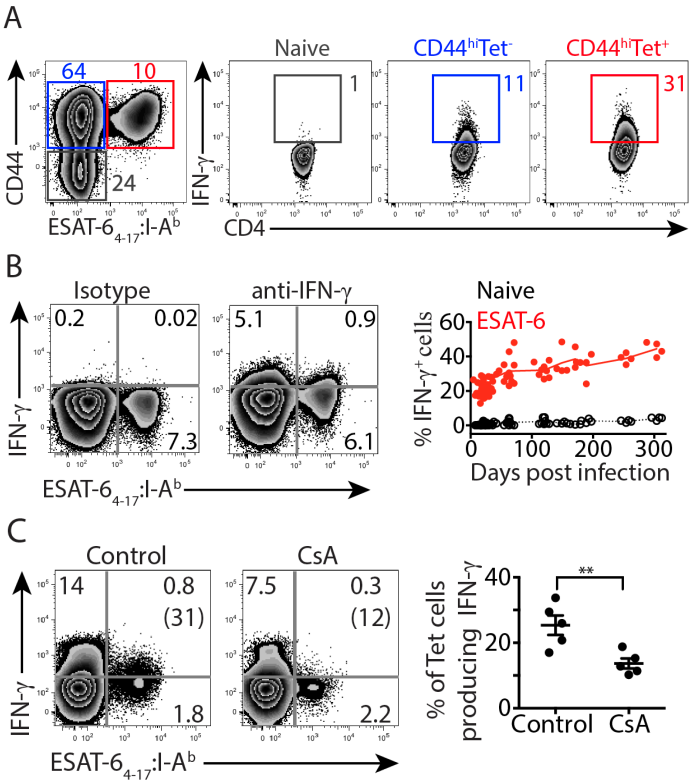

Figure 3.3: Mtb-specific CD4 T cells produce IFN-γ in vivo in a TCR signaling dependent manner. A) Representative flow cytometry plots denote gating strategy to identify lung naïve CD44^{low} (gray), CD44^{hi} non-tetramer binding (blue) and CD44^{hi} tetramer binding lung CD4 T cells and their respective ex vivo IFN-γ production 140 days post-infection. Numbers in plots depicts the percentage of cells in the respective gates. B) Representative flow cytometry plots depicts IFN-γ and isotype marched control staining of lung CD4 T cells 73 days post Mtb-infection. The right panel shows percentage of ESAT-6 tetramer binding and naïve CD44^{low} cells producing IFN-γ in vivo. C) Infected mice were treated with vehicle control or Cyclosporine A (CsA) for 4hrs and analyzed for ex vivo IFN-γ production. Numbers in parentheses depicts the frequency of ESAT-6 tetramer binding cells producing IFN-γ and are shown in the cumulative total graph on the right. Results represent 2 independent experiments with 4-5 mice per group and per time point. Data are presented as mean ± SEM **P <0.005

At 16 days post-infection, ~20% of ESAT-6-specific T cells recovered from the lungs produced IFN-γ, and this percentage gradually increased to ~40% on day 300 (Fig. 3.3B). IFN-γ production was dependent on TCR signaling in at least half of these cells; as CsA, an inhibitor of proximal TCR-mediated signaling[111]) administered four hours prior to euthanasia blocked IFN-γ production in ~50% of the cells (Fig. 3.3C).

Taken together, our results indicate that ESAT-6 derived antigen is readily available for T cell recognition throughout persistent infection. This recognition is frequent and high numbers of ESAT-6-specific T cells are maintained in the lung and co-exist with high levels of cognate antigen.

Mtb-specific CD4 T cells cluster into functionally distinct populations

ESAT-6-specific T cells in the lung can be separated into two distinct populations based on their expression of the inhibitory receptors PD-1 and KLRG1 (Fig. 3.4A). Consistent with previous studies[106], we found that KLRG1$^+$ cells produced more IFN-γ and TNF than their PD-1$^+$ counterparts after in vitro stimulation with ESAT-6 peptide or anti-CD3 and anti-CD28 antibodies (Fig. 3.4B). In contrast, KLRG1$^+$ cells produced very little IL-2 with almost all of the detected IL-2 being produced by a population of polyfunctional KLRG1$^-$PD-1$^+$ cells that also co-produced IFN-γ and TNF (Fig. 3.4C). We could not readily detect IFN-γ and TNF using the direct ex vivo approach, however, consistent with the in vitro restimulation data, a higher percentage of KLRG1$^+$ than PD-1$^+$ CD4 T cells within the ESAT-6 tetramer-binding population produced IFN-γ when assessed immediately after isolation from the lung (Fig. 3.4D). Furthermore, KLRG1$^+$ cells expressed high levels of the Th1 defining transcription factor T-bet whereas PD-1$^+$ cells had intermediate T-bet levels (Fig. 3.4E). We also assessed the proliferation of these populations of Mtb-specific CD4 T cells by staining for Ki67.

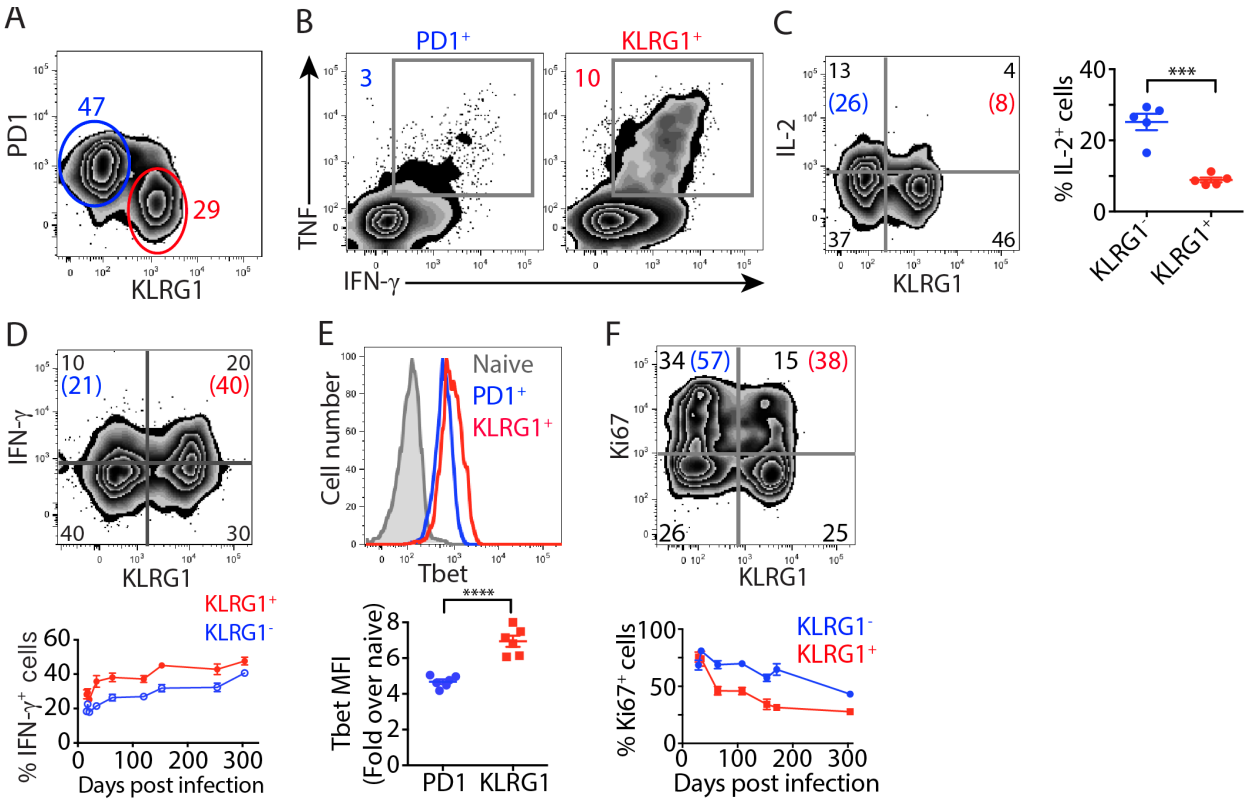

Figure 3.4: Mtb-specific CD4 T cells cluster into functionally distinct populations. A) Representative flow cytometry plot depicts PD-1 and KLRG1 expression by lung ESAT-6-tetramer binding CD4 T cells 90 days post Mtb infection. B) Lung CD4 T cells from day 140 Mtb infected mice were in vitro stimulated with ESAT-$6_{4\text{-}17}$ peptide. Representative flow cytometry plots depicts IFN-γ and TNF production by PD-1^+ and KLRG1^+ CD4 T cells. C) CD4 T cells identified in panel B were gated on IFN-γ and TNF double producers and analyzed for IL-2 production. Numbers in parentheses in representative depicts the percentage of KLRG1^-PD-1^+ (blue) or KLRG1^+PD-1^- (red) that produce IL-2 and are shown in the right panel. D) Representative flow cytometry plot depicts direct ex vivo IFN-γ production and KLRG1 expression. Numbers in parentheses represent the percentage of KLRG1^- or KLRG1^+ cells that produce IFN-γ and are depicted in the bottom panel. E) Representative histograms depict T-bet expression by lung CD4 T cells clustered as naïve (gray) or ESAT-6 tetramer binding PD-1^+ (blue) or KLRG1^+ (red). The bottom panel shows cumulative T-bet expression as mean fluorescent intensity (MFI) by PD-1^+ and KLRG1^+ ESAT-6 tetramer binding depicted as fold increase over naïve cells. F) ESAT-6 tetramer binding CD4 T cells were analyzed for Ki67 expression. Numbers in parentheses represent the percentage of KLRG1^- or KLRG1^+ cells that express Ki67 and are depicted in the panel below. Data are representative of 3 independent experiments with 4-5 mice per group and per time point. ***P <0.0005 and ****P <0.0001

We found that PD-1^+ ESAT-6-specific CD4 T cells expressed more Ki67 than KLRG1^+ cells at time points beyond 28 days post-infection (Fig. 3.4F) indicating enhanced proliferation by the PD-1^+ population. Overall these results indicate that although ESAT-6-specific T cells

expressing KLRG1 are the main in vivo producers of IFN-γ, PD-1$^+$ cells have a higher capacity to produce IL-2 and undergo more extensive proliferation.

Mtb-specific PD-1$^+$ CD4 T cells share features with T follicular helper (Tfh) cells

Mtb-specific PD-1$^+$ CD4 T cells represent a self-renewing progenitor population[106] and there is growing evidence that these cells play a central role in protective immunity to TB[88,102,107]. Thus, we sought to characterize these cells more extensively.

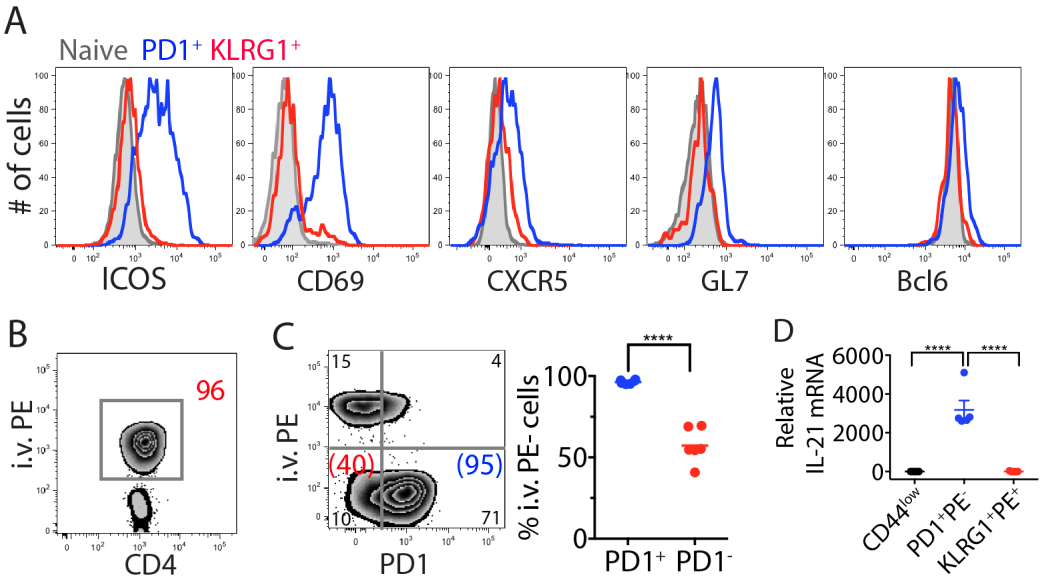

Figure 3.5: Mtb-specific PD-1$^+$ CD4 T cells exhibit characteristics of Tfh cells. A) Lung CD4 T cells from ~day 60 Mtb infected mice were clustered as naïve CD44^{low} (gray), ESAT-6 tet$^+$ PD-1$^+$ (blue) or KLRG1$^+$ (red) and analyzed for the indicated markers. B) Anti-CD90.2 T cell specific antibodies conjugated to PE were i.v. injected into uninfected mice 10 minutes before euthanasia. Representative flow cytometry plot depicts the percentage of CD4 T cells that were intravenously labeled. C) Representative flow cytometry plot show i.v. PE labeling in the context of PD-1 expression for lung ESAT-6-specific CD4 T cells 90 days post Mtb infection. Numbers in parentheses depict the percentage of PD-1$^+$KLRG1$^-$ (blue) or PD-1$^-$KLRG1$^+$ (red) ESAT-6 tet$^+$ cells protected from i.v. labeling and are shown on the right panel. D) Naïve CD44^{low}, PD-1$^+$ PE$^-$ or KLRG1$^+$PE$^+$ ESAT-6-tet$^+$ CD4 T cells were sorted from the lungs of day 120 infected mice and analyzed for IL-21 by RNA sequencing. Data in A-C are representative of at least 3 independent experiments with 3-5 mice per group. Data in D is from one experiment of 4 pooled mice per replicate, with a total of 4-5 replicates per group. Statistical significance was determined by Student`s *t* test with a ****P <0.0005

Most PD-1$^+$ESAT-6-specific CD4 T cells co-expressed the inducible co-stimulatory molecule (ICOS) and CD69, whereas a smaller fraction co-expressed the chemokine receptor CXCR5 and

the T and B cell activation marker GL7 (Fig. 3.5A). In contrast, tetramer-binding KLRG1$^+$ T cells did not express these markers. Finally, compared to KLRG1$^+$ or naïve CD44^{low} CD4 T cells, PD-1$^+$ ESAT-6-specific CD4 T cells reproducibly expressed slightly higher levels of the Tfh defining transcription factor Bcl6.

To localize PD-1$^+$ and KLRG1$^+$ CD4 T cells within the lung, PE conjugated T cell specific antibodies were injected i.v. to mice shortly before euthanasia. This technique accurately labels cells resident in the in the tissue parenchyma, including during Mtb infection, excluding those within the lung parenchyma[101,102 103,104]. In agreement with a previous report[103], $>$ 95% of CD4 T cells isolated from the lungs of uninfected mice were labeled with intravenous antibodies indicating their location within the lung-associated blood vessels (Fig. 3.5B). Interestingly, we found that the vast majority of ESAT-6-specific PD-1$^+$KLRG1$^-$ cells (>95%), but only ~50% of the PD-1$^-$KLRG1$^+$ cells, were resident in the lung parenchyma (Fig. 3.5C).

We also sorted naïve and PD-1$^+$PE$^-$ or KLRG1$^+$PE$^+$ ESAT-6-specific CD4 T cells from the lungs of mice infected 120 days earlier and analyzed IL-21 expression using RNA sequencing (Fig. 3.5D). Remarkably tissue resident cells (PD-1$^+$PE$^-$) expressed more IL-21 compared to the lung-vasculature associated cells (KLRG1$^+$PE$^+$) (Fig. 3.5D).

In summary, PD-1$^+$ Mtb-specific T cells share phenotypic features with Tfh cells and are located in the lung parenchyma. In contrast, at least 50% of the terminally differentiated KLRG1$^+$ Th1 cells reside within the lung-associated vasculature.

Mtb-specific PD-1$^+$ CD4 T cells exhibit characteristics of central memory T cells

While PD-1$^+$ Mtb-specific CD4 T cells have Tfh-like features, further analysis of cell surface and intracellular molecules revealed a mixed profile with expression of effector and memory markers (Fig. 3.6A). CD62L expression reflected an effector phenotype and was low in

both PD-1$^+$ and KLRG1$^+$ tetramer-binding populations. Although CCR7 and CD127 expression was slightly higher amongst PD-1$^+$ compared to KLRG1$^+$ cells, this expression did not approach the levels usually observed on central memory cells that develop when antigen is cleared. In contrast, as we had previously observed for ICOS and CD69 (Fig 3.5A), CXCR3, Ly6C, and CD43 showed markedly different expression patterns on these two populations (Fig. 3.6A). Most ESAT-6-specific PD-1$^+$ cells were CXCR3$^+$, Ly6C$^-$ and CD43$^+$, whereas most KLRG1$^+$ cells exhibited the opposite phenotype.

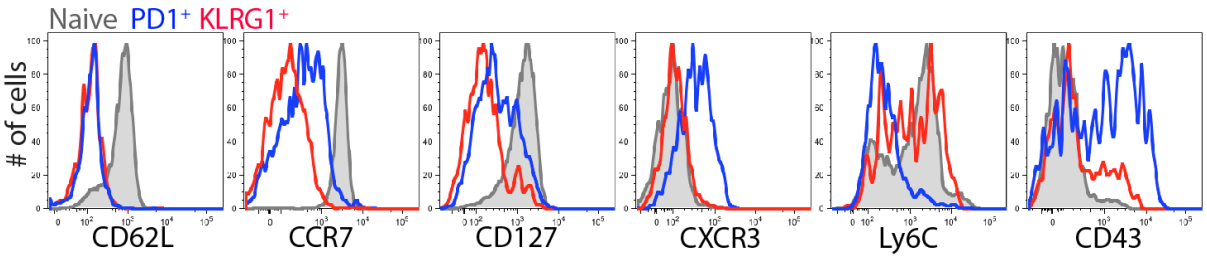

Figure 3.6: ESAT-6-specific PD-1$^+$ CD4 T cells express molecules associated memory CD4 T cells: Lung CD4 T cells from ~day 120 Mtb infected mice were clustered as naïve CD44^{low} (gray histograms), ESAT-6 tetramer binding PD-1$^+$ (blue histograms) or ESAT-6 tetramer binding KLRG1$^+$ cells (red histograms) and analyzed for expression of the indicated markers. Results represent at least 2 independent experiments with 4-5 mice per group.

In addition, PD-1$^+$ cells, like memory cells[112], were intermediate for T-bet expression, whereas KLRG1$^+$ cells, like Th1 effector cells, exhibited high T-bet expression (Fig. 3.4E). These results thus reveal that ESAT-6-specific PD-1$^+$ CD4 T cells, while expressing some markers of effector T cells, also displayed features of memory T cells. In contrast, their KLRG1$^+$ counterparts exhibited characteristics of terminally differentiated Th1 cells.

Memory T cells are defined as antigen-specific T cells that persist after antigen withdrawal and mount a rapid recall response to a subsequent challenge[113,114]. To address whether PD-1$^+$ cells can survive in the absence of ongoing antigenic stimulation, we sorted (to >95% purity) polyclonal PD-1$^+$ and KLRG1$^+$ CD4 T cells from the lungs of Mtb infected mice and transferred them into uninfected hosts (Fig. 3.7A). Recipient mice were maintained on

antibiotic treated water to prevent infection from occurring via the transferred cells, and no bacteria were detected in the spleen, liver, or lungs of the host mice.

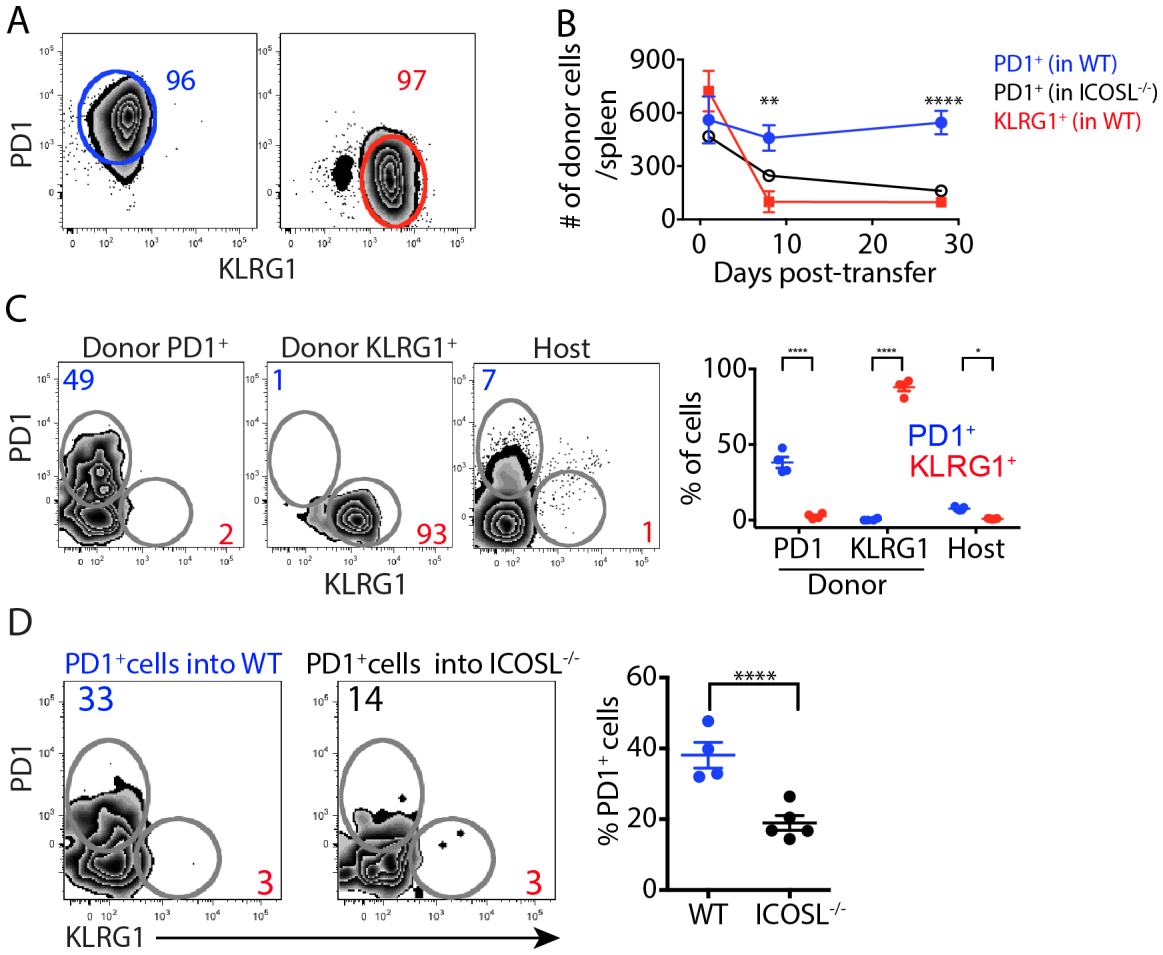

Figure 3.7: PD-1$^+$ CD4 T can survive in the absence of antigen: A) Post sort purity of polyclonal PD-1$^+$ and KLRG1$^+$ cells sorted from day 120 Mtb infected mice. B) PD-1$^+$ cells sorted in panel A were transferred into uninfected WT (blue) and ICOSL$^{-/-}$ (black) mice while KLRG1$^+$ cells were transferred only into uninfected WT mice (red). The graph depicts the number of donor cells recovered from the spleens of host mice. C) Representative flow cytometry plots and cumulative graphs depicts PD-1 and KLRG1 expression by donor cells transferred into uninfected WT mice 28 days prior as PD-1$^+$ or KLRG1$^+$. D) Representative flow cytometry plots and cumulative graph show PD-1 expression by donor cells transferred into uninfected WT or ICOSL$^{-/-}$ hosts 28 days prior as PD-1$^+$ cells. Donor cells were transferred into WT mice as PD-1$^+$ or KLRG1$^+$ in 2 independent experiments with 3-5 mice per group and per time point, whereas transfer of PD-1$^+$ into ICOSL$^{-/-}$ was done once with 4-5 mice per group and per time point. *P <0.05, **P <0.005, ***P <0.0005, ****P <0.0001

At day 1 post transfer, we recovered equivalent numbers of donor PD-1$^+$ and KLRG1$^+$ cells from spleens indicating an equivalent take rate. Although transferred PD-1$^+$ CD4 T cells

were maintained at similar numbers throughout the 28 days of the experiment, KLRG1$^+$ cells underwent attrition, and by day 8, five-fold fewer cells were recovered (Fig. 3.7B). Despite maintaining their numbers, about 50% of donor PD-1$^+$ CD4 T cells lost PD-1 expression by day 28 (Fig. 3.7C). Furthermore, unlike PD-1$^+$ cells transferred into Mtb-infected mice[106], none of the PD-1$^+$ donor cells differentiated into KLRG1$^+$ cells in uninfected recipients, and donor KLRG1$^+$ cells maintained their KLRG1$^+$ phenotype (Fig. 3.7C).

Because ICOS:ICOSL interactions are required to maintain central memory CD4 T cells[115], we also transferred PD-1$^+$ CD4 T cells into uninfected WT mice and ICOSL$^{-/-}$ mice. Interestingly, in the absence of ICOSL, donor PD-1$^+$ cells underwent attrition similar to transferred KLRG1$^+$ cells (Fig. 3.7B), and exhibited even lower PD-1 expression (Fig. 3.7D). These results show that while ICOSL signaling alone is capable of maintaining overall cell numbers, both antigen and ICOSL signaling contribute to optimal PD-1 expression. Furthermore, the results show that antigenic stimulation plays a primary role in driving differentiation into KLRG1$^+$ effectors and confirm previous findings that KLRG1$^+$ cells are terminally differentiated Th1 cells[106].

To determine whether PD-1$^+$ cells had the capacity to mount a robust recall response, we challenged uninfected mice that had received donor PD-1$^+$ or KLRG1$^+$ CD4 T cells 10 days prior with aerosolized Mtb. At 28 days post infection, we found that donor cells derived from PD-1$^+$ precursors had undergone robust expansion, while KLRG1$^+$ precursors had not (Fig. 3.8A). Furthermore, PD-1$^+$ progenitors had the capacity to differentiate into KLRG1$^+$ cells in response to Mtb challenge. In fact, the profile of PD-1 vs. KLRG1 expression for ESAT-6-specific CD4 T cells derived from transferred PD-1$^+$ cells was nearly identical to that for endogenous tetramer-binding CD4 T cells participating in the primary response to Mtb. Conversely, most of the

tetramer-binding cells derived from transferred KLRG1$^+$ cells retained a KLRG1$^+$ phenotype (Fig. 3.8B).

Overall these results show that despite being subjected to chronic antigenic stimulation and exhibiting some phenotypic markers of effector T cells, Mtb-specific PD-1$^+$ CD4 T cells share many features with classical memory cells. Like memory T cells they can persist in the absence of antigen and mount a robust recall response that generates a heterogeneous population of cells resembling the cells responding to a primary infection[112,115,116].

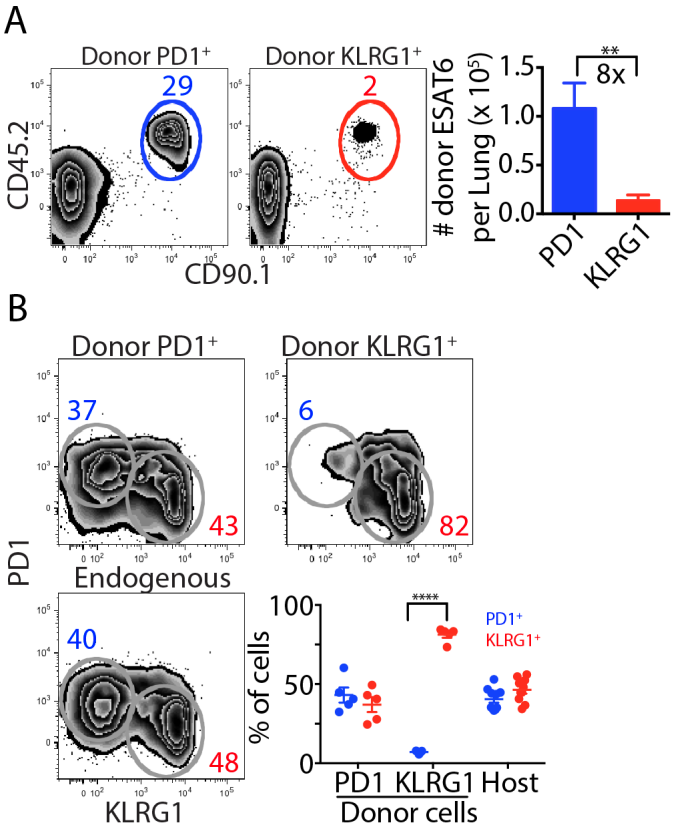

Figure 3.8: PD-1$^+$ CD4 T cells undergo enhanced recall responses. Polyclonal PD-1$^+$ and KLRG1$^+$ CD4 T cells were sorted from donor B6.PL mice ~120 days post infection and adoptively transferred into uninfected B6.SJL. Recipient mice were challenged with low dose aerosolized Mtb 10 days later. A) Representative flow cytometry plots are gated on total lung ESAT-6 tetramer binding CD4 T cells isolated from mice challenged with Mtb 28 days prior and show the proportion of donor cells transferred as PD-1$^+$ (blue) or as KLRG1$^+$ (red). The cumulative total graph depicts absolute numbers of donor cells recovered. B) Representative flow cytometry plots and cumulative graph depict expression of PD-1 and KLRG1 by ESAT-6 tetramer binding CD4 T cells transferred as donor PD-1$^+$ or KLRG1$^+$ and host cells. Data are representative of 2 independent experiments with 5 mice per group. **P≤0.005 and ****P≤0.0001.

Intrinsic ICOS expression is required to maintain Mtb-specific CD4 T cells

To determine whether ICOS:ICOSL interactions were required to maintain Mtb-specific CD4 T cells in the presence of ongoing antigenic stimulation, we reconstituted sub-lethally irradiated TCR$\beta^{-/-}\delta^{-/-}$ mice with WT and ICOS$^{-/-}$ bone marrow cells mixed in a ratio of 1:1. After immune reconstitution, the chimeric mice were infected with Mtb and the ratio of WT to ICOS$^{-/-}$ ESAT-6-specific CD4 T cells in the lungs was evaluated over time. Immediately before infection, chimeric mice had a 1:1 ratio of WT to ICOS$^{-/-}$ CD4 T cells in their blood, and this ratio did not change for naïve CD4 T cells isolated from the lungs of infected mice up to day 180 (Fig.3.9A). Interestingly, ESAT-6-specific ICOS$^{-/-}$ CD4 T cells had an early competitive advantage over WT cells; at the peak of the T cell response (~28 days post-infection) twice as many ICOS$^{-/-}$ ESAT-6-specific CD4 T cells as WT cells were recovered from the lungs. However, ICOS$^{-/-}$ CD4 T cells were compromised in their persistence during the chronic stages of infection. The ratio of ICOS$^{-/-}$ to WT CD4 T cells progressively declined and was 1:6 by 180 days post-infection (Fig. 3.9B). The enhanced early expansion and impaired maintenance of ICOS$^{-/-}$ ESAT-6-specific CD4 T cells were associated with an increased ratio of KLRG1^{+} to PD-1^{+} cells (Fig. 3.9C). Furthermore, PD-1^{+} cells efficiently phosphorylated Akt (Fig. 3.9D) and this and their IL-2 production were dependent on ICOS signaling (Fig. 3.9E).

In summary, intrinsic expression of ICOS on Mtb-specific CD4 T cells promoted Akt activation, IL-2 production, and the generation and maintenance of the self-renewing PD-1^{+} population. In the absence of ICOS-mediated signaling, robust expansion of short-lived KLRG1^{+} effectors was initially observed, but the Mtb-specific CD4 T cell response could not be sustained during chronic stages of infection.

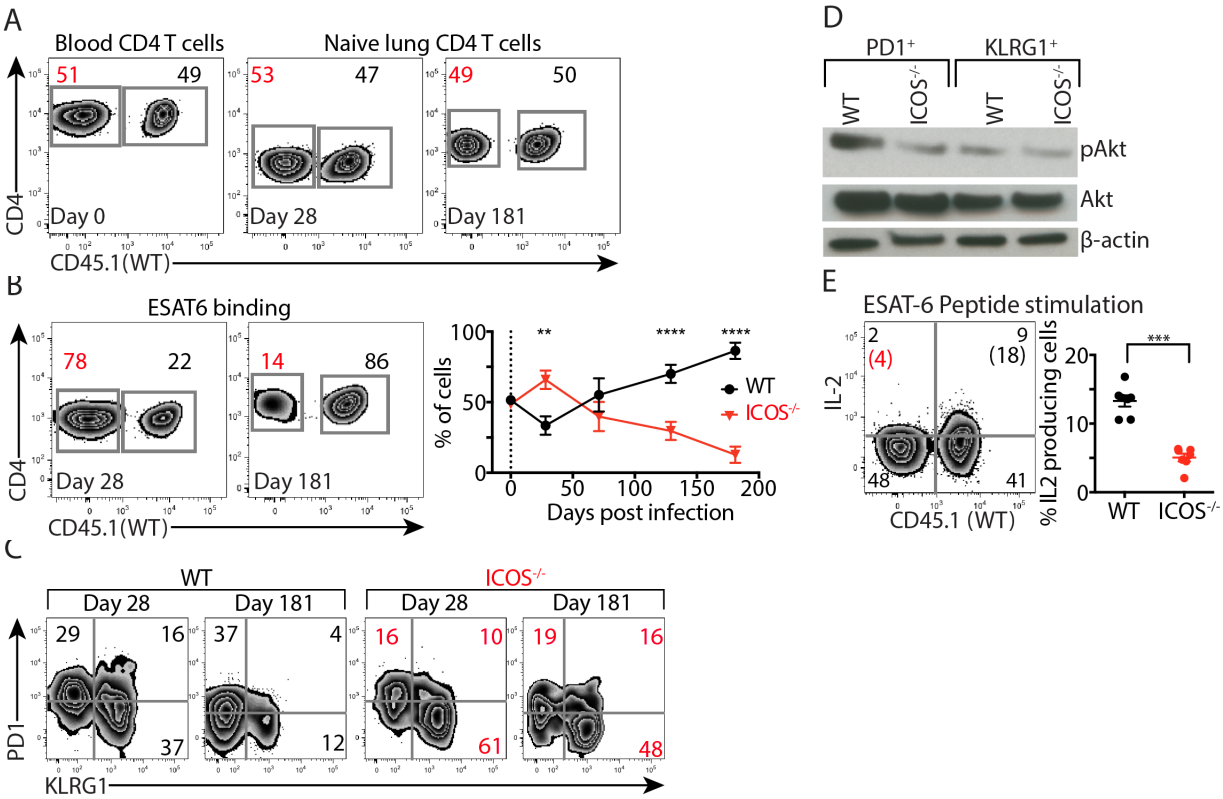

Figure 3.9: T cell intrinsic ICOS signaling is required to maintain Mtb-specific CD4 T cells. A) WT and ICOS$^{-/-}$ CD4 T cells in the blood of TCRβ$^{-/-}$δ$^{-/-}$ mice reconstituted with a 1:1 mixture of WT and ICOS$^{-/-}$ bone marrow cells 10 weeks prior (Left flow cytometry plot). The two panels on the right show the ratio of WT and ICOS$^{-/-}$ naïve CD4 T cells isolated from the lungs of mice infected at the indicated time points. B) Representative flow cytometry plots and cumulative data denote WT and ICOS$^{-/-}$ lung ESAT-6 tetramer binding CD4 T cells at the days post infection shown. C) The representative flow cytometry plots depict the expression of PD-1 and KLRG1 by WT or ICOS$^{-/-}$ ESAT-6 tetramer binding CD4 T cells at the days post infection shown. D) PD-1^{+} and KLRG1^{+} CD4 T cells of WT or ICOS$^{-/-}$ origin were sorted from chimeric mice ~70 days post infection and analyzed by western blot for phosphorylation of Akt. E) Representative flow cytometry plot denote IL-2 production by WT and ICOS$^{-/-}$ CD4 T in response to in vitro stimulation with ESAT-6$_{4-17}$ peptide ~120 days post infection. Numbers in parentheses denote percentage of WT (black) or ICOS$^{-/-}$ (red) CD4 T cells that produce IL-2 and are depicted as cumulative totals in the graph on the right. Data shown in A-C and E are representative of 3 independent experiments with 4-7 mice per group per and per time point while data in D is representative of 2 independent experiments of cells pooled from 4 mice ~70 days post infection. **P≤0.005, ***P≤0.005 and ****P≤0.0001.

B cells are not required for immunity against TB

ICOS-ICOSL signals are required for the maintenance of memory T cells after acute infections in which antigen is cleared and B cells are the primary source of ICOSL signals in this setting[117]. To determine if B cells were required for the maintenance of Mtb-specific CD4 T

cells, we infected B cell deficient ($\mu MT^{-/-}$) mice and investigated their ability to control Mtb and to induce and sustain Mtb-specific CD4 T cells. In agreement with previous reports[82], we found that $\mu MT^{-/-}$ mice controlled Mtb as well as WT mice (Fig. 3.10A) and there was no defect in their ability to induce or sustain ESAT-6-specific CD4 T cells (Fig.3.10B). Furthermore, the maintenance of ESAT-6-specific CD4 T cells with a Tfh phenotype was not defective (Fig.3.10C).

Because ICOS-ICOSL signaling, but not B cells, were required to maintain Mtb-specific CD4 T cells during TB, we investigating whether ICOSL was expressed by any non-B cell populations in the lungs of Mtb-infected mice. In contrast naïve mice where B cells are the primary source of ICOSL signals[115], we found that most cells of myeloid origin including dendritic cells and alveolar macrophages also expressed ICOSL in Mtb-infected mice (Fig. 3.11). Thus, other cell types in $\mu MT^{-/-}$ mice could potentially compensate for the lack of B cells, as the source of ICOSL signaling needed to maintain Mtb-specific CD4 T cells.

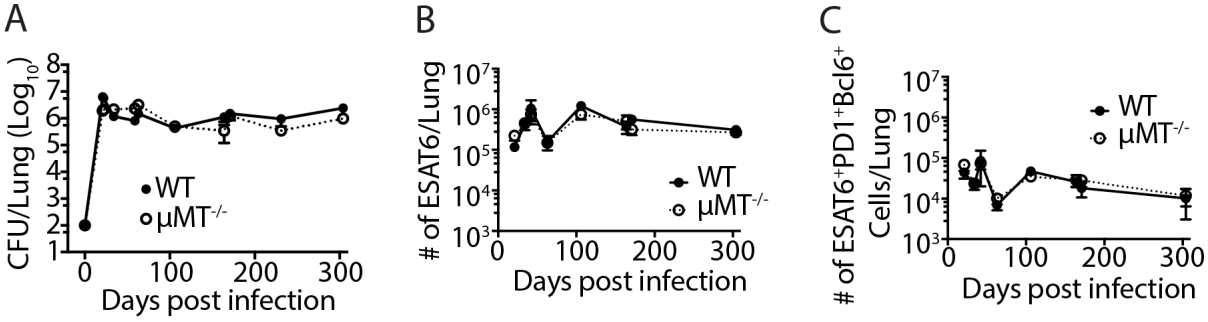

Figure 3.10: B cells are dispensable for protection and Mtb-specific CD4 T cell responses following low dose aerosol Mtb infection. A) Kinetics of lung bacterial loads in WT and $\mu MT^{-/-}$ mice infected with low dose aerosolized Mtb. B) Kinetics of lung ESAT-6 tetramer binding CD4 T cells in WT and $\mu MT^{-/-}$ mice. C) Kinetics of Tfh like ESAT-6-specific cells (co-expressing PD-1 and Bcl6). Data are representative of 2 independent experiments with 3-5 mice per group and per time point. Data are represented as mean ± SEM.

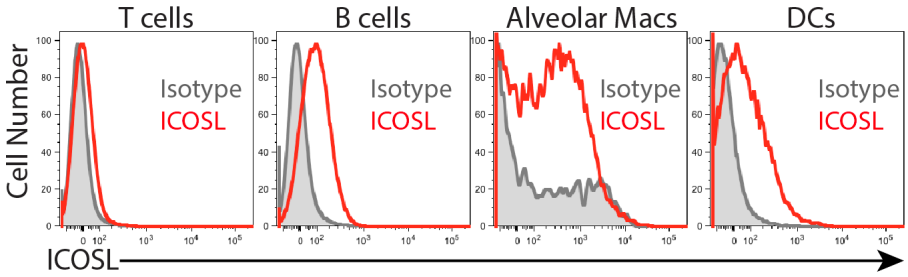

Figure 3.11: ICOSL expression in the Mtb infected lung. Representative flow cytometry plots depict ICOSL (red histograms) or isotype matched control (gray histograms) of lung cells from mice 24 days post infection. T cells were as identified as $CD3^{+}$cells, B cells as $CD19^{+}$ cells, alveolar MACs as auto-fluorescence $CD11b^{+}$ cells whereas DCs were identified as $CD11c^{+}MHCII^{+}$ cells.

B cells maintain Tfh cells in part by sustaining antigen presentation[62]. To test whether B cells play a role in antigen presentation during TB, we generated mixed bone marrow chimeric mice such that either all APCs (including B cells) were MHCII sufficient or all APCs except B cells were MHCII sufficient. We infected these mice and fount their ability to induce an ESAT-6-specific response was equivalent, whether B cells expressed MHCII molecules or not (Fig. 3.12A). Furthermore, ESAT-6-specific CD4 T cells from both groups produced equivalent amounts of IFN-γ ex vivo (Fig. 3.12B). Thus antigen-presentation by B cells is not required to maintain an IFN-γ-producing population of Mtb-specific CD4 T cells.

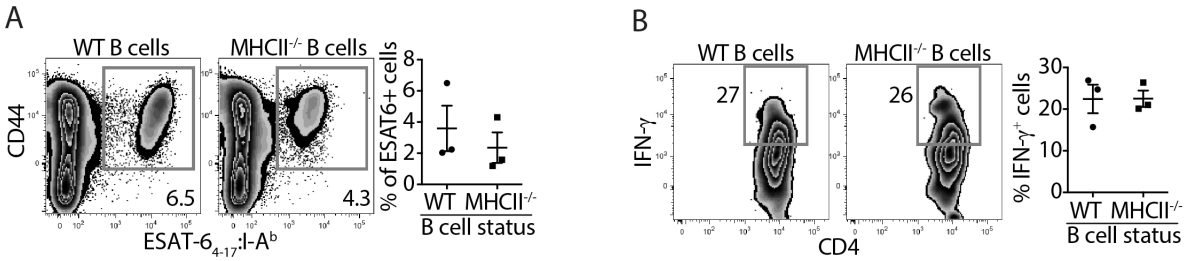

Figure 3.12: B cell antigen presentation is not required for CD4 T cell expansion and function. Mixed bone marrow chimeric mice were generated such that B cells were either of WT or $MHCII^{-/-}$ origin. These mice were then infected with Mtb for 28 days. A) Representative flow cytometry plots and cumulative graph depict the frequency of lung CD4 T cells that are specific for ESAT-6. B) Representative flow cytometry plot and cumulative graph depict the frequency of lung ESAT-6-specific CD4 T cells that produced IFN-γ directly ex vivo.

Because of the reported role of B cells in shaping the memory T cell response[115,118], we tested the effect of B cells in response to BCG vaccination. We vaccinated $\mu MT^{-/-}$ and WT mice

with BCG subcutaneously. Some mice were sacrificed ~60 days post vaccination and spleens were analyzed for the BCG specific response. The rest of the mice were challenged with Mtb. As BCG lacks ESAT-6 protein but has intact Ag85B[87], we used tetramers specific for Ag85B ($Ag85B_{240-254}$:I-A^b) to identify BCG specific CD4 T cells in the spleens of immunized mice. WT and $\mu MT^{-/-}$ mice had equivalent BCG-specific responses (Figure 3.13A), and after Mtb challenge, both showed lung bacterial burdens that were similarly reduced (by ~1 log) compared to unimmunized controls (Fig. 3.13B). Thus, B cells had no effect on the magnitude of the induced T cell response or the protective efficacy of BCG immunization.

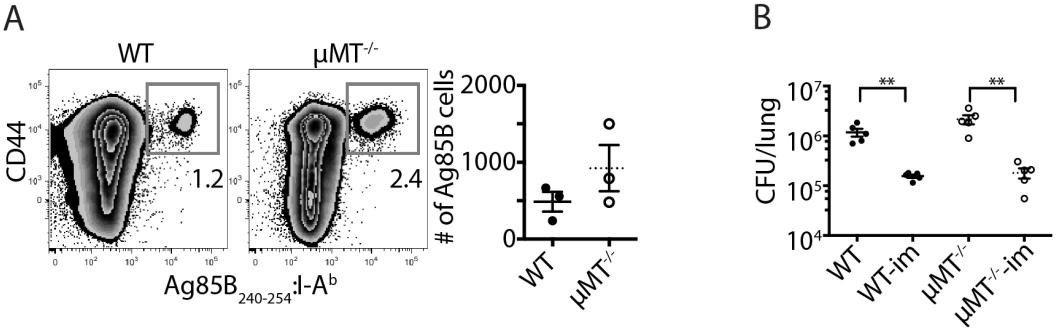

Figure 3.13: B cells have no effect on BCG immunization. A) $\mu MT^{-/-}$ and WT mice were immunized (WT-im and $\mu MT^{-/-}$-im) or left un-immunized and challenged with Mtb ~60 days later. Representative flow cytometry plots depict Ag85B-specific CD4 T cells in the spleen 60 days post vaccination. The cumulative data denotes the number of Ag85B-specific CD4 T cells recovered from the spleen. B) Lung bacterial loads in BCG immunized mice challenged with Mtb for 5 weeks. Data are from one experiment with 3 mice per group in A and 5 mice per group in B. $^{**}P < 0.005$

Intrinsic Bcl6 expression is required for Mtb-specific CD4 T cell expansion

The Tfh-associated Bcl6 transcription factor is induced in T cells by ICOS:ICOSL signaling and is required for the maintenance of central memory CD4 T cells[115,119]. To investigate the role of Bcl6 in the induction and maintenance of the CD4 T cell response during Mtb infection, we generated mixed chimeras by reconstituting lethally irradiated WT mice with WT and $Bcl6^{-/-}$ fetal liver cells. After immune reconstitution, and immediately before infection, chimeric mice had a 1:1 ratio of WT to $Bcl6^{-/-}$ CD4 T cells in their blood and this ratio was

maintained for naïve CD44^{low} CD4 T cells isolated from the lungs up to at least 44 days post Mtb infection (Fig. 3.14A).

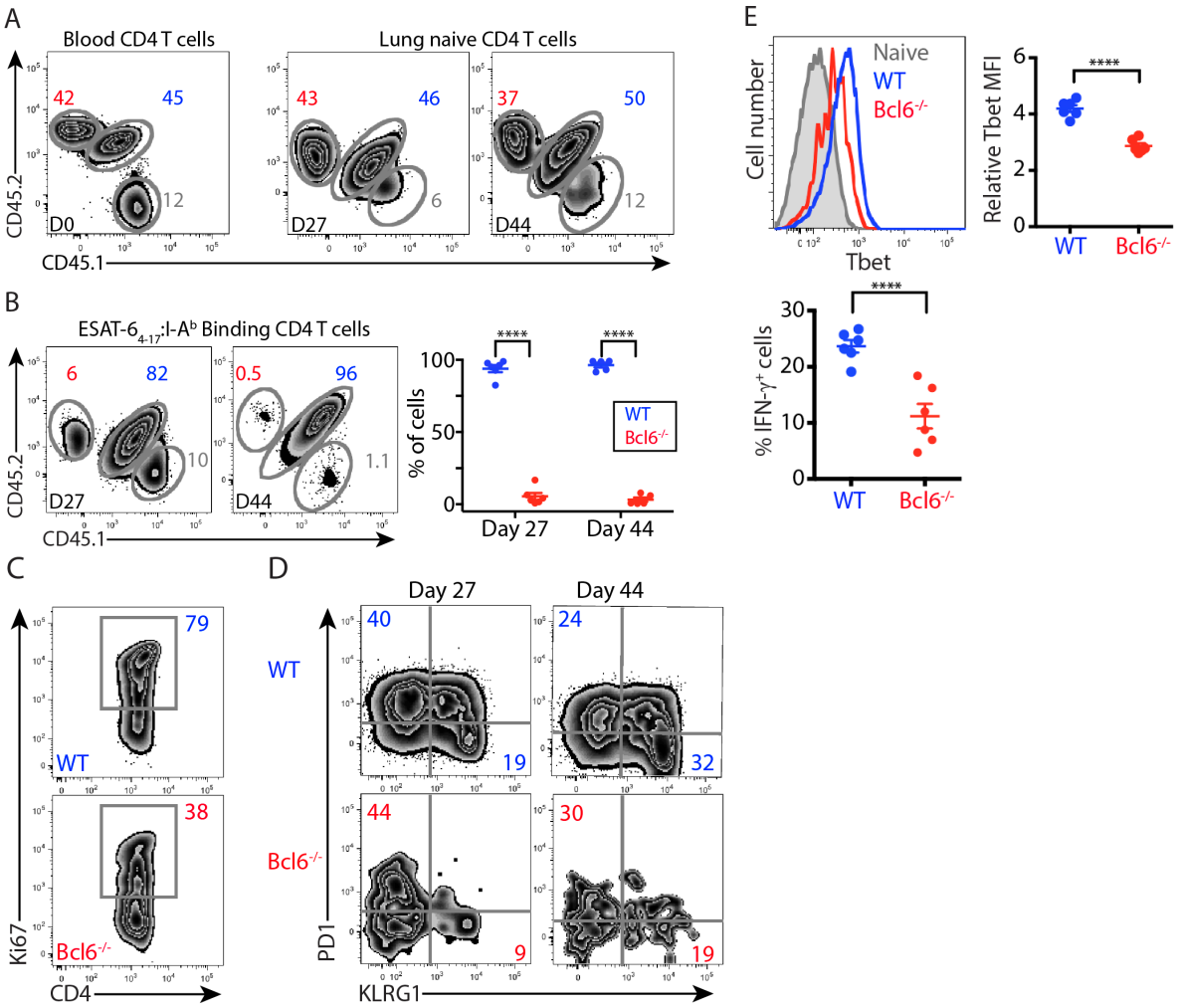

Figure 3.14: T cell intrinsic Bcl6 signaling is required to generate an Mtb-specific Th1 response. Bcl6$^{-/-}$ (red) and WT (blue) fetal liver transferred into lethally irradiated WT (gray) mice in a 1:1 ratio. A) Representative flow cytometry plots show the ratio of donor Bcl6$^{-/-}$, donor WT and host CD4 T cells in blood 10wks post immune reconstitution and among lung naïve CD4 T cells at days 27 and 44 post-infection. B) Frequency of Bcl6$^{-/-}$ (red), donor WT (blue) and host (gray) cells among total ESAT-6 tetramer binding cells are shown in the flow cytometry plots at the times post infection indicated. The cumulative graph depicts WT and Bcl6$^{-/-}$ cells as a percentage of total donor ESAT-6 tetramer binding CD4 T cells. C) Percentage of WT (top) or Bcl6$^{-/-}$ (bottom) ESAT-6 tetramer binding CD4 T cells that express Ki67 27 days post infection. D) PD-1 and KLRG1 expression by WT (top) or Bcl6$^{-/-}$ (bottom) ESAT-6 tetramer binding CD4 T cells at days post-infection indicated. E) Histograms and cumulative graph (top panel) show T-bet expression by naïve CD4 T cells (gray), WT (blue) or Bcl6$^{-/-}$ (red) ESAT-6 specific CD4 T cells. The cumulative bottom graph on shows the percentage of WT and Bcl6$^{-/-}$ ESAT-6 tetramer binding CD4 T cells that produce IFN-γ directly ex vivo 27 days post infection. Data are representative of 2 independent experiments with 3-7 mice per group and per time point. ****P≤0.0001.

Interestingly, expansion of ESAT-6-specific CD4 T cells was severely limited; at the peak of the immune response (~day 27 post infection), Bcl6$^{-/-}$ comprised only ~6% of the total ESAT-6-specific CD4 T cells in the lungs and this was reduced to <1% by day 44 (Fig. 3.14B). The reduced fraction of antigen-specific Bcl6$^{-/-}$ CD4 T cells at least partially reflected diminished proliferation; a smaller fraction of tetramer-binding Bcl6$^{-/-}$ T cells expressed Ki67 compared to their WT counterparts (Fig. 3.14C). Furthermore, ESAT-6-specific CD4 T cells lacking Bcl6 exhibited impaired functional differentiation, as evidenced by a smaller frequency of KLRG1^{+} cells (Fig. 3.14D), reduced T-bet expression, and diminished IFN-γ production assessed directly ex vivo (Fig. 3.14E). Overall, our results show that intrinsic expression of Bcl6 plays a critical role in the expansion and function of Mtb-specific CD4 T cells.

The chemokine receptor CXCR5 is regulated by Bcl6 and intrinsic expression of CXCR5 by CD4 T cells plays an important role in TB immunity[82,119]. To address the role of CXCR5 during TB we infected CXCR5$^{-/-}$ mice and found them to be defective in controlling lung bacterial burdens (Fig 3.15A) and to succumb to infection early compared to WT mice (Fig. 3.15B).

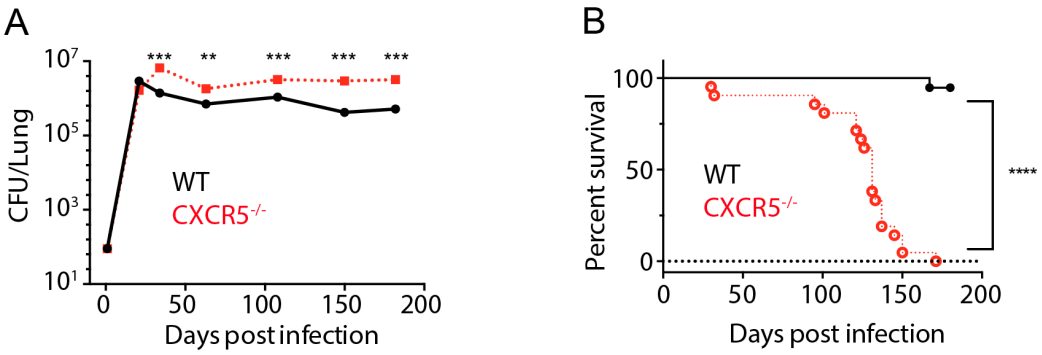

Figure 3.15: CXCR5 deficient mice are hypersusceptible to Mtb infection. A) Kinetics of lung bacterial burdens in WT (black) and CXCR5$^{-/-}$ (red) mice. B) Survival graph of WT and CXCR5$^{-/-}$ infected with low dose Mtb. Data in A are representative of 2 independent experiments with 3-5 mice per group and per time point. Data in B are from one experiment with 21 CXCR5$^{-/-}$ and 19 WT mice per group. Statistical significance in panel A was determined by Students t test and that in panel was by Log-Rank Mantel Cox test. **P≤0.005 ***P≤0.0005 and ****P≤0.0001.

To directly test the cell intrinsic role for CXCR5, we generated mixed bone marrow chimeras by mixing WT and CXCR5$^{-/-}$ bone marrow cells in a 1:1 ratio and adoptively transferring them into sub-lethally irradiated T cell deficient mice. Ten weeks post immune reconstitution and immediately before Mtb infection, the mice had a 1:1 ratio of WT: CXCR5$^{-/-}$ CD4 T cells in their blood and this ratio was maintained even for lung naïve CD4 T cells in the infected mice for at least 120 days (3.16A). In contrast to our findings in Bcl6 chimeras, WT and CXCR5$^{-/-}$ ESAT-6 tetramer binding CD4 T cells expanded similarly during early infection, however, CXCR5$^{-/-}$ cells showed diminished persistence after 120 days post-infection (Fig. 3.16B) but maintained similar PD-1/KLRG1 profiles (Fig. 3.16C), T-bet expression (Fig. 3.16D) and in vivo IFN-γ production (Fig. 3.16E) as WT CD4 T cells.

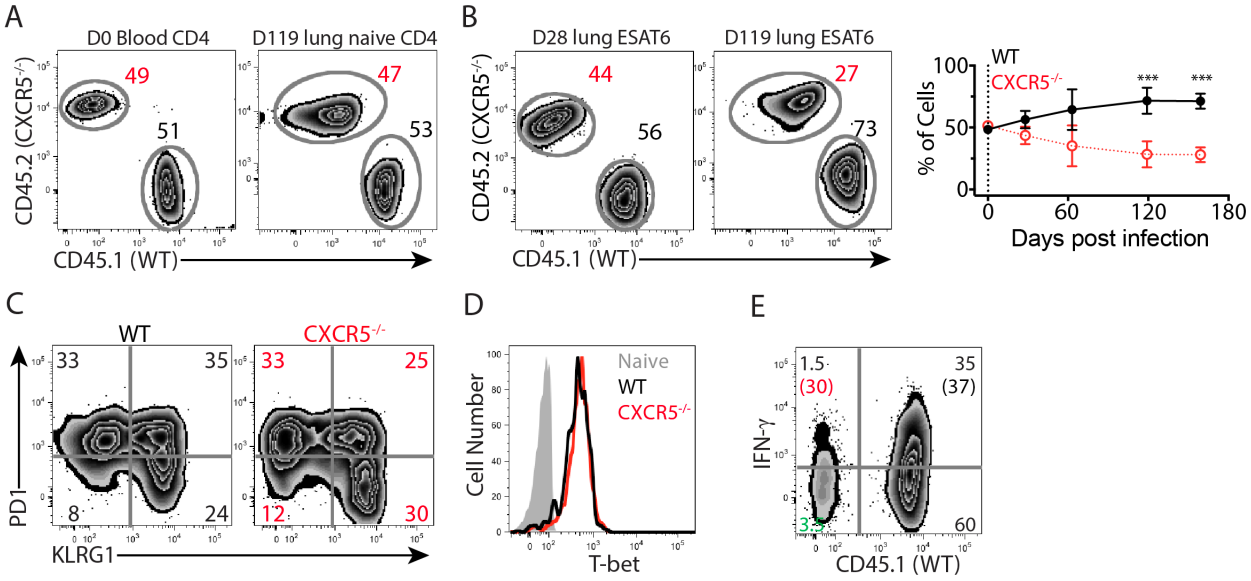

Figure 3.16: Intrinsic CXCR5 expression is required for maintenance of Mtb-specific CD4 T cells. Mixed bone marrow chimeric mice were generated with 1:1 ratio of WT and CXCR5$^{-/-}$ bone marrow cells and infected with Mtb. A) Representative FACS plots depicting ratio of WT (black) and CXCR5$^{-/-}$ (red) naïve CD4 T cells in blood before infection or lungs 119 days post infection. B) Representative FACS plots and kinetics graph show ratio of WT and CXCR5$^{-/-}$ ESAT-6-specific CD4 T cells. C) PD-1 and KLRG1 expression by WT and CXCR5$^{-/-}$ ESAT-6-specific CD4 T cells 119 days post infection. D) T-bet and E) IFN-γ expression by WT and CXCR5$^{-/-}$ ESAT6-specific CD4 T cells 119 days post infection. Numbers in parentheses in E depict the percentage of WT (CD45.1, black) or CXCR5$^{-/-}$ (red) ESAT-6-specific cells that produce IFN-γ directly ex vivo. Data are representative of 3 independent experiments with 3-7 mice per group and per time point. Statistical significance was determined by Student`s T test with $^{***}P \leq 0.0005$

Thus, while intrinsic CXCR5 expression is required to maintain Mtb-specific CD4 T cells during chronic infection, this requirement is not profound.

Overall, the CD4 T cell response to Mtb infection is sustained by a progenitor population that shares many properties with memory T cells, including its regulation by the transcription factor Bcl6.

Discussion

The pathologic hallmark of TB is the granuloma, an organized structure of immune cells that forms at sites of infection[80]. Although the dynamic nature of granulomas is becoming increasingly recognized[67,80,120], in the past granulomas were usually considered static structures that served to sequester Mtb, and perhaps even hide Mtb antigens and prevent recognition by T cells. The latter possibility gained credence from two reports showing that Mtb-specific CD4 T cells had a limited ability to recognize their cognate antigen during chronic mycobacterial infection[100,121]. However, both studies analyzed the response of CD4 T cells specific for Ag85B, an enzyme involved in Mtb cell wall synthesis, whose expression is drastically reduced during chronic Mtb infection as bacterial replication slows[122]. Here we show that CD4 T cells specific for a different Mtb antigen, ESAT-6, a secreted virulence factor that is highly expressed during all stages of infection[122], are subject to chronic antigenic stimulation. Furthermore, this stimulation appears to be ongoing and frequent. Thus, the concept that Mtb escapes T cell-mediated immunity by sequestering or reducing expression of its antigenic proteins does not hold for ESAT-6, the immunodominant antigen in both mice and humans[42,110].

The finding that PD-1-expressing, Mtb-specific CD4 T cells undergo robust proliferation and are polyfunctional cytokine producers was initially somewhat surprising because PD-1 was first identified as a marker for functionally exhausted T cells[123,124]. However, PD-1 is also

expressed on functional T cells that have been recently activated, including Tfh cells[62]. Because PD-1-mediated inhibitory signals increase the TCR threshold for antigenic stimulation[125], it is tempting to theorize that PD-1 signaling elevates the threshold of TCR signaling required to drive terminal differentiation. This theory is supported by the failure of PD-1$^+$ cells to differentiate into terminal KLRG1$^+$ Th1 cells in the absence of antigen. Furthermore if this theory is correct, CD4 T cell expression of PD-1 might serve dual beneficial roles during TB by restricting terminal differentiation, thereby prolonging the CD4 T cell response and at the same time preventing this response from being excessive. Consistent with this, CD4 T cell expression of PD-1 during TB is host protective; PD-1-deficient mice rapidly succumb to a severe inflammatory form of TB that is driven by a profound expansion of Mtb-specific CD4 T cells[108,109]. While the precise role of PD-1 in modulating antigen-specific CD4 T cell expansion, function and differentiation during TB remains unclear and needs to be further investigated, recent reports indicate that PD-1 signaling may directly target and block TCR signaling processes that supply energy to the expanding antigen-specific cells, akin to putting T cells on a diet[126]. The signaling pathways that supply energy to the clonally expanding cells are mediated mainly by co-stimulatory molecules (ICOS and CD28), and as such, signal through induction of PI3K and phosphorylation of Akt that result in IL-2 production, proliferation and enhanced survival. However PD-1 signaling through recruitment of SHIP1 is thought to block these signals[126]. Consistent with that we found that PD-1$^+$ cells express high levels of SHIP1 during Mtb infections (not shown). However, as these cells also express high levels of ICOS, likely a competition ensues between PD-1 and ICOS signaling pathways with the outcome being the net effect of the two signaling pathways. Consistent with this theory, we found that despite the high

levels of SHIP1, PD-1^{+} cells (unlike their ICOS^{-}KLRG1^{+} counterparts) phosphorylated Akt and secreted IL-2 in an ICOS dependent manner.

In this study, we also show that a proliferating population of antigen-specific CD4 T cells with memory-like properties maintains the Mtb-specific Th1 response. Although memory T cells are classically defined as antigen-specific T cells that persist after antigen clearance, a recent study using acute infection with *Listeria monocytogenes* showed that memory precursor cells are induced as early as three days after infection, when antigen is still present[115]. Here we extend these findings by showing that memory CD4 T cells can be maintained for months during Mtb infection, despite ongoing antigenic stimulation. Like central memory CD4 T cells, maintenance of these cells depends on ICOS:ICOSL signaling. Furthermore, the Mtb-specific CD4 T cell response, including the generation of memory and Th1 effector cells, is almost completely dependent on T cell intrinsic expression of Bcl6.

Central memory T cells normally circulate between blood and lymph nodes, whereas Tfh cells reside within lymphoid follicles[62,75]. Thus, it was somewhat unusual to find Mtb-specific T cells with Tfh and memory-like properties within the lung parenchyma. A likely explanation for this finding is that Mtb infection triggers ectopic lymphangiogenesis within infected lungs, resulting in granulomatous inflammation with B and T cell containing follicular structures that are dependent on CXCL13 and CXCR5 for their formation[82,84,86].

Even though ICOS, Bcl6 and CXCR5 are inter-related during Tfh development (ICOS induces Bcl6, which induces CXCR5)[119], their inter-relationship during TB is not clear. Bcl6 expression could not explain the ICOS deficiency defects, nor was CXCR5 responsible for the defects associated with Bcl6 deficiency. Thus, the relationship of ICOS, Bcl6 and CXCR5 during TB is not linear like during Tfh development and need to be investigated further. However, the

overall results suggest that interactions within the follicular structures are critical for maintaining the pulmonary Th1 response during chronic infection and, at the very least, the progenitor population has both Tfh and memory like features.

Slight et al, recently showed, and our studies confirm that $CXCR5^{-/-}$ mice are susceptible to TB, but this susceptibility can be completely reversed by providing CD4 T cells from CXCR5-sufficient mice[82]. One possible explanation for these results is that $CXCR5^{+}$ CD4 T cells mediate immunity by localizing CD4 effectors to Mtb-infected cells. Indeed, a recent study showed that direct and cognate antigen-dependent recognition of infected cells by Mtb-specific CD4 T cells is critical for controlling Mtb[45]. Our finding that CXCR5 expression by CD4 T cells contributes to the maintenance of Th1 cells during chronic infection suggests an additional possibility: that CXCR5 may direct CD4 T cells to follicular sites where they receive signals to persist and differentiate into effector cells with mycobacteriocidal properties. These possibilities are not mutually exclusive, and each warrants further investigation.

Surprisingly, $ICOS^{-/-}$ CD4 T cells had a competitive advantage over WT CD4 T cells in mixed chimeras during early infection but this advantage was not be sustained. This outcome could be explained by the fact that $ICOS^{-/-}$ cells exhibited reduced expression of PD-1 and progressed rapidly into terminally differentiated $KLRG1^{+}$ Th1 cells, indicating that ICOS signaling (together with TCR stimulation) promotes PD-1 expression in Mtb-specific CD4 T cells. Taken together, these findings support the idea that PD-1 may function to restrict CD4 T cell expansion and terminal differentiation, which may ultimately serve to maintain the Th1 response during chronic infection.

Interestingly, in contrast to the importance of B cells in the maintenance of memory CD4 T cells following acute infections, we found that $\mu MT^{-/-}$ mice lacking B cells had normal

numbers of ESAT-6-specific CD4 T cells throughout infection. This likely reflects the fact that B cells are the primary cell type expressing ICOSL in uninfected animals after antigen clearance[115,117,118], whereas we found ICOSL expression on multiple myeloid populations, including DCs and even alveolar macrophages, in the lungs of Mtb infected mice. The precise role for B cells during TB is currently subject to debate. Some results have indicated that there is excessive inflammation with neutrophil infiltration into the lungs in the absence of B cells and that can be detrimental to the host[69] while other studies indicate that B cells enhance lung pathology and dissemination of disease[127]. Yet we and others have shown that B cells have no impact on immunity to TB[82]. The discrepancy in the results could likely be explained by the difference Mtb strains used to infect mice. Slight et al,[82] and our studies used Mtb strain H37Rv whereas Mtb strain Erdman was used for the study showing that B cells controlled inflammation[69] while the study showing that B cells reduced lung pathology and prevented dissemination used Mtb strain CDC 1551[127]. Therefore, a direct head to head comparison of Mtb strains is warranted. Regardless of the strain of Mtb used, lung bacterial burdens were identical in the presence or absence of B cells in all the reported studies suggesting B cells may not have a direct effect in controlling bacteria but affect the immune mediated pathology or bacterial dissemination. Our studies have further extended the question of the role of B cells in immunity to TB by showing that antigen presentation by B cells is not a critical requirement for immunity. Significantly, we showed that in the context of vaccination, B cells did not have an impact (either positive or negative) on the final outcome of reducing lung bacterial burdens.

Bcl6 deficiency had a dramatic impact on the induction of the Mtb-specific CD4 T cell response and also limited the ability of Mtb-specific CD4 T cells to differentiate into Th1 effector cells. In contrast, ICOS deficiency enhanced the differentiation into Th1 cells. These

results are consistent with recent studies using in-vitro stimulated T cells showing that optimal Th1 polarization requires collaboration between T-bet and Bcl6[128-130]. From the studies it can be hypothesized that during Th1 polarization, a transitional cell type is induced that expresses both T-bet and Bcl-6 and is capable of producing both IFN-γ and IL-21. This transitional population of cells eventually disappears as T-bet progressively dominates in the invitro conditions. We speculate that this scenario is happening in vivo during TB, in which the inflammatory milieu is characterized by enhanced IL-12 secretion. Indeed, Mtb-specific PD-1$^+$ CD4 T cells have all the characteristics of the assumed transitional cell type: T-bet^{int}Bcl6$^+$IFN-γ$^+$IL-21$^+$. While the precise nature and phenotype of this transitional cell type has yet to be described in vivo, to our knowledge, our study is the first one to show that Bcl6 is critical for induction of a Th1 response in vivo. In fact, during acute Listeria infection, Bcl6$^{-/-}$ CD4 T cells showed normal differentiation into Th1 effectors, despite an impaired central memory response[115]. This difference between Mtb and Listeria infections highlights the importance of the Bcl6$^+$ Tfh-like precursor population in generating the Mtb-specific Th1 response.

Although a potent Th1 response has long been considered paramount for protection against Mtb, there is growing evidence that robust expansion of a less differentiated Th1-progenitor population is more important than the induction of terminally differentiated Th1 cells themselves[88,107]. In addition to immunization studies showing that vaccines that induce high numbers of less differentiated (PD-1$^+$KLRG1$^-$) Mtb-specific CD4 T cells confer superior and more durable immunity[88,107], studies with T-bet$^{+/-}$ mice further support this idea. We have shown that PD-1$^+$ memory-like CD4 T cells express Bcl6 and intermediate levels of T-bet, whereas terminally differentiated Th1 cells exhibit less Bcl6 and higher T-bet expression. Interestingly, although T-bet$^{-/-}$ mice have increased susceptibility to Mtb infection due their complete lack of

Th1 cells; T-bet$^{+/-}$ mice are paradoxically more resistant (Andrea Cooper unpublished data) and exhibit an expanded population of PD-1^{+} memory-like cells with relatively few terminally differentiated KLRG1^{+} cells. Finally, adoptive transfer studies also support the idea that PD-1^{+} memory-like CD4 T cells are more protective than their KLRG1^{+} Th1 cell counterparts. Mtb-specific PD-1^{+} T cells isolated from the lung parenchyma were found to be more protective than Mtb-specific T cells isolated from the lung associated vasculature[102].

The findings described here provide a framework for understanding how the CD4 T cell response is maintained during chronic TB. Thus, understanding the pathways that selectively drive the expansion of Mtb-specific CD4 T cells with memory-like properties may provide new avenues for the prevention and treatment of TB.

Chapter IV: Trafficking of CD4 T cells into and out of Mtb-infected lungs

Introduction

How Mtb persists in the lung despite an apparent robust Mtb-specific Th1 response represents a major question in the TB field. In fact, the ability of Mtb to withstand strong Th1-mediated immunity has been used as an argument against using a Th1 targeted vaccine approach against TB[131]. One explanation for Mtb's persistence was recently provided by experiments performed by us (as shown in Chapter III), and others[102], using intravenously administered antibodies to label T cells in the vasculature. These studies revealed that most terminally differentiated Th1 effector cells (identified by cell surface expression of KLRG1 and high levels of the transcription factor T-bet) reside in the lung-associated vasculature, and not in the lung parenchyma as was previously believed. Because control of Mtb requires direct cognate interactions between Mtb-specific CD4 T cells and infected cells[45], the protective role of T cells localized in the vasculature rather than the site of infection in the lung parenchyma is probably limited. However, these surprising findings raise even more questions than they answer. What is the origin of the Th1 effectors in the lung-associated vasculature? Why are very few terminally differentiated Th1 effectors present within the lung parenchyma? Why do a large percentage of the Th1 effectors within the lung-associated vasculature produce IFN-γ directly ex vivo?

We considered these questions in light of the granulomatous inflammatory response that occurs within Mtb-infected lungs. As outlined in Chapter I, the TB granuloma is a tertiary lymphoid structure that develops in the lung in response to Mtb infection[80,85,86]. Like secondary lymphoid structures, the granuloma contains B cell follicles and its development is dependent upon CCR7, CXCR5, and CXCL13[82,84,85]. Given the similarities between TB granulomas and

lymph nodes, we hypothesized that the rules governing T cell trafficking into and out of lymph nodes also govern T cell trafficking through TB granulomas in the lung.

Here we sought to test this idea. Unlike previously reported reported[132], we found that naïve CD44^{low} CD4 T cells were excluded from lung parenchyma of uninfected mice. However, these naïve cells were capable of trafficking into the lung tissue of Mtb infected mice. Like the migration of naïve CD4 T cells into lymph nodes, the migration of naïve CD4 T cells into Mtb-infected lungs was CCR7-dependent manner. Using MHCII tetramers to identify CD4 T cells recognizing the immunodominant Mtb epitope ESAT-6$_{4-17}$:I-A^{b}, we found that ESAT-6-specific T cells within the lung parenchyma were phenotypically similar to those within the lung draining lymph node, whereas ESAT-6 specific cells in the lung-associated vasculature resembled those in general circulation. We also used RNA sequencing to assess the genome-wide transcriptional profile of ESAT-6-specific CD4 T cells in the lung parenchyma compared to those in the vasculature. We found that the transcription factor KLF2, an important regulator of T cell migration, was highly expressed by ESAT-6-specific T cells in the vasculature compared to those in the lung parenchyma. Furthermore, KLF2 was predicted to regulate many of the genes that were differentially expressed between ESAT-6-specific CD4 T cells in the lung parenchyma and those in the vasculature (including S1PR1, a receptor for sphingosine 1-phosphate that directs T cell egress from lymphoid tissue into the blood). Finally we showed that ESAT-6-specific CD4 T cells in the lung-associated vasculature produce IFN-γ directly ex vivo but show little evidence of recent TCR activation. Although these results are still preliminary, they suggest that T cells traffic into and out of Mtb-specific lungs in the same manner that T cells traffic through lymph nodes. This model would help to explain why terminally differentiated Th1 cells

are preferentially found in the vasculature and not the lungs, and suggests new avenues for potential immunotherapeutic interventions.

Migration of naïve CD4 T cells into the lungs of Mtb-infected mice is dependent on CCR7

First we examined the relative number of naïve and activated CD4 T cells in the lung parenchyma and lung-associated vasculature following aerosol infection with Mtb. Using the in vivo lymphocyte labeling technique[101-103],we found less than 5% of naïve CD44^{low} CD4 T cells isolated from the lungs of uninfected mice reside in the lung parenchyma, with the majority of the cells found in the lung vasculature. A slightly higher percentage of CD44^{hi} CD4 T cells (~20%) were found to localize to the lung parenchyma in uninfected mice (Fig. 4.1). After Mtb infection, the percentage of both CD44^{low} and CD44^{hi} CD4 T cells in the lung parenchyma rapidly increased, peaking at ~2 months at ~60% and ~80%, respectively (Fig. 4.1). These levels were maintained thereafter for at least 8 months.

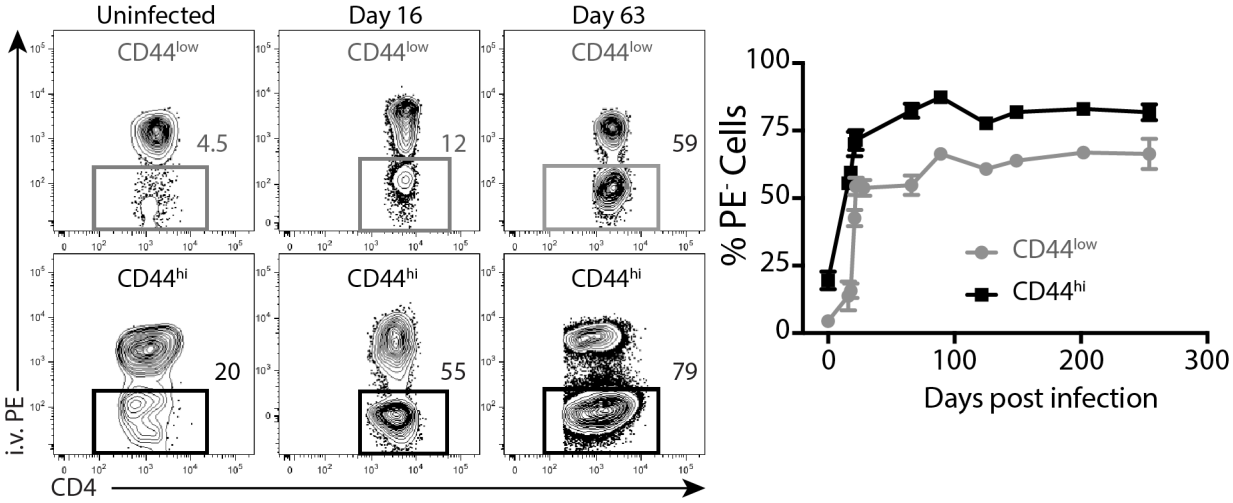

Figure 4.1: Naïve CD4 T cells migrate into the lung parenchyma of Mtb-infected mice. Numbers in the representative flow cytometry plots denote the percentage of cells protected from i.v. labeling and are shown in the cumulative data on the right. The top flow cytometry graphs are gated on CD44^{low} and the bottom on CD44^{hi} CD4 T cells. Data is representative of two independent experiments with 4-6 mice per group and per time point.

Next we examined the capacity of naïve ($CD44^{low}$) and previously activated ($CD44^{hi}$) CD4 T cells to migrate into the lung parenchyma after adoptive transfer. CD4 T cells from the spleens and lungs of mice infected with Mtb for ~2 months were isolated and ~10^7 cells were adoptively transferred into uninfected mice or recipients infected with Mtb for ~2 months. As an additional control, CD4 T cells were transferred into mice infected with *Listeria monocytogenes* in the lungs (3 days after intranasal infection). Recipient mice were sacrificed 12-20 hrs after transfer, a time point when there was no additional activation or proliferation of the donor cells (data not shown). In agreement with the endogenous CD4 T cell data, <5% of naïve $CD44^{low}$ CD4 T cells migrated into the uninfected lung parenchyma compared to a slightly higher percentage (~15%) of $CD44^{hi}$ cells that were able to migrate into the uninfected lung. Remarkably, both $CD44^{low}$ and $CD44^{hi}$ cells migrated equally into the lungs of Mtb infected mice (Fig. 4.2). In contrast, $CD44^{hi}$, but not $CD44^{low}$ CD4 T cells migrated into the parenchyma of Listeria-infected lungs.

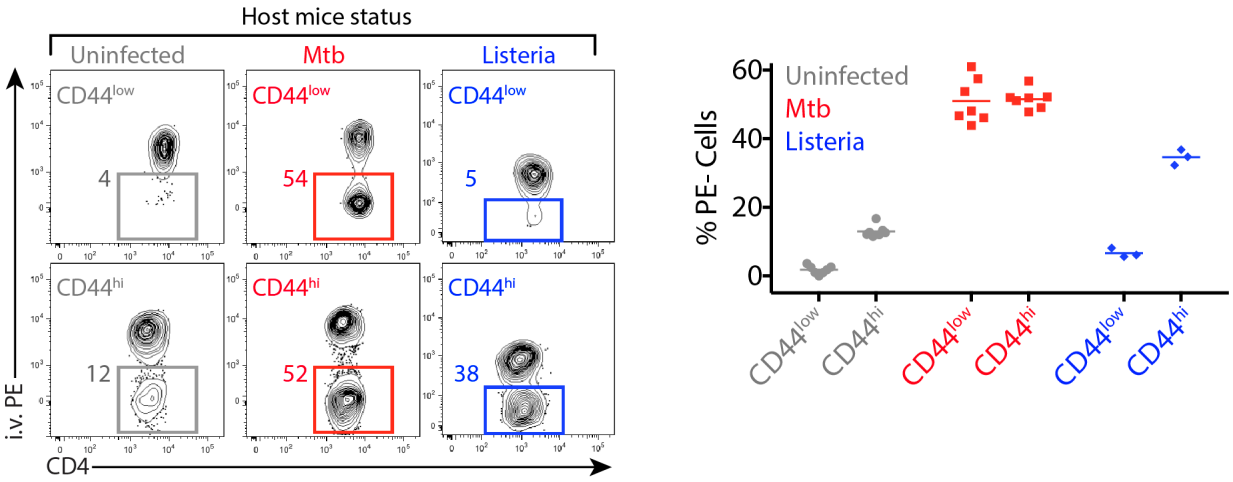

Figure 4.2: $CD44^{low}$ CD4 T cells migrate into Mtb-infected, but not Listeria-infected lungs. CD4 T cells from day 60 Mtb-infected mice were transferred into uninfected, day 60 Mtb or day 3 intranasal Listeria-infected mice and analyzed ~15 hrs post transfer. Representative flow cytometry plots and cumulative data showing the percentage of donor $CD44^{low}$ (top panels) and $CD44^{hi}$ cells (bottom panels) recovered from the lung parenchyma (i.v. PE^-). Data are representative of two independent experiments with 3-7 mice per group.

Thus, the migration of CD44^{low} cells into the lung parenchyma does not occur in all inflammatory settings, indicating that the nature of pulmonary inflammation during Mtb infection specifically promotes this process.

Because the Mtb induced granuloma is essentially a tertiary lymphoid structure that forms in the lung due to ectopic lymphangiogenesis[67,80,82,85,86], we hypothesized that the signals that drive migration of naïve T cells into lymph nodes might also drive the migration of naïve CD4 T cells into the lungs of Mtb infected mice. The migration of naïve T cells into lymph nodes depends upon T cell intrinsic expression of CCR7, a chemokine receptor that binds CCL21 (a chemokine also produced in TB granulomas[75]). To test the role of CCR7 in the migration of T cells into Mtb-infected lungs we co-transferred a 1:1 ratio of congenically-marked, WT and CCR7$^{-/-}$ CD4 T cells isolated from uninfected mice into uninfected or Mtb-infected recipients. The migration of the transferred cells into the lungs and lymph nodes was assessed 12 hours later, after labeling intravascular T cells. When the analysis was performed without considering intravascular labeling, CCR7$^{-/-}$ CD4 T cells migrated poorly into lymph nodes, but their recovery from uninfected and Mtb-infected lungs appeared to be similar to WT CD4 T cells (Fig. 4.3A). Similar findings were previously interpreted to mean that CD4 T cells undergo CCR7 independent migration into the lungs[103,132]. However when the T cell location was segregated as either parenchymal or intravascular by intravenous labeling, the migration patterns were dramatically different. The only setting in which naïve CD44^{low} CD4 T cells migrated into the lung parenchyma was when WT T cells were transferred into Mtb-infected. Neither WT nor CCR7$^{-/-}$ naïve CD44^{low} CD4 T cells migrated into the lungs of uninfected mice, and CCR7$^{-/-}$ CD44^{low} cells showed very minimal migration into Mtb-infected lungs (Fig.4.10B). In contrast, WT and CCR7$^{-/-}$ CD44^{hi} CD4 T cells showed similar migration into Mtb-infected

lungs (Fig. 4.10C). Combined these results indicate that migration of naïve CD4 T cells into Mtb-infected lungs is CCR7 dependent as is migration into lymph nodes. Conversely, migration of CD44^{hi} CD4 T cells into Mtb-infected lungs is independent of CCR7.

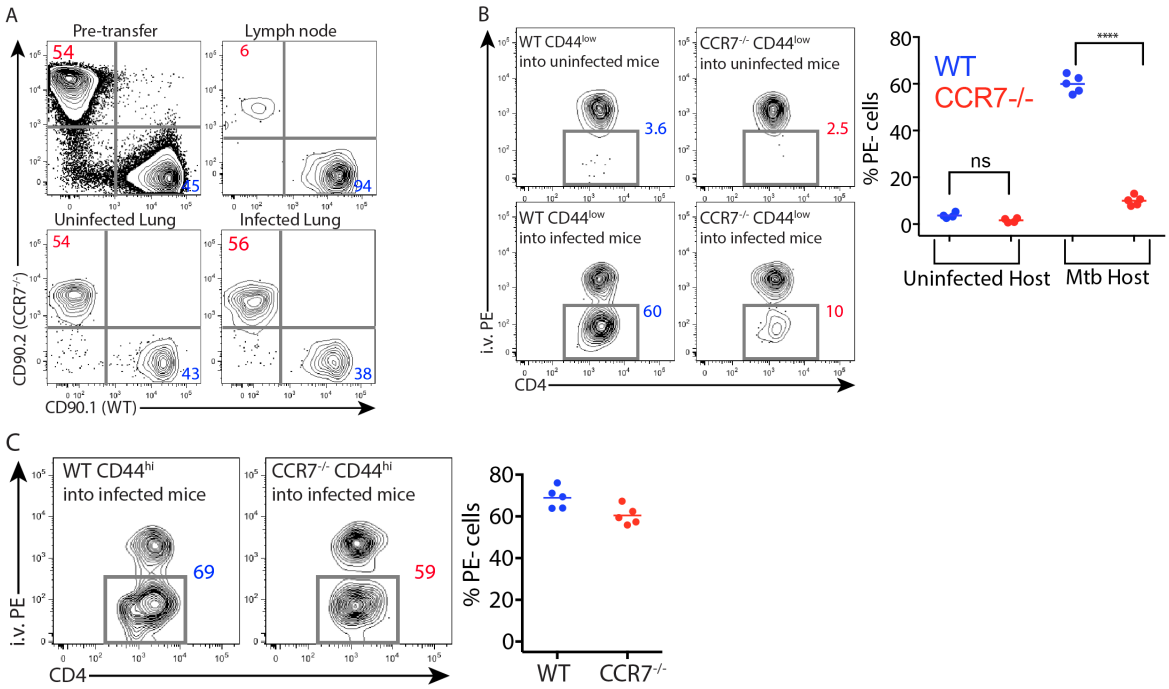

Figure 4.3: Migration of naïve CD4 T cells into Mtb-infected lungs is CCR7 dependent. A) Representative flow cytometry plots depict the ratio of WT and CCR7$^{-/-}$ CD4 T cells from uninfected donors before transfer and 12 hrs post transfer in the lymph node, uninfected lung or infected lung. B) Representative flow cytometry plots and cumulative data depict the i.v. PE labeling status of naïve CD44^{low} WT and CCR7$^{-/-}$ CD4 T cells recovered from the lungs of uninfected or Mtb-infected recipients 12hrs post-transfer. C) Representative flow cytometry plots and cumulative data depict i.v. PE labeling status of activated CD44^{hi} WT and CCR7$^{-/-}$ CD4 T cells recovered from the lungs of Mtb-infected hosts 12hrs post-transfer. Data are from one experiment with 4-5 mice per group. ****P≤0.0001

Mtb-specific CD4 T cells in the lung parenchyma resemble those in the pLN, whereas those in the lung vasculature resemble those in general circulation

Next we sought to characterize the nature of the Mtb-specific T cell response in the lung parenchyma compared to the vasculature, as identified in Chapter III of this dissertation and by Sakai and collegues[102]. We found that the percentage of ESAT-6-specific CD4 T cells that localized to the lung parenchyma was relatively stable throughout infection.

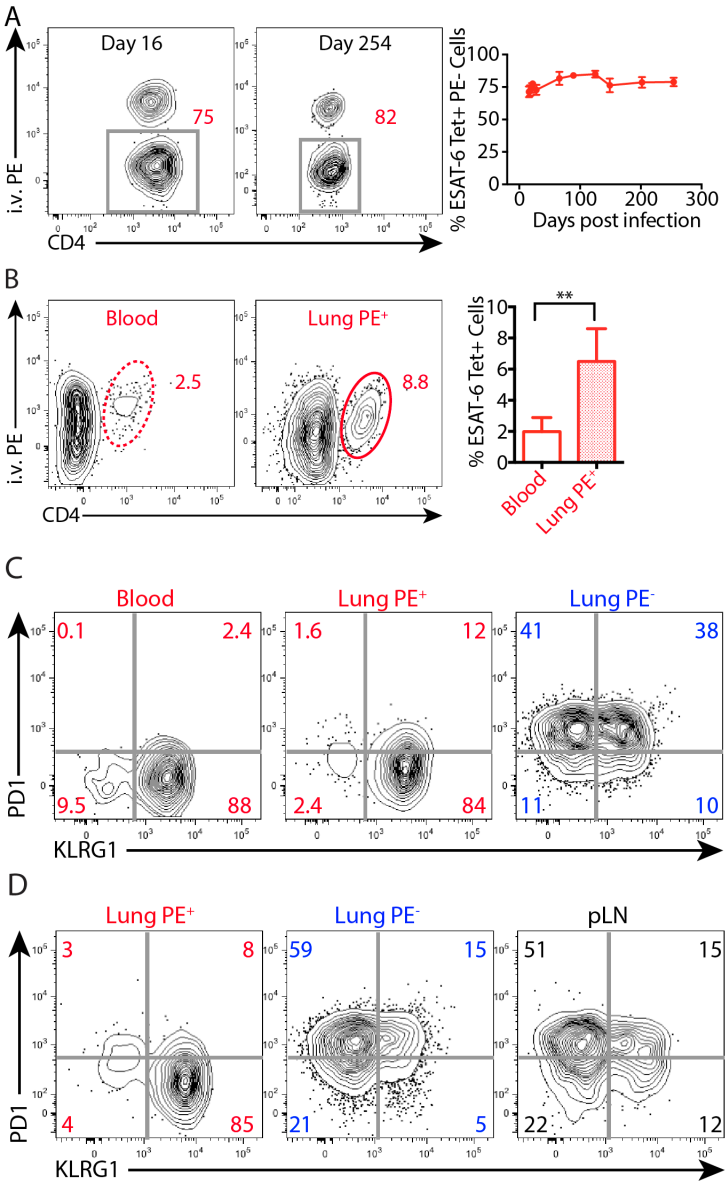

Figure 4.4: Mtb-specific CD4 T cells in the lung parenchyma resemble those in the pLN. A) Representative flow cytometry plots and a cumulative data over the course of infection depicting the frequency of ESAT-6-tetramer binding cells that localize within the lung parenchyma. B) Representative flow cytometry plots and cumulative data depict the frequency of ESAT-6-specific cells within the CD4 T cells recovered from the lung vasculature (i.v. PE^+) and blood in general circulation. The mice had been infected for 202 days with Mtb. C) Representative flow cytometry plots depicting PD1 and KLRG1 expression by ESAT-6-specific CD4 T cells localized in the blood, lung vasculature (PE^+), and lung parenchyma (PE^-) 89 days post infection. D) Representative flow cytometry plots denote PD1 and KLRG1 expression by ESAT-6-specific CD4 T cells isolated from the lung vasculature, lung parenchyma or lung draining lymph node (pLN) 44 days post Mtb infection. Data are from one experiment with 4-6 mice per group. $^{**}P \leq 0.005$

At 16 days post infection ~75% of ESAT-6-specific CD4 T cells were found within the lung parenchyma and this ratio did not change for at least 8 months when ~80% of the cells were in the lung parenchyma (Fig. 4.4A). Interestingly, the percentage of ESAT-6-specific cells amongst total CD4 T cells in the lung vasculature was over 3-fold greater than the percentage in general circulation in the blood (Fig. 4.4B). Thus, the abundance of ESAT-6-specific T cells in the lung vasculature is not simply a result of circulation, but suggests that these cells must have a prolonged dwell time in the lung associated vasculature.

We next sought to compare the phenotypes of Mtb-specific CD4 T cells in the lung vasculature, lung parenchyma, draining lymph nodes and general circulation. We hypothesized that if T cell trafficking through TB granulomas follow the rules of lymph node trafficking, then ESAT-6-specific CD4 T cells within the lung parenchyma should resemble those in lymph nodes, whereas cells in the lung vasculature should be similar to those in general circulation. Consistent with these ideas, based on PD1 and KLRG1 expression, lung vasculature-associated ESAT-6-specific CD4 T cells closely resemble those in general circulation in terms of PD1 and KLRG1 expression (>80% exclusively expressed KLRG1). Conversely, ESAT-6-specific cells in the lung parenchyma exhibited a distinct phenotype, with most cells expressing PD1 and a much lower percentage of $PD1^{-}KLRG1^{+}$ cells (Fig. 4.4C), and this phenotype was very similar to those in the pLN (Fig. 4.4D).

As Mtb-specific CD4 T cells in general circulation and lung vasculature phenotypically resembles each other, we wanted to determine if they were similar functionally by measuring their ability to secrete IFN-γ in vivo. We found that when analyzed directly ex vivo, without further restimulation, ESAT-6-specific CD4 T cells in lung vasculature made significantly more IFN-γ compared to those in general circulation (Fig. 4.5). However, the cells in general

circulation still made significantly more IFN-γ compared to naïve CD4 T cells. Combined, these results indicate that even though Mtb-specific CD4 T cells in the lung vasculature are phenotypically similar to those in general circulation, they more actively produce IFN-γ in vivo.

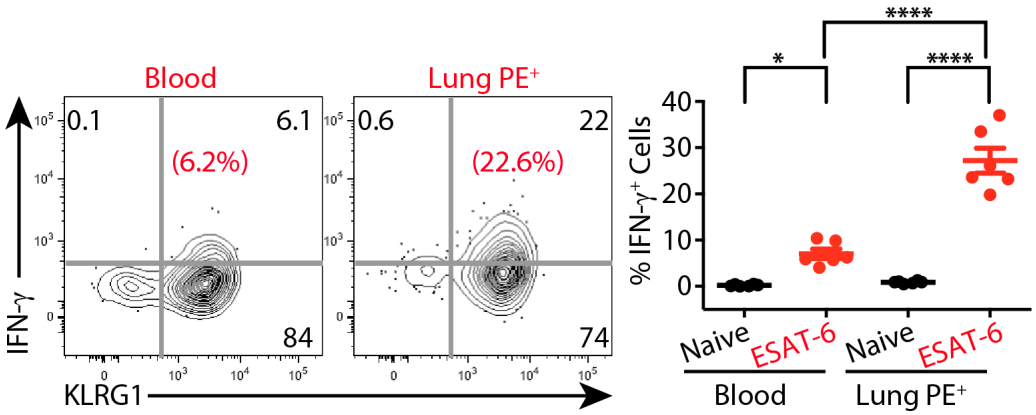

Figure 4.5: Mtb-specific CD4 T cells in the lung vasculature secrete high amounts of IFN-γ compared to those in general circulation. Representative flow cytometry plots depict IFN-γ and KLRG1 expression by ESAT-6-specific CD4 T cells from general circulation or in lung vasculature. Numbers in parentheses depict the percentage of all cells in each location that produced IFN-γ in vivo and is shown in the cumulative. Mice had been infected for 89 days with Mtb. Data are representative of 2 independent experiments with 4-6 mice per group. $^{*}P \leq 0.05$ and $^{****}p \leq 0.0001$

Mtb-specific KLRG1^{+} CD4 T cells in the lung parenchyma more closely resemble PD1^{+} cells in the lung parenchyma than KLRG1^{+} cells in the lung vasculature

From the experiments above and as outlined in Chapter III, a majority of the ESAT-6-tetramer binding cells isolated from the lung vasculature express KLRG1, and this is in agreement with a recent publication[102]. However, we consistently found that 20-50% of the ESAT-6-specific CD4 T cells are actually within the lung parenchyma. As reported in Chapter III, Mtb-specific PD1^{+} CD4 T cells (mostly in the lung parenchyma) expressed higher levels of CD69 and CXCR3 but low levels of T-bet compared to KLRG1^{+} cells. We therefore sought to determine whether the KLRG1^{+} CD4 T cells present in the lung parenchyma more closely resemble PD-1^{+} cells that also reside in the lung or KLRG1^{+} cells in the vasculature.

Interestingly, ESAT-6-specific KLRG1^{+} in the lung parenchyma (i.v. PE^{-}) expressed levels of CD69 and CXCR3 that were intermediate between KLRG1^{+} cells in the vasculature (i.v. PE^{+}) and PD-1^{+} cells in the lung parenchyma (Fig. 4.6A and Fig. 4.6B).

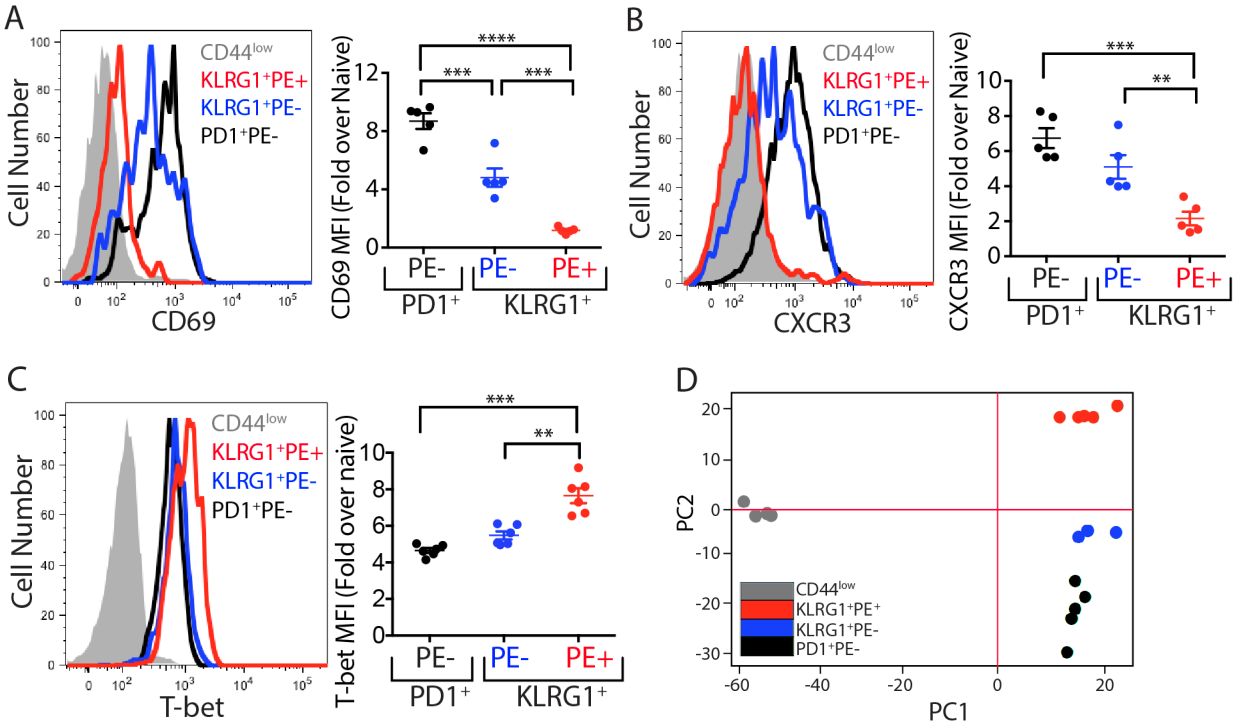

Figure 4.6: Tissue resident Mtb-specific CD4 T cells cluster together and are significantly different from cells in the lung vasculature. Lung CD4 T cells from day 120 Mtb infected mice were clustered as naïve CD44^{low} (gray), ESAT-6-specific PD1^{+}PE^{-} (black), ESAT-6-specific KLRG1^{+}PE^{-} (blue) and ESAT-6-specific KLRG1^{+}PE^{+} (red) and analyzed for: A) CD69, B) CXCR3 and C) T-bet expression. D) The four populations of cells were sorted and their transcriptome was analyzed by RNA sequencing. Graph depicts principal component analysis of the whole transcriptome. Data in A-C are representative of 3 independent experiments with 4-6 mice per group. Data in D are from one experiment with 3 pooled mice to make one replicate and each data point represents a replicate. $^{**}P\leq0.005$, $^{***}P\leq0.0005$ and $^{****}p\leq0.0001$

However, T-bet expression more closely resembled that in PD-1^{+} cells than the high levels observed in ESAT-6-specific KLRG1^{+} CD4 T cells in the vasculature (i.v. PE^{+}) (Fig.4.6C). These findings suggested that KLRG1^{+} cells in the lung tissue were closely related to the PD-1^{+} cells in the tissue and not to the KLRG1^{+} cells in the vasculature.

To analyze the similarities between these populations globally, we sorted each of the above population of cells ($CD44^{low}$, ESAT-6-$tet^{+}PD\text{-}1^{+}PE^{-}$, ESAT-6-$tet^{+}KLRG1^{+}PE^{-}$ and ESAT-6-$tet^{+}KLRG1^{+}PE^{+}$) and isolated RNA for genome-wide transcriptome analysis by RNAseq. Transcriptomes from each population were compared using principal component analysis, which assigns statistical vectors that accounts for variation within the data. When the first principal component (PC1, the model that best describes differences between the samples) is plotted against the second principal component (PC2, the next best description of differences that is independent of PC1) in X and Y-axes, data are linearized with closely related data points clustering together. With this analysis we found that samples from each group clustered with themselves and differentially from samples from other groups (Fig. 4.6D). Not surprisingly, we found that samples containing $CD44^{low}$ samples were quite different from the other samples containing tetramer-binding cells. In assessing the different ESAT-6-specific populations, however, we found that the $KLRG1^{+}$ population within the lung parenchyma was more closely related to the $PD\text{-}1^{+}$ population than to the $KLRG1^{+}$ cells in the vasculature.

Lung vasculature-localized ESAT-6-specific CD4 T cells have enhanced Th1 functional capacity compared to their tissue resident counterparts

The high levels of T-bet and direct ex vivo IFN-γ production in $KLRG1^{+}$ ESAT-6-specific CD4 T cells in the vasculature prompted us to further investigate their capacity to produce inflammatory cytokines. We stimulated polyclonal CD4 T cells from Mtb infected mice with ESAT-$6_{4\text{-}17}$ peptides or anti-CD3/28 antibodies in vitro for 4 hrs and analyzed the production of IFN-γ and TNF by $KLRG1^{+}$ CD4 T cells. We found that compared to their tissue

resident counterparts, KLRG1$^+$ CD4 T cells in the vasculature produced more IFN-γ and TNF after stimulation with ESAT$_{4-17}$ peptides (Fig.4.7B) or anti-CD3/28 (Fig. 4.7C).

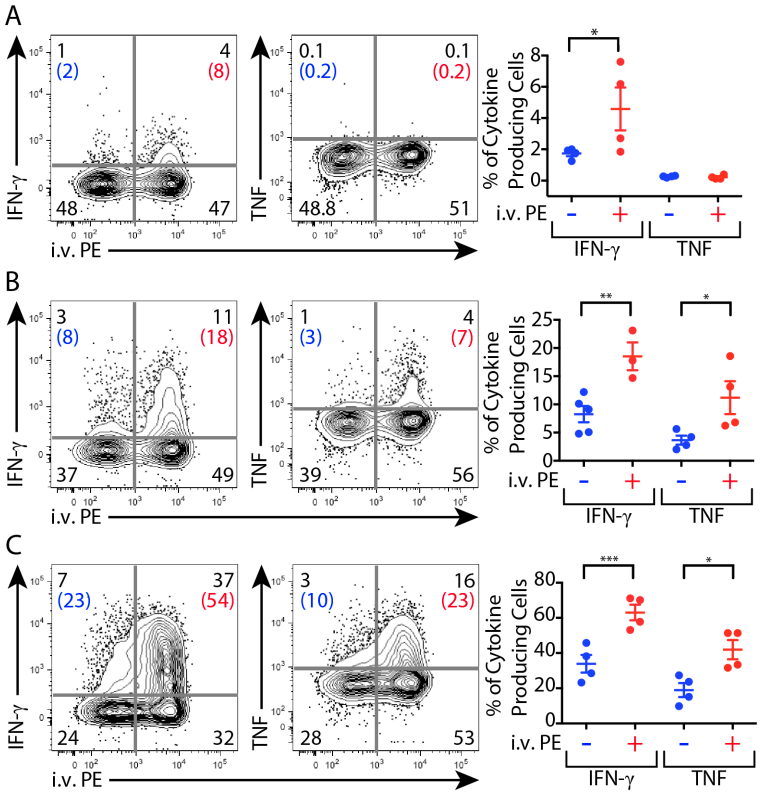

Figure 4.7: Lung vasculature-associated Mtb-specific KLRG1$^+$ CD4 T cells have enhanced Th1 functional capacity. A) Representative flow cytometry plots depict IFN-γ or TNF production and i.v. PE labeling status of lung KLRG1$^+$ cells after in vitro culture with: A) Medium control, B) ESAT-6$_{4-17}$ peptide and C) Anti-CD3/28 antibodies. Numbers in parentheses denote the percentage of i.v. PE$^-$ (blue) or i.v. PE$^+$ (red) that produce IFN-γ and are shown in the respective cumulative data on the right. Data shown are from day 66 Mtb infected mice and are representative of least 3 independent experiments. *P≤0.05 **P≤0.005 ***P≤0.0005

Thus, KLRG1$^+$ ESAT-6-specific CD4 T cells in the lung parenchyma resemble PD-1$^+$ cells in the lung in terms of their reduced cytokine producing capacity.

Lung vasculature Mtb-specific CD4 T cells are weakly stimulated via TCR

The finding that Mtb-specific CD4 T cells in the lung vasculature exhibit high T-bet expression and an increased capacity to secrete Th1 cytokines prompted us to evaluate if they were making more IFN-γ in vivo. In agreement with a recent report[102], when we analyzed IFN-γ production

directly ex vivo without restimulation, we found that ESAT-6-specific KLRG1$^+$ CD4 T cells in the vasculature made more IFN-γ than those in the lung parenchyma. We were surprised that T cells in the vasculature were producing the highest levels of IFN-γ because the vast majority of Mtb-infected cells were resident in the lung parenchyma as assessed using a recombinant Mtb strain expressing mCherry (data not shown). Furthermore, the few Mtb-infected cells observed in the vasculature had a less activated phenotype than those in the lung parenchyma, and showed reduced expression of MHCII and CD86. To investigate whether Mtb-specific CD4 T cells in the vasculature received TCR-mediated signals, we Mtb infected Nur77^{GFP} reporter mice that express GFP under the Nr4a1 promoter. The Nr4a1 is downstream of TCR signaling and GFP expression peaks within 24 hours of stimulation through the TCR and dissipates within 48-72 hours. Thus, these mice are a useful tool for measuring TCR signal strength[133]. As previously shown ESAT-6-specific KLRG1$^+$ CD4 T cells in the lung vasculature produced significantly more IFN-γ directly ex vivo than those in the lung parenchyma (Fig. 4.8A). However, when the cells were analyzed for GFP expression, ESAT-6-specific PD-1$^+$ CD4 T cells had the highest level of GFP expression. Interestingly, KLRG1$^+$ cells in the vasculature expressed very little GFP (Fig. 4.8B), whereas KLRG1$^+$ cells in the lung parenchyma expressed higher levels. In fact, KLRG1$^+$ cells in the vasculature actually expressed less GFP than naïve CD44^{low} cells isolated from the lungs of the same mice. The very low GFP expression by ESAT-6-specific KLRG1$^+$ cells in the vasculature that produce the highest amount of IFN-γ suggests that this cytokine production is TCR independent.

Gene expression profile of Mtb-specific CD4 T cells in lung vasculature vs. parenchyma

Next we revisited the genome-wide transcriptome analysis to identify potential signaling pathways that might shape the distinct localization of different ESAT-6-specific CD4 T cell

populations. We gave special attention to genes known to play a role in T cell egress from lymph nodes, retention in the blood, or migration into inflamed tissues.

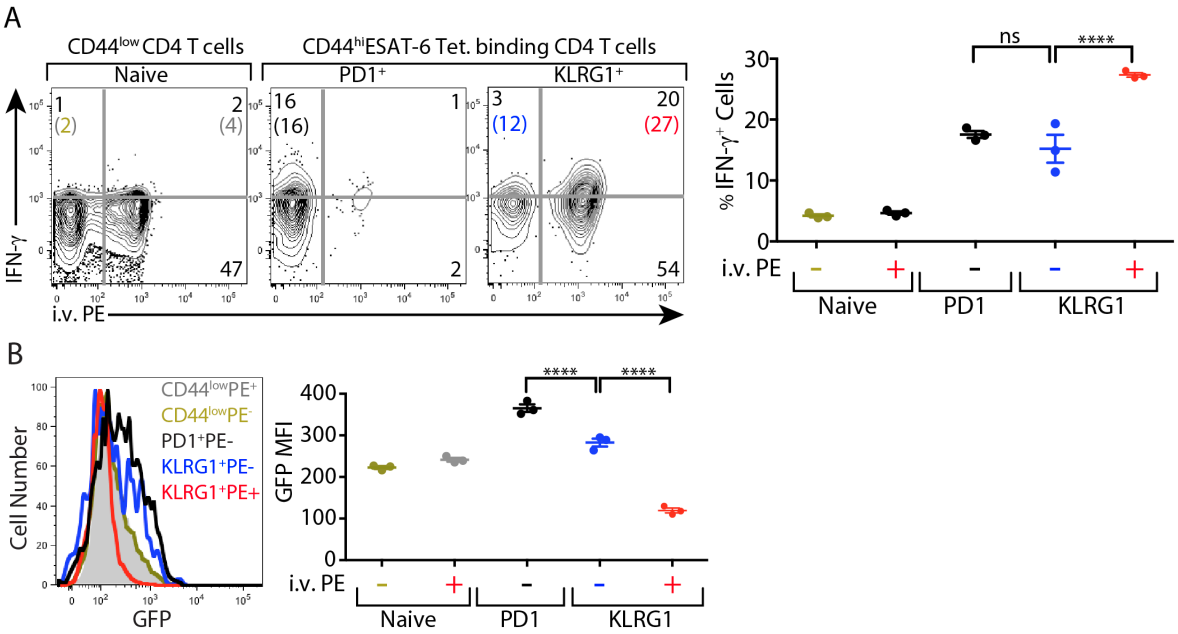

Figure 4.8: ESAT-6-specific CD4 T cells in the lung vasculature produce more IFN-γ but receive weak TCR stimulation. A) Representative flow cytometry plots denote IFN-γ expression and i.v. PE labeling of lung CD4 T cells with the indicated phenotype isolated 90 days post Mtb infection of Nur77^{GFP} mice. Numbers in parentheses denote the percentage of i.v. PE^{-} or i.v. PE^{+} cells that produce IFN-γ directly ex vivo and are shown in the cumulative data in the right. B) Representative histograms and cumulative graph depict GFP expression by the cells identified in panel A. Data are representative of two independent experiments. ****P≤0.0001.

Kruppel like transcription factors (KLF) are a family of transcription factors that regulate gene expression effecting a diverse array of biological processes[134]. KLF2 in particular has been reported to regulate expression of integrin, S1P and chemokine receptors and therefore plays a major role in regulating lymphocyte trafficking[135]. We first analyzed RNAseq data of lung lymphocytes isolated ~120 days post Mtb infection, for expression of KLF transcription factors. Of the 17 identified KLF transcription factors, only KLF2 and KLF6 were highly expressed in the data set, and only KLF2 was differentially expressed between ESAT-6-specific CD4 T cells in the lung parenchyma and the vasculature (Fig.4.9A). Given this differential expression of KLF2, we next sought to determine if other genes differentially expressed between ESAT-6-

specific cells in the lung parenchyma and vasculature might be regulated by KLF2. We first sought to identify genes in the mouse genome that are predicted to be targets of KLF2 or KLF4, which shares the KLF2 the DNA binding motif (CCCACCCC). As the KLF2 and KLF4 motif is very common in gene promoter regions we filtered the binding sites through ENCODE DNAse I footprints to identify genes with chromatin structure that facilitates transcription factor binding. Through this analysis, we found ~13,000 genes predicted to be regulated by KLF2. From our data set comparing ESAT-6-specific KLRG1^{+} CD4 T cells either in the vasculature or parenchyma, we found 102 genes that were significantly down regulated and 77 genes that were significantly up regulated. Of the up regulated genes, 66 were predicted to be KLF2 regulated, a significant enrichment (hypergeometic p-value of 6.4×10^{-8}). Additionally of the down-regulated genes, 76 were predicted to be KLF2 regulated and this enrichment was also significant with a hypergeometic p-value of 7.6×10^{-4} (Fig.4.9B). Finally we sought to identify some of the genes that were either up regulated or down regulated in the lung vasculature. We found S1PR1, S1PR5 and CX3CR1 to be up regulated in the lung vasculature whereas CXCR3 and CCR8 were down regulated (Fig. 4.9C). The down-regulation of CXCR3 in the vasculature was in agreement with our flow cytometry data (Chapter III), whereas CX3CR1 up regulation is agreement with flow cytometry analysis of vasculature resident CD4 T cells reported recently[102,117]. These results strongly suggest that KLF2 plays an important role in driving the differential gene expression between KLRG1+ cells in the lung parenchyma and the vasculature. Furthermore, the regulation of S1PR1 suggests that KLF2 not only controls the ability of T cells to egress from lymph nodes into the blood[135], but may also control the egress of T cells from Mtb-infected lungs

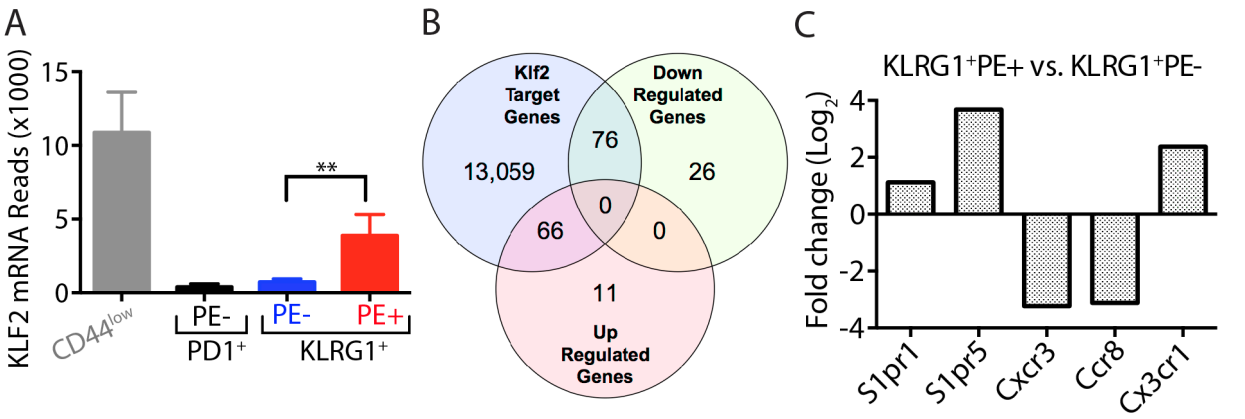

Figure 4.9: Differential gene expression by lung parenchyma vs. tissue resident Mtb-specific CD4 T cells. A) KLF2 mRNA as determined by RNA sequencing of lung naïve CD44^{low}, ESAT-6-specific PD1^{+}PE^{-}, KLRG1^{+}PE^{-} and KLRG1^{+}PE^{+}. B) Venn diagram depicts overlap between genes predicted to be KLF2 regulated vs. genes up regulated or down regulated in a head to head comparison of ESAT-6-specific KLRG1^{+}PE^{+} and KLRG1^{+}PE^{-}. D) Expression profile of some of the genes regulated by KLF2. Data shown are from day 120 Mtb infected mice with 3 pooled mice making one replicate and 3-5 replicates per group. **P≤0.005

Mtb-specific KLRG1^{+} CD4 T cells are defective in their ability to migrate into the lung parenchyma

Although S1P – S1PR1 signaling is required for T cells to egress from lymph nodes into the blood, once in the blood, T cells must down regulate their S1P receptor expression in order to migrate out of blood into tissues or lymph nodes[74]. Because our transcriptional analysis showed high levels of S1PR1 and the transcription factor KLF2 in ESAT-6-specific CD4 T cells in the vasculature, we hypothesized that they would migrate from blood into lung tissue poorly. To test this hypothesis, we transferred CD4 T cells isolated from mice infected with Mtb for ~60 days into congenically marked uninfected or Mtb infected mice and analyzed their ability to migrate into lung tissue ~12-20 hrs post-transfer. First, we assessed donor ESAT-6-specific CD4 T cells based on their PD1 or KLRG1 expression. We found ~50% of the PD-1^{+} cells successfully migrated into the lung parenchyma of uninfected mice (Fig. 4.10A). This migration was further enhanced by Mtb infection, as ~80% of donor PD1^{+} cells successfully migrated into the lungs (Fig. 4.10B). In contrast, only ~6% of the ESAT-6-specific KLRG1^{+} cells were able to migrate

into the uninfected lung (Fig. 4.10A) and this ratio increased only marginally (to ~10%) in Mtb-infected mice (Fig. 4.10B). These results suggest that Mtb-specific KLRG1^{+} cells are defective in their ability to migrate into lung tissue.

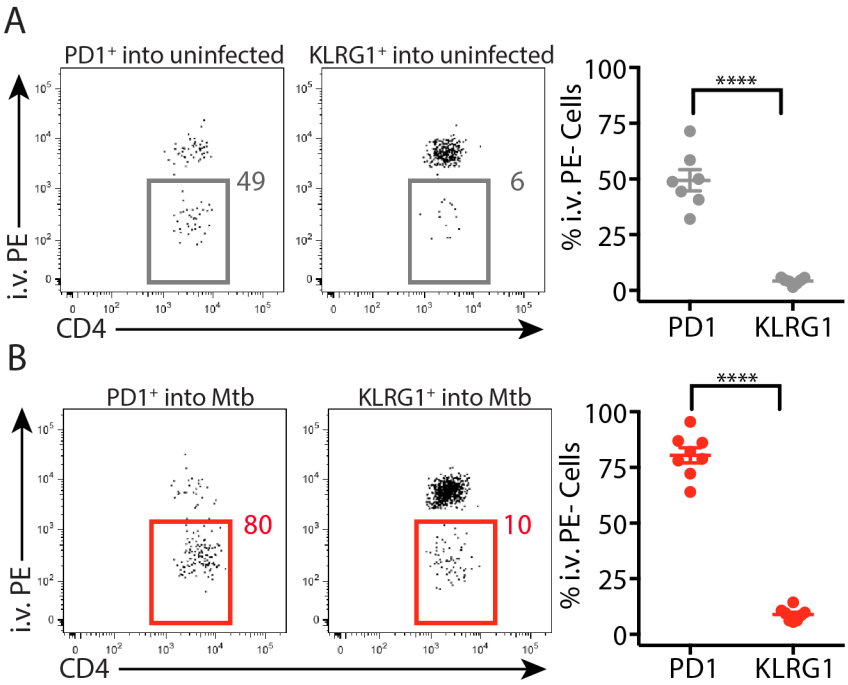

Figure 4.10: Mtb-specific KLRG1^{+} CD4 T cells are defective in their ability to migrate into lung tissue. CD4 T cells were isolated from ~day 60 Mtb infected mice and 5-10 x 10^{6} cells were transferred into congenically marked uninfected or ~day 60 Mtb infected mice. Donor cells were recovered ~14-20 hrs later. Representative flow cytometry plots and cumulative data depict the percentage of i.v. PE^{-} ESAT-6-specific PD1^{+} and KLRG1^{+} donor cells recovered from A) Lungs of uninfected recipient mice and B) lungs of Mtb-infected recipient mice. Data shown are from 2 independent experiments with 3-8 mice per group. ****P≤0.0001

Discussion

Appropriate lymphocyte trafficking is fundamental for immunity, with naïve lymphocytes continuously recirculating between the lymphatics, lymph nodes and blood[74,136]. Any perturbation of this migratory circuit can have detrimental effects on the host's ability to effectively control or clear infections. Indeed, it has been demonstrated in various disease conditions that failure to express molecules and receptors essential for lymphocyte migration can lead to poor prognosis and disease outcome[82,137-139]. Additionally, drugs that change the

migration kinetics of lymphocytes have been used to treat some autoimmune diseases[140,141]. However, how lymphocytes migrate during TB and what effect this migration has on the overall immune response has not been studied.

Here we found that the majority of Mtb-specific CD4 T cells with the highest Th1 functional capacity are located within the lung vasculature and not in the lung parenchyma where Mtb-infected cells are predominantly found. Furthermore, these cells were generally incapable of migrating into the lung parenchyma following infection. This inability to move into the lung is likely to contribute to the failure of the immune system to confer optimal protection to Mtb even though the Th1 response mounted is seemingly robust. In support of this idea, a recent study showed that cells isolated from the lung vasculature failed to migrate into the lungs and conferred less protection than cells isolated from the lung parenchyma that were able to migrate back into the lung[102]. These findings help to explain one of the most puzzling questions in the immunology of tuberculosis: A Th1 response is absolutely required for protection against tuberculosis, but the magnitude of that response does not correlate with protection against Mtb infection[19,29,30,92].

A key question that was not answered in these experiments, but that will be a focus of my future studies, is the relationship between the cells in the lung parenchyma to those in general circulation and in the draining lymph node. It has been shown previously that Mtb-specific PD-1^+ CD4 T cells (predominantly within the lung parenchyma) give rise to the KLRG1^+ cells (mainly within the lung vasculature)[106]. This raises the question of the lineage relationship between these cells. It is likely that the parenchyma resident KLRG1^+ cells are a transitional stage between the PD1^+ in the tissue and the KLRG1^+ cells in the vasculature. In support of this idea, we found that tissue resident KLRG1^+ cells closely resemble PD1^+ cells but significantly

differ from the KLRG1^{+} cells in the vasculature. It will be important to address from which location the cells migrate into the vasculature. We hypothesize that KLRG1^{+} cells in the lung vasculature during chronic Mtb infections arise independently from two locations: a) the draining lymph node and b) the lung. In support of this hypothesis, we found Mtb-specific CD4 T cells in the lung parenchyma had a phenotype resembling that of cells found within the draining lymph nodes. However, it is unlikely that the lymph node is the sole source of these cells, as they are too few in number to account for the large number of cells we find in the lung vasculature. The spleen maybe the source of the cells in the vasculature but it seems unlikely because the total number of antigen-specific cells in this tissue is not as high as in the lungs.

Other important questions that remain include whether these Mtb-specific Th1 cells can be induced to migrate into the lungs or be retained there, and whether T-bet^{hi} effector T cells in the Mtb-infected lungs are prone to death in this inflammatory environment. In support of the latter possibility, it has been reported that reactive nitric oxide species generated by activated macrophages are toxic to T-bet^{hi} cells[73]. Furthermore, TGFβ is known to mediate apoptosis or block development of T-bet expressing cells and the concentration of this cytokine is increased in the lungs of Mtb infected mice and in humans with active TB[71,142]. In support of the idea that TGFβ plays an important role in regulating these events, we found that mice that lacked TGFβ signaling in their T cells had increased numbers of ESAT-6-specific KLRG1^{+} T-bet^{hi} cells in their lung parenchyma that produced significantly more IFN-γ (data not shown). Thus, it is possible that high T-bet expression is incompatible with CD4 T cell survival in the Mtb-infected lung, and that to survival of these cells require that they either egress from the lung, or reduce their T-bet expression. Further studies will be required to explore these possibilities.

Even though naïve cells migrate into the lungs of Mtb-infected mice in a CCR7 dependent manner, activated cells can migrate into both uninfected and Mtb-infected lungs in a manner independent of CCR7. Therefore it's likely that other mechanisms exist that drive migration of PD-1^+ cells into the lungs. We hypothesize that the migration of PD-1^+ CD4 T cells into the lungs is CXCR3-dependent, as this population expresses very high levels of CXCR3 and chemokines that bind this receptor (CXCL9, CXCL10, and CXCL11) are present at high concentrations in Mtb-infected lungs[54,79,137]. CXCR3 may also direct the migration of these cells into uninfected lungs, as this chemokine receptor was recently shown to drive the migration of memory CD8 T cells into the lungs of uninfected mice which apparently had CXCL10 expression in the airway[143].

The consequences of ectopic lymphangiogenesis on the ability of the immune system to effectively control TB needs further evaluation. Specifically, further insights are needed regarding how the granuloma affects lymphocyte migration into and out of the lung. The paradigm of the immune system is that T cells are activated in lymphoid tissue and fully differentiated effector cells migrate to the site of infection and only return to the lymph node after differentiating into central memory T cells after antigen is cleared. This migration back into the lymph nodes is CCR7 dependent[75]. Our results suggest that T cell trafficking through the TB granulomas is governed by the same rules that direct trafficking through the lymph nodes. Thus, it may be inherent to the biology of tertiary lymphoid structures that fully differentiated effector Th1 cells egress into the blood, even though the granuloma is also the primary site of infection. This trafficking pattern may benefit Mtb by limiting the ability of effector Th1 cells to interact with Mtb-infected cells. If this is the case, then drugs that interfere with lymphocyte egress from the lymph nodes that are currently used to alleviate autoimmunity, may serve to maintain Mtb-

specific CD4 T cells in the granuloma and perhaps to help control Mtb. We are currently testing one of this drugs (fingolimod)[141] in the mouse model of Mtb.

Finally it requires to be determined what triggers Mtb-specific Th1 cells located in the vasculature secrete high amounts of IFN-γ. TCR signaling is unlikely to contribute significantlys to the ability of these cells to produce IFN-γ because the Nur77^{GFP} mouse reports weaker TCR signals in these cells and we found APCs in the lung vasculature to be less activated. Additionally, most of the infected cells were in the parenchyma and not in the vasculature. Thus, the hypothesis we favor is that the lung vasculature cells produce IFN-γ in a bystander fashion, perhaps in response to inflammatory cytokines like IL-12 and IL-18 that are highly expressed in the Mtb infected lungs[54,64,144]. We are currently testing this hypothesis. Conversely, it can also be postulated that tissue resident cells are inhibited either by anti-inflammatory cytokines in the lung tissue or by strong and persistent TCR-mediated stimulation, or both. Suppression by persistent TCR signaling is the basis of the experiments discussed in Chapter V whereas inhibition by anti-inflammatory cytokines is the focus of current ongoing experiments.

In summary, we have found that Mtb-specific Th1 cells predominantly localize within the lung vasculature and not the lung parenchyma as previously thought. Furthermore, we found that the Mtb induced granuloma takes the form of and functions like an ectopic lymphoid tissue profoundly affecting lymphocyte migration kinetics during TB.

Chapter V: Persistent antigenic stimulation impairs the function and protective capacity of Mtb-specific CD4 T cells

Introduction

Following infection with Mtb, the bacteria and the host response co-exist in a dynamic equilibrium for a prolonged period, usually for the lifetime of the host[54]. In Chapter III, we found that ESAT-6-specific CD4 T cells are subject to frequent and ongoing antigenic stimulation, but the consequences of this persistent stimulation on the function and protective capacity of these T cells is unknown. In some other disease conditions, persistent antigenic stimulation leads to functional exhaustion of T cells, which is characterized by a hierarchical loss of their ability to produced immune modulatory cytokines[145-147]. In its severe form, functional exhaustion can lead to deletion of antigen-specific clones[148]. In the past, however, Mtb-specific CD4 T cells were thought to retain their functional capacity throughout chronic infection, as evidenced by the robust production of IFN-γ and TNF by Mtb-specific T cells isolated from lungs[30,68,89].

Our findings in Chapter IV, and a recent published report[102]; have caused reconsideration of this idea. Previous studies did not differentiate between Mtb-specific T cells located in the lung-associated vasculature and those residing in the parenchyma of the infected lung. When we labeled T cells located in the vasculature, we found that these cells were the most robust producers of inflammatory cytokines. By comparison, IFN-γ and TNF production by ESAT-6-specific T cells in the lung parenchyma was diminished. We also found that cells in the lung vasculature received relatively weaker TCR signals compared to those in the lung parenchyma. We therefore hypothesized that chronic antigenic stimulation may contribute to the reduced functional capacity of ESAT-6-specific CD4 T cells in the lung.

We investigated this possibility by comparing the functional capacity of CD4 T cells specific for ESAT-6 (an Mtb virulence factor that is expressed throughout infection) to those specific for Ag85B (a mycolyl transferase involved in Mtb cell synthesis) whose expression is reduced after the first three weeks of infection when bacterial replication slows[122]. We found that ESAT-6-specific CD4 T cells, compared to Ag85B-specific cells, were severely limited in their capacity to produce IFN-γ. This reduced functional capacity impacted the ability to control Mtb, because stimulating lung CD4 T cells with Ag85B peptide (but not ESAT-6 peptide) resulted in a reduced bacterial burden in the lung. Our results indicate that CD4 T cells have a limited potential to control Mtb during persistent infection either because their cognate antigen is not expressed, or because it is continuously expressed and triggers functional exhaustion. These findings help explain why Mtb evades immune eradication despite what was previously thought to be a robust Th1 response in the lungs.

ESAT-6 but not Ag85B-specific CD4 T cells are maintained at high levels during Mtb infection

First, we used MHCII tetramers to directly compare the kinetics of ESAT-6 and Ag85B-specific CD4 T cell accumulation and persistence in the lungs of mice after infection with low dose aerosolized Mtb. ESAT-6 and Ag85B specific CD4 T cells were first detected in the lungs ~16 days post infection, when each population accounted for <1% of the lung CD4 T cells (Fig. 5.1A). Both ESAT-6 and Ag85B cells increased in equivalent numbers until the peak of the T cell response at ~28 days post infection, at which point they each accounted for ~6-10% of lung CD4 T cells. After day 28, ESAT-6-specific CD4 T cells were maintained in high numbers for at least 5 months. In contrast, the numbers of Ag85B-specific CD4 T cells decreased dramatically

and were recovered at 10-fold fewer numbers compared to ESAT-6-specific cells between days 52 and 150 post infection (Fig. 5.1A). Additionally, even though both ESAT-6 and Ag85B-specific cells expressed similar levels of PD1 and KLRG1 at the peak of the immune response (~28 days), late in the infection, the Ag85B-specific CD4 T cell population had a reduced proportion of KLRG1^{+} cells (Fig. 5.1B).

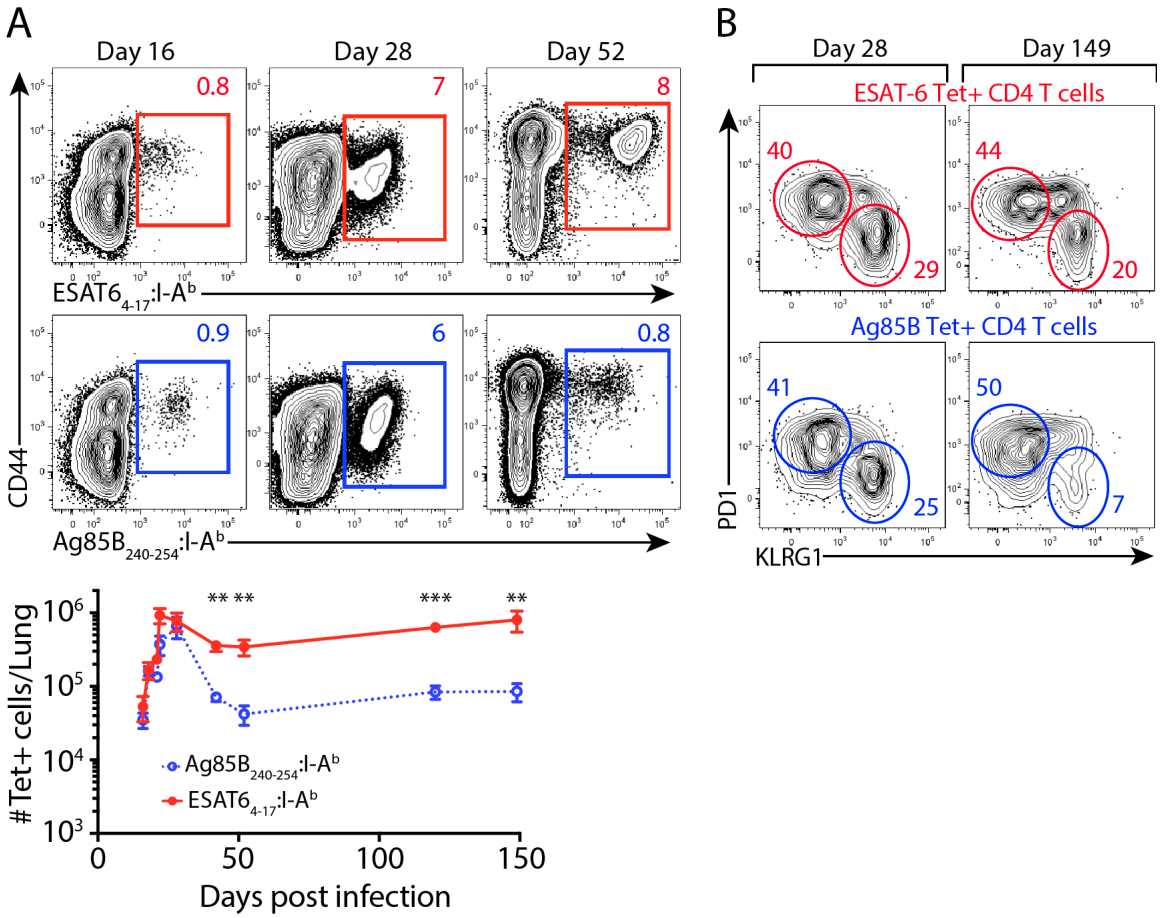

Figure 5.1: ESAT-6 but not Ag85B-specific CD4 T cells are maintained at high levels throughout the course of Mtb infection. A) Representative flow cytometry plots and cumulative data below depict the kinetics of ESAT-6 and Ag85B tetramer binding cells in the lung. B) The representative glow cytometry plots depict PD1 and KLRG1 expression by ESAT-6 and Ag85B-specific CD4 T cells at the time points post infection shown. Data are representative of two independent experiments with 4-5 mice per group and per time point. **P≤0.005, ***P≤0.0005

We postulated that the differences in numbers of ESAT-6 and Ag85B-specific CD4 T cells late during chronic infection were due to disparities in antigen availability, as had been

previously suggested by differences in ESAT-6 and Ag85B mRNA levels in the lungs following Mtb-infections[122]. To directly test this idea we transferred a 1:1 ratio of CFSE labeled, congenically marked CD4 T cells from ESAT-6 Tg (C7) or Ag85B Tg (P25) mice into Mtb-infected mice at various time points. Recipient mice were sacrificed 5 days after transfer and proliferation of donor cells recovered from the lungs was determined by CFSE dilution. We found that both ESAT-6 and Ag85B-specific T cells proliferated to similar degrees (>90% had diluted CFSE) when cells were transferred into mice infected for 10 days (Fig. 5.2A). However the proliferation of transferred cells differed significantly during the chronic phase of infection. Although transferred ESAT-6-specific cells continued to exhibit high levels of proliferation at 4 weeks and 6 months after post-infection, proliferation of Ag85B-specific cells was diminished at these times (Fig. 5.2A).

To test directly whether the reduced proliferation of Ag85B-specific CD4 T cells was due to lack of antigen availability, we generated a strain of Mtb that constitutively express Ag85B (Mtb_Ag85B). When CFSE-labeled ESAT-6 and Ag85B-specific CD4 T cells were transferred into mice infected with Mtb_Ag85B, Ag85B-specific T cells exhibited a high level of proliferation even during the chronic phase of infection (days 35 and 56 post-infection), comparable to that observed for ESAT-6-specific T cells (Fig. 5.2B). In addition, we used MHCII tetramers to track endogenous Mtb-specific CD4 T cells. In contrast to the attrition of Ag85B-specific CD4 T cells (Fig. 5.1A) in mice infected with WT Mtb, ESAT-6-specific and Ag85B-specific CD4 T cells were maintained at equal numbers (Fig. 5.2C) for at least 103 days in mice infected with Mtb_Ag85B. These findings show that Ag85B, compared to ESAT-6, is less available for T cell recognition during chronic infection with WT Mtb, and that this

decreased antigen availability causes increased attrition of Ag85B-specific CD4 T cells and reduced differentiation into KLRG1^{+} effectors.

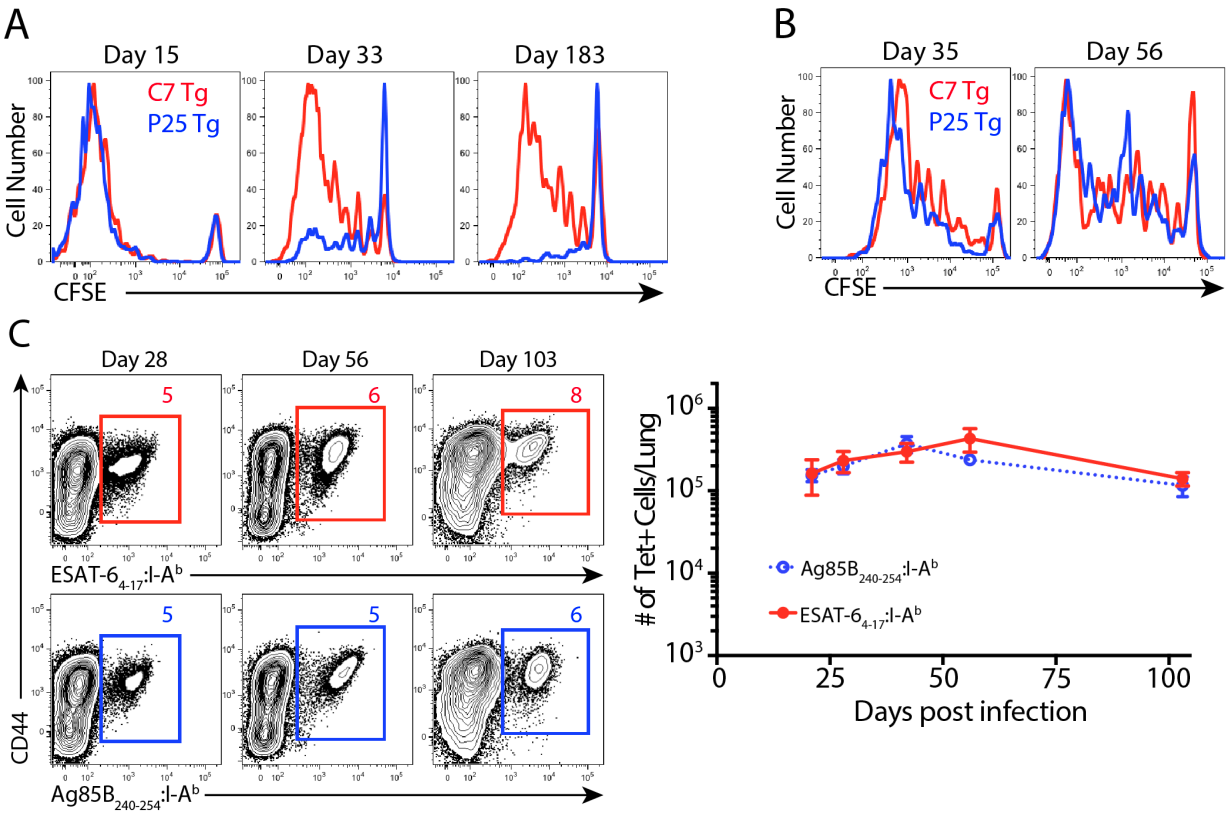

Figure 5.2: Antigen availability dictates the maintenance of Mtb-specific CD4 T cells. A) CFSE labeled C7 and P25 TCR Tg CD4 T cells were adoptively into mice previously infected with WT Mtb. Cells recovered from the lungs 5 days post transfer were assessed for CFSE dilution. Representative histograms depict CFSE dilution by C7 (red) or P25 (blue) TCR Tg cells recovered from the lungs 5 days post transfer. The days shown on the plots are days post infection when the analysis was performed. B) Mice were infected with Mtb that was engineered to express Ag85B (Mtb_Ag85B) constitutively and the experiment described in A was repeated. Representative histograms depict CFSE dilution by C7 (red) and P25 (blue) Tg cells 5 days post transfer. C) Representative flow cytometry plots and cumulative kinetics depicting the frequency (top) or absolute number (bottom) of ESAT-6 and Ag85B tetramer binding cells recovered from mice infected with an Mtb strain that constitutively express Ag85B. D) The representative flow cytometry plots depict PD1 and KLRG1 expression by ESAT-6 and Ag85B-specific CD4 T cells isolated from the lungs of Mtb_Ag85B at days 28 and 56 post infection or WT Mtb at day 52 post infection. Data are from one experiment with 4-5 mice per group and per time point.

Ag85B-specific CD4 T cells exhibit a memory phenotype

Memory T cells are defined as antigen-specific T cells that persist after cessation of antigenic stimulation[115,149]. However, as highlighted in Chapter III of this dissertation, some

antigen-specific CD4 T cells with memory characteristics develop and persist despite chronic antigenic stimulation. Because Ag85B-specific CD4 T cells experience frequent antigenic stimulation during early infection, but reduced stimulation later, we postulated that these cells would exhibit a phenotype more closely resembling memory cells. We found that compared to ESAT-6-specific CD4 T cells, Ag85B-specific cells showed a trend for higher expression of CD62L, but this difference was not statistically significant (Fig. 5.3A). However, Ag85B-specific T cells expressed higher levels of CCR7 (Fig. 5.3B) and CD127 (IL-7Rα) (Fig. 5.3C), even though the expression of these memory-associated molecules did not reach the levels found in naïve or central memory T cells. In summary, these results show that Ag85B-specific cells more closely resemble the phenotype of memory cells than do ESAT-6-specific cells.

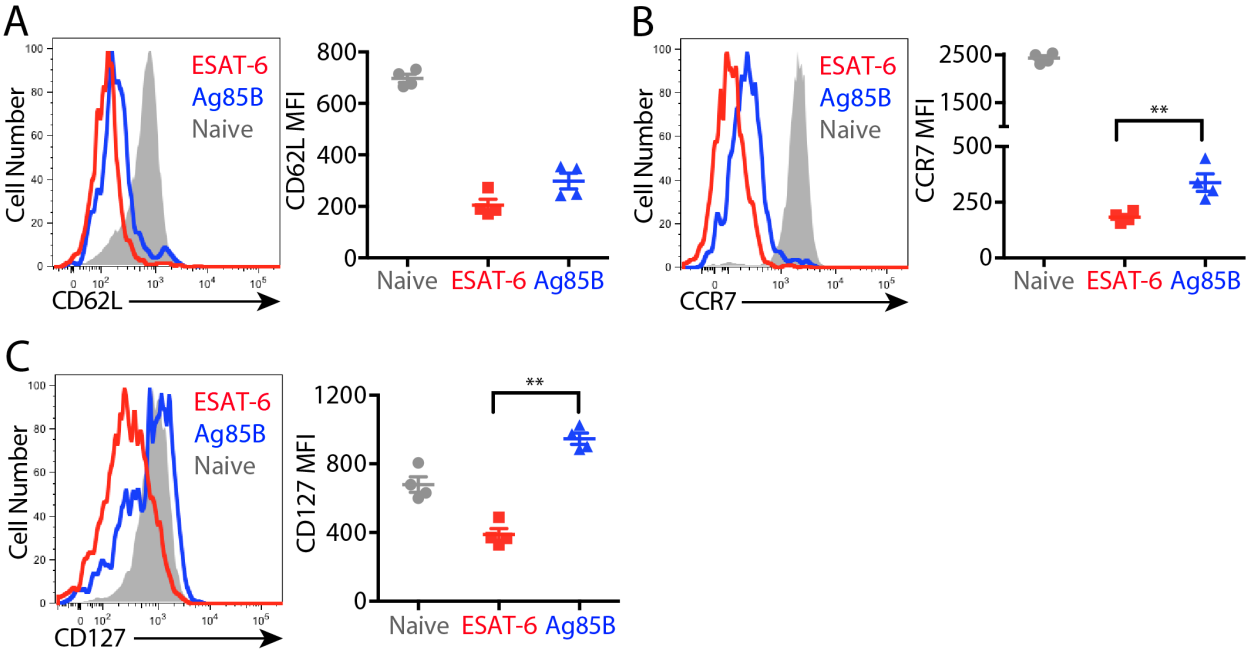

Figure 5.3: Ag85B but not ESAT-6-specific CD4 T cells express memory-associated surface markers: Representative histograms and cumulative data depict MFI of: A) CD62L B) CCR7 and C) CD127 expression by naïve CD44^{low} (gray), Ag85B-specific (blue) and ESAT-6-specific (red) CD4 T cells isolated from the lungs. Data in A are from 4 mice infected for 67 days while B and C are from 4 mice infected for 212 days. $^{***}P \leq 0.0005$

Impaired Th1 functional capacity by ESAT-6- but not Ag85B-specific CD4 T cells

To begin to test this idea, we compared the frequency of ESAT-6-specific T cells or Ag85B-specific T cells detected by either MHCII tetramer staining or by intracellular cytokine staining after in vitro peptide re-stimulation. At early time points after infection (16 days post-infection) we detected similar frequencies of Mtb-specific T cells in the lung using either tetramer or intracellular staining, and this was true for CD4 T cells recognizing either ESAT-6 or Ag85B (Fig. 5.4A).

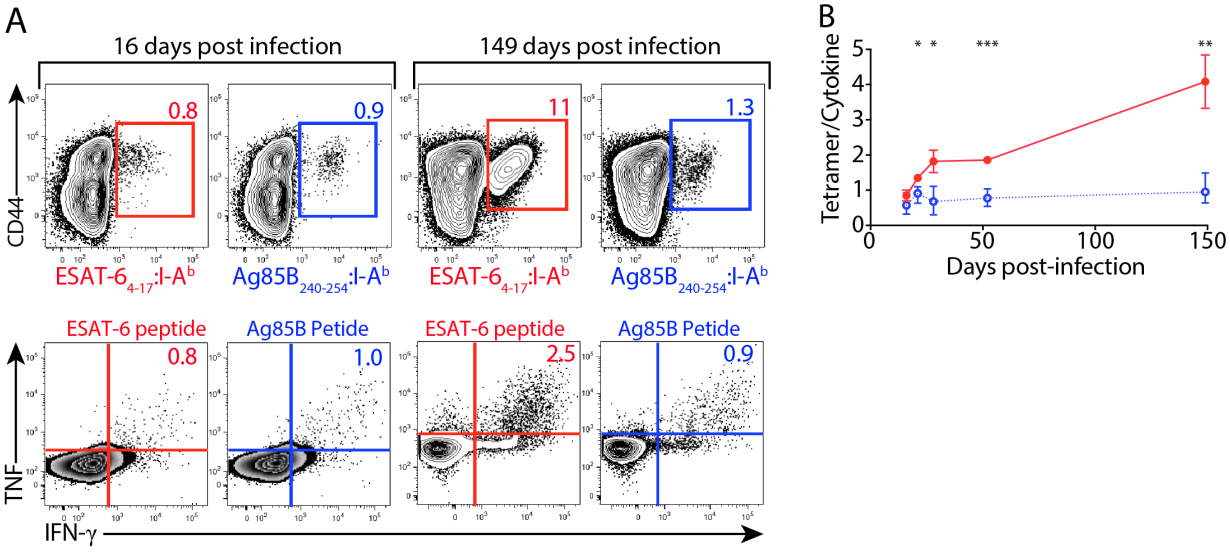

Figure 5.4: ESAT-6 but not Ag85B-specific CD4 T cells have reduced Th1 functional capacity. A) Representative flow cytometry plots depict detection of Mtb-specific CD4 T cells by tetramer staining (top panels) or IFN-γ and TNF co-production following in vitro re-stimulation (bottom panels). Numbers in the panels depict frequency of CD4 T cells that bind tetramer (top) or co-produce IFN-γ and TNF (bottom). Mice were infected for 16 or 149 days with Mtb. ESAT-6 tet$^+$ or cytokine producing cells are shown in red while Ag85B tet$^+$ or cytokine producing cells are shown in blue. B) Graph depicts the ratio of antigen-specific CD4 T cells as defined by tetramer binding vs antigen-specific CD4 T cells as defined by in vitro cytokine production. Data are representative of two independent experiments with 4-5 mice per group and per time point. $^*P\leq0.05$, $^{**}P\leq0.005$ and $^{***}P\leq0.0005$

As the infection progressed, however, the ratio of ESAT-6-specific CD4 T cells detected by tetramer binding compared to intracellular cytokine production gradually increased, and by 5 months post infection we detected ~4 fold more ESAT-6-specific cells by tetramer staining

compared to intracellular cytokine production (Fig. 5.4A and B). In contrast, this ratio remained at ~1:1 for Ag85B-specific T cells throughout the observed course of infection (Fig. 5.4). These results strongly suggest that many ESAT-6-specific CD4 T cells lose their cytokine producing capacity during chronic infection, whereas this function is retained in most Ag85B-specific cells.

Ag85B- but not ESAT-6-specific CD4 T cells have an increased capacity to produce IFN-γ but do not do so in vivo

We next sought to investigate this reduced Th1 functional capacity further by examining cytokine production in vivo within the milieu of the infected lung. We injected 100μg of ESAT-$6_{4\text{-}17}$, $Ag85B_{240\text{-}254}$, or control $OVA_{323\text{-}339}$ peptides i.v into mice and determined cytokine production by tetramer-binding CD4 T cells directly ex vivo (in the absence of in vitro re-stimulation) two hours later. Consistent with our previous assessment of cytokine production in vitro (Figure 5.4), we found that Ag85B-specific CD4 T cells had a dramatically greater capacity to produce IFN-γ than their ESAT-6-specific counterparts. Following infusion of Ag85B peptide, the proportion of tetramer-binding cells producing IFN-γ increased from 27% to 81%, whereas after ESAT-6 infusion, a smaller increase was observed; 31% to 52% (Fig. 5.5A). The differences were even more dramatic when the mean the MFI of IFN-γ expression was assessed on a per cell basis. The IFN-γ MFI in Ag85B-specific T cells increased ~16 fold after peptide infusion, whereas only a ~3 fold increase was observed for ESAT-6-specific CD4 T cells (Fig. 5.5B). Importantly, this enhanced IFN-γ production by Ag85B-specific CD4 T cells was directly due to the fact that they were subjected to less antigenic stimulation during chronic infection; Ag85B-specific CD4 T cells recovered from the lungs of mice infected with Mtb_Ag85B had a reduced capacity to produce IFN-γ that was similar to the capacity of ESAT-6-specific cells (Fig.

5.4B). Despite their increased capacity for IFN-γ production, when mice infected with WT Mtb were assessed directly ex vivo in the absence of peptide infusion, Ag85B-specific CD4 T cells exhibited similar IFN-γ production as ESAT-6-specific cells (Fig. 5.4A). Taken together, these results indicate that cytokine production by ESAT-6-specific T cells is restricted due to chronic antigenic stimulation, whereas cytokine production by Ag85B-specific T cells is limited to a similar degree by reduced antigen availability.

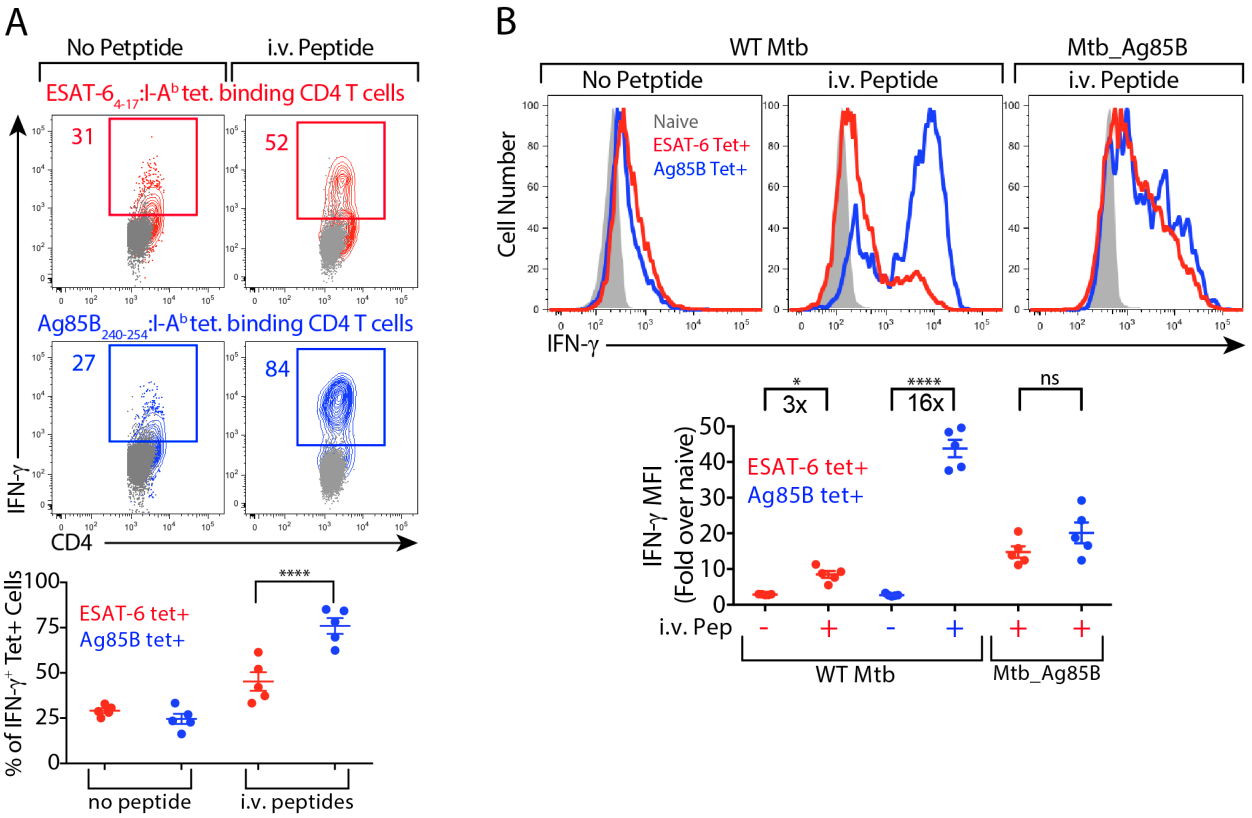

Figure 5.5: Persistent antigenic stimulation contributes to reduced Th1 functional capacity in ESAT-6-specific CD4 T cells. A) Representative flow cytometry plots and cumulative data (bottom panel) depict the proportion of naïve (gray), ESAT-6-specific (red) and Ag85B-specific (blue) lung CD4 T cells that produce IFN-γ in vivo following i.v. infusion of cognate peptides. Mice had been infected with Mtb for 28 days and IFN-γ production was analyzed 2hrs after peptide infusion. B) Representative histograms depict MFI of IFN-γ by naïve (gray), ESAT-6-specific (red) and Ag85B-specific lung CD4 T cells 2hrs after i.v. injection of ESAT-6 or Ag85B peptides. Mice had been infected for 28 days with WT or Mtb constitutively expressing Ag85B, as indicated. Data are from one experiment with 5 mice per group. $^{*}P \leq 0.05$, $^{**}P \leq 0.005$ and $^{****}P \leq 0.0001$

We next investigated whether the capacity of ESAT-6-specific CD4 T cells to produce other cytokines were impaired. We infused mice that had been infected with Mtb 7 months prior with either ESAT-6 or Ag85B peptide and assessed IFN-γ, TNF and IL-2 production in tetramer binding T cells directly ex vivo 2 hours later.

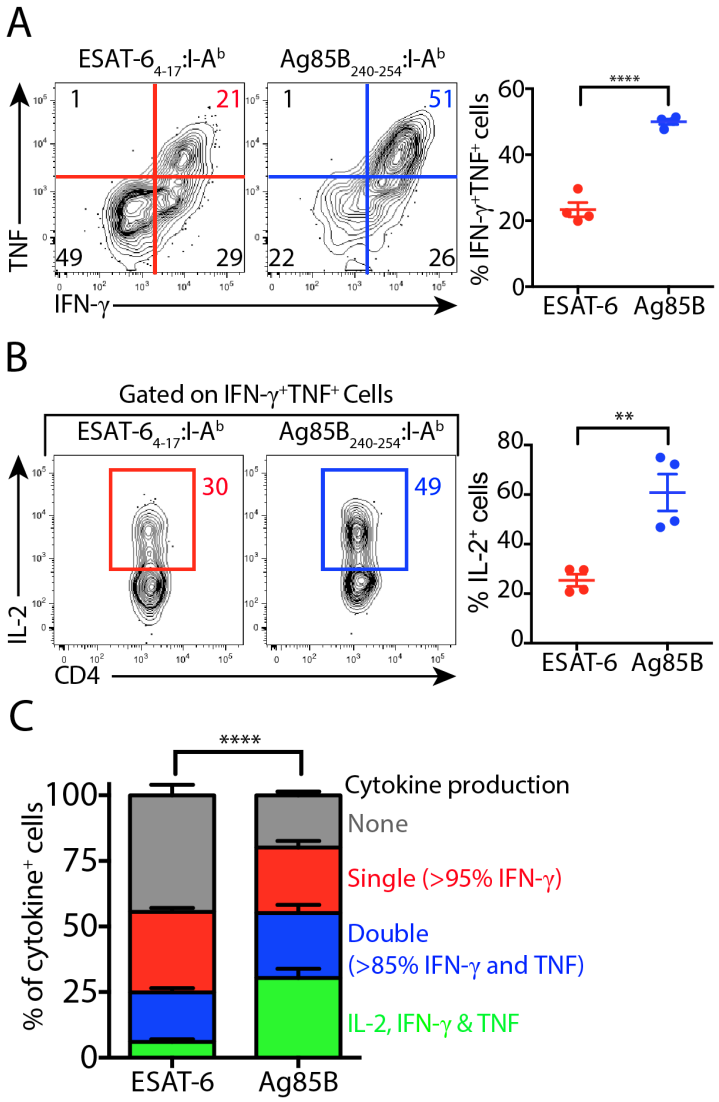

Figure 5.6: ESAT-6- compared to Ag85B-specific CD4 T cells, are impaired in polyfunctional cytokine production. A) Representative flow cytometry plots and cumulative data denote IFN-γ and TNF production by ESAT-6 and Ag85B tetramer-binding cells analyzed directly ex vivo 2hrs after i.v. cognate peptide infusion. B) Representative flow cytometry plots and cumulative data depict IL-2 production by cells gated as indicated that co-produced IFN-γ and TNF. C) Combinatorial analysis for IFN-γ, TNF and IL-2 production. Mice were infected with Mtb for 212 days. Data are representative of 2 independent experiments with 4-5 mice per group. $^{**}P \leq 0.005$ and $^{****}P \leq 0.0001$

We found that ~50% of Ag85B-specific CD4 T cells co-produced IFN-γ and TNF, whereas only about ~20% of the ESAT-6-specific CD4 T cells did (Fig. 5.6A). Furthermore, over half of the Ag85B-specific cells that produced both IFN-γ and TNF also produced IL-2, whereas only 20-30% of this population produced IL-2 amongst ESAT-6-specific cells (Fig. 5.6B). Nevertheless, for both ESAT-6 and Ag85B specific CD4 T cells, IL-2 production was almost exclusively restricted to the cells that co-produced IFN-γ and TNF. Overall, ~30% of Ag85B-specific CD4 T cells were capable of triple cytokine production compared to only ~6% of ESAT-6-specific cells (Fig. 5.5C). Combined, these results indicated that there is a severe and generalized defect in cytokine producing capacity by ESAT-6-specific CD4 T cells during chronic Mtb infections.

Provision of additional cognate Ag85B but not ESAT-6 leads to enhanced bacteria control

We investigated whether the functional impairment of ESAT-6-specific CD4 T cells restricted their ability to control lung bacterial burdens. Three weekly infusions of either ESAT-6 or Ag85B peptide were administered to Mtb infected mice beginning on day 25 post-infection. Control mice received a peptide of irrelevant specificity (OVA). Three days after the last peptide dose (day 42 post-infection), the frequency of Ag85B and ESAT-6-specific lung CD4 T cells and the lung bacterial burdens were assessed. As expected, Ag85B-specific CD4 T cells were reduced by 10-fold in control mice receiving OVA peptide. In mice receiving Ag85B peptide, however, Ag85B-specific CD4 T cells were recovered at numbers close to those for ESAT-6-specific cells (Fig. 5.7A), and even more importantly, exhibited a ~5 fold reduction in lung bacterial burden (Fig. 5.6B). In contrast, administration of ESAT-6 peptide did not alter the number of ESAT-6-specific CD4 T cells recovered from the lung, and had no effect on the bacterial load. When Ag85B peptide was administered to mice infected with Mtb_Ag85B, it had

no effect on the lung bacterial burden (Fig. 5.6C). Thus, stimulating Ag85B-specific CD4 T cells with exogenous peptide conferred protection in excess to that provided by ESAT-6-specific CD4 T cells, despite their ongoing stimulation by Mtb-derived antigens. Overall, our results demonstrate that chronic antigenic stimulation of Mtb-specific CD4 T cells limits their capacity to control bacterial burdens in the lung.

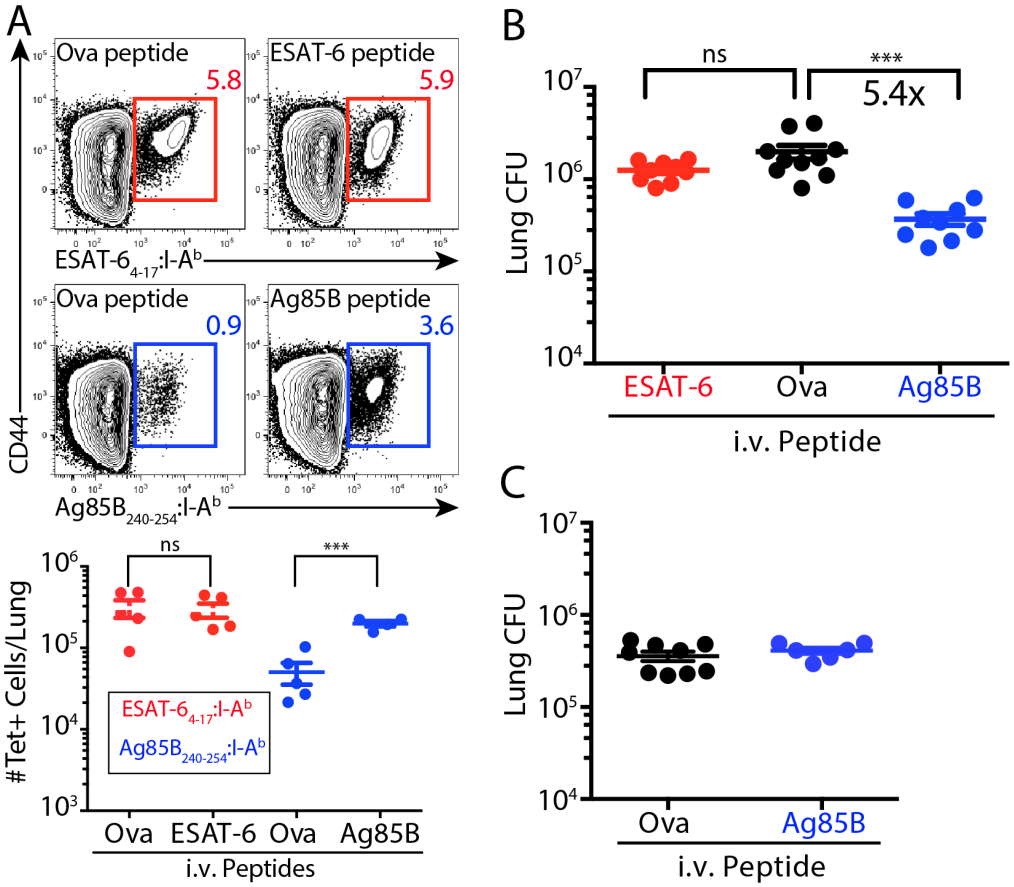

Figure 5.7: Peptide infusions increases the protection conferred by Ag85B- but not ESAT-6-specific CD4 T cells: A) Representative flow cytometry plots and cumulative data below depict the frequency and absolute number of ESAT-6- and Ag85B-specific CD4 T cells recovered from mice treated with 3 weekly i.v. peptide doses. Mice received ESAT-6, Ag85B or Ova peptides and were sacrificed 42 days post infection. B) Lung bacterial burdens in mice described in A. C) Mice were infected with Mtb_Ag85B and treated with 3 weekly i.v. Ag85B or Ova peptides and lung bacterial burdens determined. Mice were sacrificed 42 days post infection. Data are from one experiment with 6-10 mice per group. $^{***}P \leq 0.0005$

Identifying regulators of immune dysfunction in chronically stimulated Mtb-specific CD4 T cells through genome-wide transcriptional profiling

To identify candidate regulators of the immune dysfunction observed in ESAT-6-specific CD4 T cells, we performed whole genome RNA sequencing of ESAT-6 and Ag85B-specific CD4 T cells in the presence and absence of in vivo peptide stimulation. Mtb-infected mice (42 days post-infection) were co-injected i.v. with ESAT-6 and Ag85B-peptides, whereas controls received Ova peptide. Two hours later, $CD44^{low}$, ESAT-6 and Ag85B tetramer-binding CD4 T cells were isolated from the lungs. RNA was isolated and after quantification, identical amounts of RNA from each population were amplified in a linear manner and sequenced. Using principal component analysis samples from each group clustered with themselves and differentially from samples from other groups (Fig. 5.8A). Furthermore, $CD44^{low}$ samples were quite different compared to the other samples containing tetramer-binding cells. In addition, samples containing unstimulated cells (sorted from mice receiving Ova peptide) and samples containing peptide-stimulated cells were also distinct, but even within each of these groups Ag85B and ESAT-6-specific cells separated nicely into distinct groups. Because the analysis was performed in an unbiased manner, the fact that samples from each group clustered together validates the analysis.

Next, we identified genes that were differentially expressed between unstimulated and stimulated ESAT-6 or Ag85B tetramer-binding cells. A total of 3314 genes were differentially expressed among the groups and were plotted as a Venn diagram to identify differentially expressed genes common among the groups (Fig. 5.8B). Of the 1179 genes that showed increased expression in stimulated ESAT-6-specific cells, 755 were also up regulated in stimulated Ag85B-specific cells, whereas 421 were unique. Likewise, of the 1372 genes that

showed decreased expression in stimulated ESAT-6-specific cells, 620 were also down regulated in stimulated Ag85B-specific cells, whereas 749 were unique.

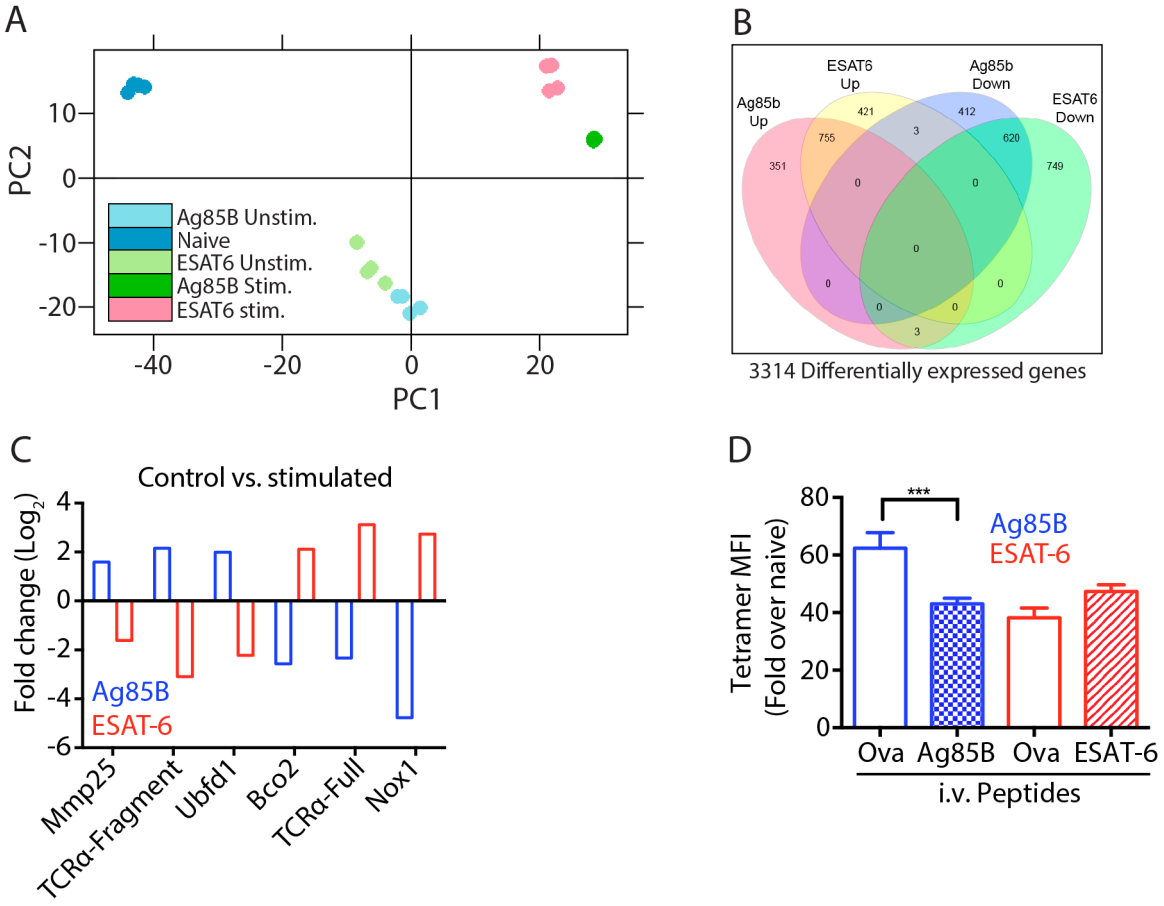

Figure 5.8: Differential gene expression profile by Ag85B and ESAT-6-specific CD4 T cells following in vivo peptide stimulation. Lung CD4 T cells were sorted as naïve $CD44^{low}CCR7^{hi}$, ESAT-6-specific $PD1^{+}$ cells and Ag85B-specific $PD1^{+}$ from day 42 Mtb infected mice. Control mice were i.v. injected with 50µg Ova peptide while the stimulated group was co-injected with 50µg each of ESAT-6 and Ag85B peptides 2hrs before sacrifice. A) Principal component analysis of RNAseq data. B) Venn diagrams depicting overlap of differentially-expressed genes among the groups following i.v. peptide stimulation. C) Some differentially-expressed genes when comparing control vs. peptide stimulated Ag85B and ESAT-6-specific CD4 T cells. D) Flow cytometry data depicting tetramer MFI after 2hrs of in vivo peptide stimulation. Data are from one experiment with 4 mice pooled to make one replicate and with 4 replicates per group. $^{***}P \leq 0.0005$

Intriguingly, the analysis revealed three genes that were up regulated in Ag85B-specific cells, but down regulated in ESAT-6-specific cells after peptide stimulation (Table 1) and another set of three genes that were up regulated in ESAT-6-specific cells, but down regulated in Ag85B-specific cells after peptide stimulation (Table 2).

Gene	Reported function
Mmmp25	Glycosyl-Phosphatidyl-Inositol (GPI)-linked cell surface metalloproteinase involved in the breakdown of extracellular matrix that has been implicated in tumor invasion and metastasis
TCRα fragment	Unclear function
Ubfd1	Ubiquitin domain-containing protein 1, a protein that binds polyubiquitinated protein and has been suggested to be a regulator of NF-kappa-B

Table 1: Genes up-regulated in Ag85B but down-regulated in ESAT-6-specific CD4 T cells following in vivo peptide stimulation.

Gene	Reported function
Bco2	Beta carotene oxygenase 2, an enzyme involved in vitamin A biosynthesis
TCRα (full length)	Unclear function
Nox1	NADPH oxidase 1, an enzyme involved in the generation of reactive oxygen species

Table 2: Genes up-regulated in ESAT-6 but down-regulated in Ag85B-specific CD4 T cells following in vivo peptide stimulation.

This outcome was not restricted with RNA data: analysis of the MFI of tetramer binding revealed that the binding capacity of Ag85B declined significantly following peptide stimulation, but showed a trend toward increase even though it was not statistically significant (Fig. 5.8D) likely reflecting the expression levels of TCR alpha and beta chains. These data suggest that these opposite expression profiles reflect real differences even at the protein level (at least for TCRα expression), and investigating the functional consequences of these differences should be a rich area for future studies.

Discussion

One of the major unsolved questions in the immunology of TB is why the host immune response is unable to eradicate Mtb despite an apparent abundance of IFN-γ producing T cells in

the lung, the primary site of infection. In Chapters III and IV we showed that most IFN-γ producing CD4 effector T cells do not reside in the lung parenchyma, as previously had been assumed, but instead are located in the lung-associated vasculature. In this chapter, we extend these findings to show that Mtb-specific CD4 T cells located in the lung parenchyma are restricted in their capacity to control chronic Mtb infection for two distinct and opposite reasons. Some are limited because of reduced expression of their cognate antigen during chronic infection (e.g., Ag85B), whereas CD4 T cells recognizing different Mtb antigens (e.g., ESAT-6) become functionally compromised due to chronic antigenic exposure. These findings have important implications for designing T cell-based vaccines and therapeutic approaches to prevent and treat TB.

As outlined in Chapter I, a major obstacle to the host immune response to TB is the prolonged period in which Mtb is allowed to replicate and establish a niche before the arrival of Mtb-specific T cells in the lung. This delayed T cell response is orchestrated by Mtb and caused by two factors: 1) the delayed transport of Mtb from the lung to the pLN, and 2) the inhibition of effector T cell expansion in the pLN by Mtb-specific regulatory T cells[41,43,47-49]. The end result of this delay is that Th1 cells do not get to the lungs (the site of infection) in sufficient numbers to curb Mtb replication until day 21 post infection and do not reach peak numbers until 28-35 days post infection. Our findings indicate that by the time T cells arrive in the lungs, the bacterial burden and antigenic load that they encounter rapidly leads to their exhaustion. Confounding the problem further is that the inflammatory milieu in the lung at the time of T cell arrival contains high levels of anti-inflammatory cytokines (e.g. TGFβ and IL-10) and lipid mediators (lipoxins) that severely limit the function of Th1 cells [68-71]. Thus, our results helps explain why early T cell

recognition of Mtb-infected cells within the lung, before Mtb establishes a high bacterial burden, is associated with enhanced immune control over Mtb.

This idea is supported by mathematical modeling and animal studies that show that the best correlate with protection against Mtb is the rapidity by which T cells get into the lung [49,59,60]. For example, airway vaccination with BCG confers better protection than the parenteral route largely because it induces effector T cells in the airway that can respond rapidly to Mtb after aerosol infection[59,60]. Conversely, parenteral vaccination with BCG or a secondary immune response following treatment of the primary Mtb infection accelerates the arrival of T cells in the lungs by only 2-3 days[59,60,150]. However, many unanswered questions remain. A recent study showed that i.v. transfer of Mtb-specific Th1 cells provided no detectable protection for the first week following Mtb challenge[96]. These results have led to the idea that alveolar macrophages do not present MHCII-restricted Mtb epitopes during the first week of infection. However, we believe it is likely that i.v. transferred T cells did not reach the site of initial infection in the airways. Addressing how early it is possible for T cells to recognize Mtb-infected cells, and the degree to which early recognition can mediate protection, is a major focus of my current work, and will provide a nice complement to the studies presented here.

Our findings also question whether vaccines should target rare or subdominant epitopes as opposed to the current practice of targeting immunodominant epitopes. Perhaps epitopes expressed throughout infection at low levels, or epitopes that T cells recognize with low affinity would drive less T cell exhaustion. In support of this conclusion a recent study showed that immunization with recombinant ESAT-6 protein lacking the immunodominant epitope revealed cryptic responses to subdominant epitopes that were not seen after immunization with the full-

length protein[107]. Responses to these subdominant epitopes were qualitatively different from the response to the immunodominant epitope and conferred superior and more durable protection.

Our results also suggest potential avenues for novel immunotherapeutic interventions. Consistent with previous reports[100,121,122], we found that Ag85B expression (and probably several other Mtb antigens including Ag85B family) is reduced during chronic infection. CD4 T cells recognizing these antigens remain functionally competent, but contribute little to immunity because of the low expression of their cognate antigen. While a previous report showed that mice treated with daily Ag85B infusions had a slightly reduced lung bacterial burden (a two-fold difference)[100], treatments with other peptides such as ESAT-6 were not performed. In our studies, we observed better efficacy when the peptide infusions were performed weekly (~5-fold difference), probably because rest periods between stimulations helps T cells maintain their functional competency. Although these studies provide a starting point for investigating whether antigen infusion may have therapeutic potential, a five-fold difference in bacterial load may be insufficient for clinical relevance. However, it is possible that greater efficacy could be achieved by combining antigen infusions with other approaches to augment the protective T cell response. For example, our findings in Chapter IV suggest that effector T cells with high IFN-γ producing capacity may leave the lung in an S1PR-dependent manner. If this hypothesis is validated, blocking this egress may provide additional benefit. In addition, we have preliminary data suggesting that intrinsic TGFβR signaling in T-bet^{hi} CD4 T cells severely impacts their survival in the inflammatory milieu of the lung parenchyma (data not shown). Thus modification of T cell migration kinetics by use of S1P agonists (e.g. Fingolimolid) or enhancing the Th1 functional capacity (and/or survival) of Mtb-specific CD4 T cells by inhibition of TGFβ signaling may represent other complementary immunotherapeutic targets. Fingolimolid is currently approved

for treatment of multiple sclerosis and several inhibitors of TGFβ signaling are currently being tested in clinical trials in the cancer field[59,141]. Experience with these agents in the clinical arena could help facilitate their usage for TB should their efficacy be established.

Finally, another potential avenue for immunotherapy might be to reverse the functional exhaustion of chronically stimulated CD4 T cells, such as those recognizing ESAT-6. Even in the exhausted state, T cells are likely able to mediate some protection[52], but our studies clearly show that the protection provided by ESAT-6-specific CD4 T cells is suboptimal, at best. Although the PD-1 pathway has been targeted therapeutically to reverse T cell exhaustion in chronic viral and parasitic infections and in cancer[123,124,151], this approach is unlikely to be effective in TB because PD1 has a host-protective role[108,109]. Comparative analysis of the genome wide transcriptional analysis of Ag85B and ESAT-6-specific CD4 T cells with and without peptide stimulation should reveal novel regulators of the immune dysfunction of chronically-stimulated CD4 T cells. Once these candidate regulators are identified, future efforts will seek to validate their precise role. Use of inhibitors of these regulatory networks, likely in conjunction with antibiotic therapy, may provide new avenues to shorten treatment and improve outcomes for multi-drug resistant TB, which currently requires up to two years of treatment, at a cost of ~$250,000/patient, and still carries a high mortality rate.

Summary

Our findings provide a new framework for understanding the CD4 T cell response to TB. In Chapter III, we found that Mtb-specific CD4 T cells are subject to chronic antigenic stimulation, yet exhibit memory-like properties and are maintained by ICOS and Bcl6 dependent pathways. In Chapter IV, we show that PD-1^{+} CD4 T cells with memory properties reside within the parenchyma of the lung, whereas $KLRG1^{+}$ terminally differentiated Th1 cells primarily reside in the lung associated vasculature. Our data suggest a completely new model for understanding how CD4 T cells traffic through the lung during TB. Because the granuloma is a tertiary lymphoid structure, egress of terminally differentiated T cells into the blood via S1P1R signaling may be inherent to the biology of such structures. In Chapter V, we show that the particular Mtb antigen that is recognized shapes the location and function of Mtb-specific CD4 T cells. CD4 T cells that recognize persistently expressed antigens become functionally exhausted and are restricted in their ability to control Mtb. Combined; these findings have important implications for devising new vaccines and immunotherapeutics to combat TB.

References

1. [The etiology of tuberculosis by Dr. Robert Koch. From the Berliner Klinische Wochenschrift, Volume 19 (1882)]. *Zentralbl Bakteriol Mikrobiol Hyg A* **251**, 287-96 (1982).

2. Barrera, L. & De Kantor, I.N. Nontuberculous mycobacteria and Mycobacterium bovis as a cause of human disease in Argentina. *Trop Geogr Med* **39**, 222-7 (1987).

3. Mfinanga, S.G. *et al.* Mycobacterial adenitis: role of Mycobacterium bovis, non-tuberculous mycobacteria, HIV infection, and risk factors in Arusha, Tanzania. *East Afr Med J* **81**, 171-8 (2004).

4. Piersimoni, C. & Scarparo, C. Pulmonary infections associated with non-tuberculous mycobacteria in immunocompetent patients. *Lancet Infect Dis* **8**, 323-34 (2008).

5. Wolf, A.J. *et al.* Mycobacterium tuberculosis infects dendritic cells with high frequency and impairs their function in vivo. *J Immunol* **179**, 2509-19 (2007).

6. Clark, R.A. *et al.* Hematogenous dissemination of Mycobacterium tuberculosis in patients with AIDS. *Rev Infect Dis* **13**, 1089-92 (1991).

7. Jarvis, J.N. *et al.* Adult meningitis in a setting of high HIV and TB prevalence: findings from 4961 suspected cases. *BMC Infect Dis* **10**, 67 (2010).

8. Chackerian, A.A., Alt, J.M., Perera, T.V., Dascher, C.C. & Behar, S.M. Dissemination of Mycobacterium tuberculosis is influenced by host factors and precedes the initiation of T-cell immunity. *Infect Immun* **70**, 4501-9 (2002).

9. CDC. Transmission and Pathogenesis of Tuberculosis. in *Tuberculosis (TB)* Vol. 2014 (http://www.cdc.gov/tb/default.htm).

10. WHO. Global tuberculosis report 2013. in *Geneva, World Health Organization* (2013).

11. Shea, K.M., Kammerer, J.S., Winston, C.A., Navin, T.R. & Horsburgh, C.R., Jr. Estimated rate of reactivation of latent tuberculosis infection in the United States, overall and by population subgroup. *Am J Epidemiol* **179**, 216-25 (2014).

12. Feldman, W.H. & Baggenstoss, A.H. The occurrence of virulent tubercle bacilli in presumably non-tuberculous lung tissue. *Am J Pathol* **15**, 501-15 (1939).

13. Barry, C.E., 3rd *et al.* The spectrum of latent tuberculosis: rethinking the biology and intervention strategies. *Nat Rev Microbiol* **7**, 845-55 (2009).

14. Lin, P.L. & Flynn, J.L. Understanding latent tuberculosis: a moving target. *J Immunol* **185**, 15-22 (2010).

15. Narain, J.P., Raviglione, M.C. & Kochi, A. HIV-associated tuberculosis in developing countries: epidemiology and strategies for prevention. *Tuber Lung Dis* **73**, 311-21 (1992).

16. Trunz, B.B., Fine, P. & Dye, C. Effect of BCG vaccination on childhood tuberculous meningitis and miliary tuberculosis worldwide: a meta-analysis and assessment of cost-effectiveness. *Lancet* **367**, 1173-80 (2006).

17. Arguin, P.M., Marano, N. & Freedman, D.O. Globally mobile populations and the spread of emerging pathogens. *Emerg Infect Dis* **15**, 1713-4 (2009).

18. WHO. Multidrug and extensively drug-resistant TB (M/XDR-TB) : 2010 global report on surveillance and response - See more at: http://apps.who.int/iris/handle/10665/44286_-sthash.t0YTnpWT.dpuf. (2010).

19. Andersen, P. TB vaccines: progress and problems. *Trends Immunol* **22**, 160-8 (2001).

20. Targeted tuberculin testing and treatment of latent tuberculosis infection. American Thoracic Society. *MMWR Recomm Rep* **49**, 1-51 (2000).

21. Linas, B.P., Wong, A.Y., Freedberg, K.A. & Horsburgh, C.R., Jr. Priorities for screening and treatment of latent tuberculosis infection in the United States. *Am J Respir Crit Care Med* **184**, 590-601 (2011).

22. Bayer, R. *et al.* Directly observed therapy and treatment completion for tuberculosis in the United States: is universal supervised therapy necessary? *Am J Public Health* **88**, 1052-8 (1998).

23. Lienhardt, C. & Ogden, J.A. Tuberculosis control in resource-poor countries: have we reached the limits of the universal paradigm? *Trop Med Int Health* **9**, 833-41 (2004).

24. Roeder, P.L. Rinderpest: the end of cattle plague. *Prev Vet Med* **102**, 98-106 (2011).

25. Whitty, C.J. Milroy Lecture: eradication of disease: hype, hope and reality. *Clin Med* **14**, 419-21 (2014).

26. Salerno-Goncalves, R. & Sztein, M.B. Cell-mediated immunity and the challenges for vaccine development. *Trends Microbiol* **14**, 536-42 (2006).

27. Gershon, A.A. The current status of live attenuated varicella vaccine. *Arch Virol Suppl*, 1-6 (2001).

28. Seder, R.A. & Hill, A.V. Vaccines against intracellular infections requiring cellular immunity. *Nature* **406**, 793-8 (2000).

29. Andersen, P. & Woodworth, J.S. Tuberculosis vaccines - rethinking the current paradigm. *Trends Immunol* (2014).

30. Leal, I.S., Smedegard, B., Andersen, P. & Appelberg, R. Failure to induce enhanced protection against tuberculosis by increasing T-cell-dependent interferon-gamma generation. *Immunology* **104**, 157-61 (2001).

31. Guirado, E., Schlesinger, L.S. & Kaplan, G. Macrophages in tuberculosis: friend or foe. *Semin Immunopathol* **35**, 563-83 (2013).

32. Cambier, C.J. *et al.* Mycobacteria manipulate macrophage recruitment through coordinated use of membrane lipids. *Nature* **505**, 218-22 (2014).

33. Flynn, J.L. & Chan, J. Immune evasion by Mycobacterium tuberculosis: living with the enemy. *Curr Opin Immunol* **15**, 450-5 (2003).

34. Fang, F.C. Antimicrobial reactive oxygen and nitrogen species: concepts and controversies. *Nat Rev Microbiol* **2**, 820-32 (2004).

35. Ehrt, S. & Schnappinger, D. Mycobacterial survival strategies in the phagosome: defence against host stresses. *Cell Microbiol* **11**, 1170-8 (2009).

36. Deretic, V. *et al.* Mycobacterium tuberculosis inhibition of phagolysosome biogenesis and autophagy as a host defence mechanism. *Cell Microbiol* **8**, 719-27 (2006).

37. Divangahi, M., Behar, S.M. & Remold, H. Dying to live: how the death modality of the infected macrophage affects immunity to tuberculosis. *Adv Exp Med Biol* **783**, 103-20 (2013).

38. Tian, T., Woodworth, J., Skold, M. & Behar, S.M. In vivo depletion of CD11c+ cells delays the CD4+ T cell response to Mycobacterium tuberculosis and exacerbates the outcome of infection. *J Immunol* **175**, 3268-72 (2005).

39. Andersson, H. *et al.* Apoptotic Neutrophils Augment the Inflammatory Response to Mycobacterium tuberculosis Infection in Human Macrophages. *PLoS One* **9**, e101514 (2014).

40. Blomgran, R., Desvignes, L., Briken, V. & Ernst, J.D. Mycobacterium tuberculosis inhibits neutrophil apoptosis, leading to delayed activation of naive CD4 T cells. *Cell Host Microbe* **11**, 81-90 (2012).

41. Urdahl, K.B., Shafiani, S. & Ernst, J.D. Initiation and regulation of T-cell responses in tuberculosis. *Mucosal Immunol* **4**, 288-93 (2011).

42. Reiley, W.W. *et al.* ESAT-6-specific CD4 T cell responses to aerosol Mycobacterium tuberculosis infection are initiated in the mediastinal lymph nodes. *Proc Natl Acad Sci U S A* **105**, 10961-6 (2008).

43. Wolf, A.J. *et al.* Initiation of the adaptive immune response to Mycobacterium tuberculosis depends on antigen production in the local lymph node, not the lungs. *J Exp Med* **205**, 105-15 (2008).

44. Samstein, M. *et al.* Essential yet limited role for CCR2+ inflammatory monocytes during Mycobacterium tuberculosis-specific T cell priming. *Elife (Cambridge)* **2**, e01086 (2013).

45. Srivastava, S. & Ernst, J.D. Cutting edge: Direct recognition of infected cells by CD4 T cells is required for control of intracellular Mycobacterium tuberculosis in vivo. *J Immunol* **191**, 1016-20 (2013).

46. Srivastava, S. & Ernst, J.D. Cell-to-cell transfer of M. tuberculosis antigens optimizes CD4 T cell priming. *Cell Host Microbe* **15**, 741-52 (2014).

47. Scott-Browne, J.P. *et al.* Expansion and function of Foxp3-expressing T regulatory cells during tuberculosis. *J Exp Med* **204**, 2159-69 (2007).

48. Shafiani, S. *et al.* Pathogen-specific Treg cells expand early during mycobacterium tuberculosis infection but are later eliminated in response to Interleukin-12. *Immunity* **38**, 1261-70 (2013).

49. Shafiani, S., Tucker-Heard, G., Kariyone, A., Takatsu, K. & Urdahl, K.B. Pathogen-specific regulatory T cells delay the arrival of effector T cells in the lung during early tuberculosis. *J Exp Med* **207**, 1409-20 (2010).

50. Scanga, C.A. *et al.* Depletion of CD4(+) T cells causes reactivation of murine persistent tuberculosis despite continued expression of interferon gamma and nitric oxide synthase 2. *J Exp Med* **192**, 347-58 (2000).

51. Deffur, A., Mulder, N.J. & Wilkinson, R.J. Co-infection with Mycobacterium tuberculosis and human immunodeficiency virus: an overview and motivation for systems approaches. *Pathog Dis* **69**, 101-13 (2013).

52. Diedrich, C.R. & Flynn, J.L. HIV-1/mycobacterium tuberculosis coinfection immunology: how does HIV-1 exacerbate tuberculosis? *Infect Immun* **79**, 1407-17 (2011).

53. Muller, I., Cobbold, S.P., Waldmann, H. & Kaufmann, S.H. Impaired resistance to Mycobacterium tuberculosis infection after selective in vivo depletion of L3T4+ and Lyt-2+ T cells. *Infect Immun* **55**, 2037-41 (1987).

54. Cooper, A.M. Cell-mediated immune responses in tuberculosis. *Annu Rev Immunol* **27**, 393-422 (2009).

55. Clay, H., Volkman, H.E. & Ramakrishnan, L. Tumor necrosis factor signaling mediates resistance to mycobacteria by inhibiting bacterial growth and macrophage death. *Immunity* **29**, 283-94 (2008).

56. Gallegos, A.M. *et al.* A gamma interferon independent mechanism of CD4 T cell mediated control of M. tuberculosis infection in vivo. *PLoS Pathog* **7**, e1002052 (2011).

57. Herbst, S., Schaible, U.E. & Schneider, B.E. Interferon gamma activated macrophages kill mycobacteria by nitric oxide induced apoptosis. *PLoS One* **6**, e19105 (2011).

58. Vandal, O.H., Pierini, L.M., Schnappinger, D., Nathan, C.F. & Ehrt, S. A membrane protein preserves intrabacterial pH in intraphagosomal Mycobacterium tuberculosis. *Nat Med* **14**, 849-54 (2008).

59. Beverley, P.C., Sridhar, S., Lalvani, A. & Tchilian, E.Z. Harnessing local and systemic immunity for vaccines against tuberculosis. *Mucosal Immunol* **7**, 20-6 (2014).

60. Tchilian, E.Z. *et al.* Simultaneous immunization against tuberculosis. *PLoS One* **6**, e27477 (2011).

61. Heitmann, L. *et al.* The IL-13/IL-4R-alpha axis is involved in tuberculosis-associated pathology. *J Pathol* (2014).

62. Crotty, S. Follicular helper CD4 T cells (TFH). *Annu Rev Immunol* **29**, 621-63 (2011).

63. Torrado, E. & Cooper, A.M. IL-17 and Th17 cells in tuberculosis. *Cytokine Growth Factor Rev* **21**, 455-62 (2010).

64. Khader, S.A. *et al.* IL-23 is required for long-term control of Mycobacterium tuberculosis and B cell follicle formation in the infected lung. *J Immunol* **187**, 5402-7 (2011).

65. Schaible, U.E. *et al.* Apoptosis facilitates antigen presentation to T lymphocytes through MHC-I and CD1 in tuberculosis. *Nat Med* **9**, 1039-46 (2003).

66. Urdahl, K.B., Liggitt, D. & Bevan, M.J. CD8+ T cells accumulate in the lungs of Mycobacterium tuberculosis-infected Kb-/-Db-/- mice, but provide minimal protection. *J Immunol* **170**, 1987-94 (2003).

67. Lin, P.L. *et al.* Sterilization of granulomas is common in active and latent tuberculosis despite within-host variability in bacterial killing. *Nat Med* **20**, 75-9 (2014).

68. Abebe, F., Mustafa, T., Nerland, A.H. & Bjune, G.A. Cytokine profile during latent and slowly progressive primary tuberculosis: a possible role for interleukin-15 in mediating clinical disease. *Clin Exp Immunol* **143**, 180-92 (2006).

69. Maglione, P.J., Xu, J. & Chan, J. B cells moderate inflammatory progression and enhance bacterial containment upon pulmonary challenge with Mycobacterium tuberculosis. *J Immunol* **178**, 7222-34 (2007).

70. Naundorf, S. *et al.* IL-10 interferes directly with TCR-induced IFN-gamma but not IL-17 production in memory T cells. *Eur J Immunol* **39**, 1066-77 (2009).

71. Toossi, Z., Gogate, P., Shiratsuchi, H., Young, T. & Ellner, J.J. Enhanced production of TGF-beta by blood monocytes from patients with active tuberculosis and presence of TGF-beta in tuberculous granulomatous lung lesions. *J Immunol* **154**, 465-73 (1995).

72. Denis, M. Killing of Mycobacterium tuberculosis within human monocytes: activation by cytokines and calcitriol. *Clin Exp Immunol* **84**, 200-6 (1991).

73. Pearl, J.E. *et al.* Nitric oxide inhibits the accumulation of CD4+CD44hiTbet+CD69lo T cells in mycobacterial infection. *Eur J Immunol* **42**, 3267-79 (2012).

74. Schwab, S.R. & Cyster, J.G. Finding a way out: lymphocyte egress from lymphoid organs. *Nat Immunol* **8**, 1295-301 (2007).

75. Comerford, I. *et al.* A myriad of functions and complex regulation of the CCR7/CCL19/CCL21 chemokine axis in the adaptive immune system. *Cytokine Growth Factor Rev* **24**, 269-83 (2013).

76. Shiow, L.R. *et al.* CD69 acts downstream of interferon-alpha/beta to inhibit S1P1 and lymphocyte egress from lymphoid organs. *Nature* **440**, 540-4 (2006).

77. Matloubian, M. *et al.* Lymphocyte egress from thymus and peripheral lymphoid organs is dependent on S1P receptor 1. *Nature* **427**, 355-60 (2004).

78. Arnon, T.I. *et al.* GRK2-dependent S1PR1 desensitization is required for lymphocytes to overcome their attraction to blood. *Science* **333**, 1898-903 (2011).

79. Groom, J.R. *et al.* CXCR3 chemokine receptor-ligand interactions in the lymph node optimize CD4+ T helper 1 cell differentiation. *Immunity* **37**, 1091-103 (2012).

80. Ramakrishnan, L. Revisiting the role of the granuloma in tuberculosis. *Nat Rev Immunol* **12**, 352-66 (2012).

81. Pitzalis, C., Jones, G.W., Bombardieri, M. & Jones, S.A. Ectopic lymphoid-like structures in infection, cancer and autoimmunity. *Nat Rev Immunol* **14**, 447-62 (2014).

82. Slight, S.R. *et al.* CXCR5(+) T helper cells mediate protective immunity against tuberculosis. *J Clin Invest* **123**, 712-26 (2013).

83. Saunders, B.M. & Britton, W.J. Life and death in the granuloma: immunopathology of tuberculosis. *Immunol Cell Biol* **85**, 103-11 (2007).

84. Khader, S.A. *et al.* In a murine tuberculosis model, the absence of homeostatic chemokines delays granuloma formation and protective immunity. *J Immunol* **183**, 8004-14 (2009).

85. Olmos, S., Stukes, S. & Ernst, J.D. Ectopic activation of Mycobacterium tuberculosis-specific CD4+ T cells in lungs of CCR7-/- mice. *J Immunol* **184**, 895-901 (2010).

86. Kahnert, A. *et al.* Mycobacterium tuberculosis triggers formation of lymphoid structure in murine lungs. *J Infect Dis* **195**, 46-54 (2007).

87. Pym, A.S., Brodin, P., Brosch, R., Huerre, M. & Cole, S.T. Loss of RD1 contributed to the attenuation of the live tuberculosis vaccines Mycobacterium bovis BCG and Mycobacterium microti. *Mol Microbiol* **46**, 709-17 (2002).

88. Lindenstrom, T., Knudsen, N.P., Agger, E.M. & Andersen, P. Control of chronic mycobacterium tuberculosis infection by CD4 KLRG1- IL-2-secreting central memory cells. *J Immunol* **190**, 6311-9 (2013).

89. Caruso, A.M. *et al.* Mice deficient in CD4 T cells have only transiently diminished levels of IFN-gamma, yet succumb to tuberculosis. *J Immunol* **162**, 5407-16 (1999).

90. Elias, D., Akuffo, H. & Britton, S. PPD induced in vitro interferon gamma production is not a reliable correlate of protection against Mycobacterium tuberculosis. *Trans R Soc Trop Med Hyg* **99**, 363-8 (2005).

91. Fletcher, H.A. Correlates of immune protection from tuberculosis. *Curr Mol Med* **7**, 319-25 (2007).

92. Mittrucker, H.W. *et al.* Poor correlation between BCG vaccination-induced T cell responses and protection against tuberculosis. *Proc Natl Acad Sci U S A* **104**, 12434-9 (2007).

93. Scriba, T.J. *et al.* Dose-finding study of the novel tuberculosis vaccine, MVA85A, in healthy BCG-vaccinated infants. *J Infect Dis* **203**, 1832-43 (2011).

94. Tameris, M.D. *et al.* Safety and efficacy of MVA85A, a new tuberculosis vaccine, in infants previously vaccinated with BCG: a randomised, placebo-controlled phase 2b trial. *Lancet* **381**, 1021-8 (2013).

95. Dent, A.L., Shaffer, A.L., Yu, X., Allman, D. & Staudt, L.M. Control of inflammation, cytokine expression, and germinal center formation by BCL-6. *Science* **276**, 589-92 (1997).

96. Gallegos, A.M., Pamer, E.G. & Glickman, M.S. Delayed protection by ESAT-6-specific effector CD4+ T cells after airborne M. tuberculosis infection. *J Exp Med* **205**, 2359-68 (2008).

97. Ariga, H. *et al.* Instruction of naive CD4+ T-cell fate to T-bet expression and T helper 1 development: roles of T-cell receptor-mediated signals. *Immunology* **122**, 210-21 (2007).

98. Yu, D. *et al.* The transcriptional repressor Bcl-6 directs T follicular helper cell lineage commitment. *Immunity* **31**, 457-68 (2009).

99. Higdon, L.E., Deets, K.A., Friesen, T.J., Sze, K.Y. & Fink, P.J. Receptor revision in CD4 T cells is influenced by follicular helper T cell formation and germinal-center interactions. *Proc Natl Acad Sci U S A* **111**, 5652-7 (2014).

100. Bold, T.D., Banaei, N., Wolf, A.J. & Ernst, J.D. Suboptimal activation of antigen-specific CD4+ effector cells enables persistence of M. tuberculosis in vivo. *PLoS Pathog* **7**, e1002063 (2011).

101. Anderson, K.G. *et al.* Intravascular staining for discrimination of vascular and tissue leukocytes. *Nat Protoc* **9**, 209-22 (2014).

102. Sakai, S. *et al.* Cutting edge: control of Mycobacterium tuberculosis infection by a subset of lung parenchyma-homing CD4 T cells. *J Immunol* **192**, 2965-9 (2014).

103. Anderson, K.G. *et al.* Cutting edge: intravascular staining redefines lung CD8 T cell responses. *J Immunol* **189**, 2702-6 (2012).

104. Pereira, J.P., An, J., Xu, Y., Huang, Y. & Cyster, J.G. Cannabinoid receptor 2 mediates the retention of immature B cells in bone marrow sinusoids. *Nat Immunol* **10**, 403-11 (2009).

105. Moon, J.J. *et al.* Naive CD4(+) T cell frequency varies for different epitopes and predicts repertoire diversity and response magnitude. *Immunity* **27**, 203-13 (2007).

106. Reiley, W.W. *et al.* Distinct functions of antigen-specific CD4 T cells during murine Mycobacterium tuberculosis infection. *Proc Natl Acad Sci U S A* **107**, 19408-13 (2010).

107. Woodworth, J.S. *et al.* Protective CD4 T cells targeting cryptic epitopes of Mycobacterium tuberculosis resist infection-driven terminal differentiation. *J Immunol* **192**, 3247-58 (2014).

108. Barber, D.L., Mayer-Barber, K.D., Feng, C.G., Sharpe, A.H. & Sher, A. CD4 T cells promote rather than control tuberculosis in the absence of PD-1-mediated inhibition. *J Immunol* **186**, 1598-607 (2011).

109. Lazar-Molnar, E. *et al.* Programmed death-1 (PD-1)-deficient mice are extraordinarily sensitive to tuberculosis. *Proc Natl Acad Sci U S A* **107**, 13402-7 (2010).

110. Ravn, P. *et al.* Human T cell responses to the ESAT-6 antigen from Mycobacterium tuberculosis. *J Infect Dis* **179**, 637-45 (1999).

111. Schreiber, S.L. & Crabtree, G.R. The mechanism of action of cyclosporin A and FK506. *Immunol Today* **13**, 136-42 (1992).

112. Marshall, H.D. *et al.* Differential expression of Ly6C and T-bet distinguish effector and memory Th1 CD4(+) cell properties during viral infection. *Immunity* **35**, 633-46 (2011).

113. Bevan, M.J. Understand memory, design better vaccines. *Nat Immunol* **12**, 463-5 (2011).

114. Sallusto, F., Lanzavecchia, A., Araki, K. & Ahmed, R. From vaccines to memory and back. *Immunity* **33**, 451-63 (2010).

115. Pepper, M., Pagan, A.J., Igyarto, B.Z., Taylor, J.J. & Jenkins, M.K. Opposing signals from the Bcl6 transcription factor and the interleukin-2 receptor generate T helper 1 central and effector memory cells. *Immunity* **35**, 583-95 (2011).

116. Hale, J.S. *et al.* Distinct memory CD4+ T cells with commitment to T follicular helper- and T helper 1-cell lineages are generated after acute viral infection. *Immunity* **38**, 805-17 (2013).

117. Yoshinaga, S.K. *et al.* T-cell co-stimulation through B7RP-1 and ICOS. *Nature* **402**, 827-32 (1999).

118. Mollo, S.B., Zajac, A.J. & Harrington, L.E. Temporal requirements for B cells in the establishment of CD4 T cell memory. *J Immunol* **191**, 6052-9 (2013).

119. Choi, Y.S. *et al.* ICOS receptor instructs T follicular helper cell versus effector cell differentiation via induction of the transcriptional repressor Bcl6. *Immunity* **34**, 932-46 (2011).

120. Davis, J.M. *et al.* Real-time visualization of mycobacterium-macrophage interactions leading to initiation of granuloma formation in zebrafish embryos. *Immunity* **17**, 693-702 (2002).

121. Egen, J.G. *et al.* Intravital imaging reveals limited antigen presentation and T cell effector function in mycobacterial granulomas. *Immunity* **34**, 807-19 (2011).

122. Rogerson, B.J. *et al.* Expression levels of Mycobacterium tuberculosis antigen-encoding genes versus production levels of antigen-specific T cells during stationary level lung infection in mice. *Immunology* **118**, 195-201 (2006).

123. Day, C.L. *et al.* PD-1 expression on HIV-specific T cells is associated with T-cell exhaustion and disease progression. *Nature* **443**, 350-4 (2006).

124. Barber, D.L. *et al.* Restoring function in exhausted CD8 T cells during chronic viral infection. *Nature* **439**, 682-7 (2006).

125. Honda, T. *et al.* Tuning of antigen sensitivity by T cell receptor-dependent negative feedback controls T cell effector function in inflamed tissues. *Immunity* **40**, 235-47 (2014).

126. Riley, J.L. PD-1 signaling in primary T cells. *Immunol Rev* **229**, 114-25 (2009).

127. Bosio, C.M., Gardner, D. & Elkins, K.L. Infection of B cell-deficient mice with CDC 1551, a clinical isolate of Mycobacterium tuberculosis: delay in dissemination and development of lung pathology. *J Immunol* **164**, 6417-25 (2000).

128. Oestreich, K.J., Huang, A.C. & Weinmann, A.S. The lineage-defining factors T-bet and Bcl-6 collaborate to regulate Th1 gene expression patterns. *J Exp Med* **208**, 1001-13 (2011).

129. Oestreich, K.J., Mohn, S.E. & Weinmann, A.S. Molecular mechanisms that control the expression and activity of Bcl-6 in TH1 cells to regulate flexibility with a TFH-like gene profile. *Nat Immunol* **13**, 405-11 (2012).

130. Nakayamada, S. *et al.* Early Th1 cell differentiation is marked by a Tfh cell-like transition. *Immunity* **35**, 919-31 (2011).

131. Nunes-Alves, C. *et al.* In search of a new paradigm for protective immunity to TB. *Nat Rev Microbiol* **12**, 289-99 (2014).

132. Caucheteux, S.M., Torabi-Parizi, P. & Paul, W.E. Analysis of naive lung CD4 T cells provides evidence of functional lung to lymph node migration. *Proc Natl Acad Sci U S A* **110**, 1821-6 (2013).

133. Moran, A.E. *et al.* T cell receptor signal strength in Treg and iNKT cell development demonstrated by a novel fluorescent reporter mouse. *J Exp Med* **208**, 1279-89 (2011).

134. Pearson, R., Fleetwood, J., Eaton, S., Crossley, M. & Bao, S. Kruppel-like transcription factors: a functional family. *Int J Biochem Cell Biol* **40**, 1996-2001 (2008).

135. Carlson, C.M. *et al.* Kruppel-like factor 2 regulates thymocyte and T-cell migration. *Nature* **442**, 299-302 (2006).

136. Pals, S.T., Horst, E., Scheper, R.J. & Meijer, C.J. Mechanisms of human lymphocyte migration and their role in the pathogenesis of disease. *Immunol Rev* **108**, 111-33 (1989).

137. Hsieh, M.F. *et al.* Both CXCR3 and CXCL10/IFN-inducible protein 10 are required for resistance to primary infection by dengue virus. *J Immunol* **177**, 1855-63 (2006).

138. Zhang, B., Chan, Y.K., Lu, B., Diamond, M.S. & Klein, R.S. CXCR3 mediates region-specific antiviral T cell trafficking within the central nervous system during West Nile virus encephalitis. *J Immunol* **180**, 2641-9 (2008).

139. Charo, I.F. & Ransohoff, R.M. The many roles of chemokines and chemokine receptors in inflammation. *N Engl J Med* **354**, 610-21 (2006).

140. Proudfoot, A.E. Chemokine receptors: multifaceted therapeutic targets. *Nat Rev Immunol* **2**, 106-15 (2002).

141. Brinkmann, V. *et al.* Fingolimod (FTY720): discovery and development of an oral drug to treat multiple sclerosis. *Nat Rev Drug Discov* **9**, 883-97 (2010).

142. Li, M.O. & Flavell, R.A. TGF-beta: a master of all T cell trades. *Cell* **134**, 392-404 (2008).

143. Slutter, B., Pewe, L.L., Kaech, S.M. & Harty, J.T. Lung airway-surveilling CXCR3(hi) memory CD8(+) T cells are critical for protection against influenza A virus. *Immunity* **39**, 939-48 (2013).

144. Khader, S.A. *et al.* Interleukin 12p40 is required for dendritic cell migration and T cell priming after Mycobacterium tuberculosis infection. *J Exp Med* **203**, 1805-15 (2006).

145. Mueller, S.N. & Ahmed, R. High antigen levels are the cause of T cell exhaustion during chronic viral infection. *Proc Natl Acad Sci U S A* **106**, 8623-8 (2009).

146. Wherry, E.J. T cell exhaustion. *Nat Immunol* **12**, 492-9 (2011).

147. Han, S., Asoyan, A., Rabenstein, H., Nakano, N. & Obst, R. Role of antigen persistence and dose for CD4+ T-cell exhaustion and recovery. *Proc Natl Acad Sci U S A* **107**, 20453-8 (2010).

148. Sullivan, J.A., Kim, E.H., Plisch, E.H. & Suresh, M. FOXO3 regulates the CD8 T cell response to a chronic viral infection. *J Virol* **86**, 9025-34 (2012).

149. Wherry, E.J., Barber, D.L., Kaech, S.M., Blattman, J.N. & Ahmed, R. Antigen-independent memory CD8 T cells do not develop during chronic viral infection. *Proc Natl Acad Sci U S A* **101**, 16004-9 (2004).

150. Jung, Y.J., Ryan, L., LaCourse, R. & North, R.J. Properties and protective value of the secondary versus primary T helper type 1 response to airborne Mycobacterium tuberculosis infection in mice. *J Exp Med* **201**, 1915-24 (2005).

151. Wong, R.M. *et al.* Programmed death-1 blockade enhances expansion and functional capacity of human melanoma antigen-specific CTLs. *Int Immunol* **19**, 1223-34 (2007).